Thymol Synthesis by Acid Catalysed Isopropylation of *m*-Cresol

by

Jacobus van der Merwe

BSc (Eng) Chem (UCT)

Submitted to the University of Cape Town
in partial fulfilment of the requirement for the degree of

MASTER OF SCIENCE IN ENGINEERING

Department of Chemical Engineering
UNIVERSITY OF CAPE TOWN

Synopsis

The initial motivation for this study was to identify a suitable window of operation for thymol synthesis from iso-propanol and *m*-cresol mediated by a commercially available H-MFI zeolite catalyst.

A preliminary investigation uncovered seeming anomalies in the course of the synthesis process, in particular counterintuitive trends with respect to *m*-cresol conversion and thymol selectivity at low space velocity. Consequently, the study sought to establish the reaction pathway responsible for these observations in an attempt to gain an understnding for future thymol yield optimisation studies.

Under the reaction conditions studied, complete dehydration of iso-propanol was observed. Further reaction of the propene to olefinic species with carbon numbers higher than 3 was also seen.

Results showed that the cause of the so-called “volcano curve” in respect of *m*-cresol conversion was found in the system’s propensity for the formation of cresylic rings which were alkylated with side chains consisting of carbon atoms between 4-8, particularly under severe reaction conditions. This fraction was formed via the alkylation of the *m*-cresol with the said olefinic pool.

The thymol synthesis system was also found to be thermodynamically limited at high reaction temperature and low space velocity.

Acknowledgements

To **Prof. Jack C.Q. Fletcher,** my academic supervisor, for the privilege and opportunity to conduct this research and guidance given in this regard – I know that time is a valuable commodity to you.

To **Mr Walter Böhringer,** my co-supervisor, for the long hours spent during the study and open-door policy. You truly are generous when it comes to your students.

c*change and IKEY® for funding of my masters studies.

Friends and family for all their encouragement and support.

Clariant for the supply of the zeolites used in this study.

The University of Cape Town with reference to the Department of Chemical Engineering for the use of their facilities and resources.

Nicola Toma for help with Aspen and molecular modelling.

Prof. Klaus Moller for advice in terms of simulations used in this study.

Werner Janse van Rensburg for advice and guidance in terms of molecular modelling.

Alexey Cherkaev for translation of the Russian journal article.

David Tsui for translation of the Japanese patents.

Nico Fischer for translation of the German patent.

Roald Brosius for the use of his GC equipment.

Plagiarism declaration

I know the meaning of plagiarism and declare that all the work in the document, save for that which is properly acknowledged, is my own.

..... Date .....
Jacobus van der Merwe

Table of Contents

Synopsis i
Acknowledgements ii
Plagiarism declaration iii
Table of Contents iv
List of Figures viii
List of Tables xii
List of Equations xiv
List of Symbols xv
Glossary xvi

1 Introduction 1

2 Literature review 5

2.1 Identification of H-MFI as most suitable catalyst 5
2.2 Zeolite H-MFI 6
2.3 Shape Selectivity of Zeolites 7
2.4 Zeolite deactivation 7
2.5 Thymol synthesis with iso-propanol at UCT 8
2.6 Influence of thermodynamic equilibrium in thymol synthesis 10
2.6.1 m-Cresol conversion limitation during thymol synthesis 10
2.6.2 Equilibrium distribution of thymol position isomers 11
2.6.3 Thermodynamic equilibrium for iso-propanol dehydration 12
2.7 Preliminary experimental results 13
2.8 Equilibrium limitations in phenolic conversions 14
2.8.1 Isomerisation of cresol 15
2.8.2 Transalkylation between phenol and xylenol 15
2.8.3 Alkylation of phenol with iso-propanol 16
2.9 Reaction mechanism for *m*-cresol isopropylation 16
2.10 Acid Catalysed Propylation of Aromatic Compounds 17

3 Objectives of study 18

3.1 Aim of the study 18
3.2 Special study objectives 18
3.3 Hypothesis 18
3.4 Key questions 18

4 Experimental 19

4.1 Catalysts 19
4.2 Feed stocks and other materials used 19
4.3 Experimental apparatus 20
4.3.1 Reactor and reactor heating systems 21
4.3.2 Liquid feed delivery 23
4.3.3 Gas supplies 23
4.3.4 Pressure control 23
4.3.5 Sampling 24
4.3.5.1 Thymol product sampling (for off-line analysis) 24
4.3.5.2 Iso-propanol dehydration product sampling (for on-line analysis) 25
4.3.5.3 Iso-propanol dehydration product sampling (for off-line analysis) 25
4.4 Procedures 26
4.4.1 Loading of the reactor 26
4.4.2 Pressure testing 27
4.4.3 Catalyst drying and activation 27
4.4.4 Start-up procedure: thymol synthesis experiments 28
4.4.5 Start-up procedure: iso-propanol dehydration experiments 29
4.4.6 Increasing system pressure: thymol synthesis experiments 29
4.4.7 Standard conditions employed for experiments 30
4.4.8 Shut-down procedure for thymol synthesis experiments 30
4.4.9 Shut-down procedure dehydration experiments 31
4.4.10 Setup of an isothermal profile over the catalyst bed 31
4.5 Product analysis 33
4.5.1 Identification of compounds 33
4.5.2 Groupings of fractions for thymol synthesis experiments 34
4.6 Data evaluation 36
4.6.1 Response factors and corrected peak areas for the thymol synthesis experiments 36
4.6.2 Molar calculations 37
4.6.3 Conversion 37
4.6.4 Selectivity 38
4.6.5 Yield 38
4.6.6 Average number of carbon atoms in side chains 38
4.6.7 Thymol synthesis thermodynamic equilibrium constant 38
4.6.8 Selectivity of Alkylating agent dehydration experiment 39
4.7 Obtaining thermodynamic data 39

5 Results 40
5.1 Theoretical considerations – thermodynamic equilibrium limitations 40
5.2 Initial experimental findings 42
5.2.1 Quasi-steady state data 42
5.2.2 Catalyst stability vs. time-on-stream 43
5.2.3 Effect of reaction conditions on catalyst stability 45
5.2.4 Exclusion of external mass transfer limitations 45
5.2.5 Repeatability and data scatter 46
5.3 Thymol synthesis 47
5.3.1 Alkylating agents vs. reaction rate and catalyst stability 47
5.3.2 Variation of space velocity 47
5.3.3 Variation of reaction pressure 53
5.3.4 Variation of reaction temperature 55
5.4 Dehydration of iso-propanol 57
5.4.1 Variation of space velocity 58
5.4.2 Temperature series 59

6 Discussion 60
6.1 Thermodynamic limitations relevant to this study 60
6.2 Integrity of experimental results 62
6.3 Conversion of iso-propanol 63
6.4 Thymol synthesis 64
6.4.1 Effect of pressure and water 64
6.4.2 Effect of temperature 65
6.4.3 Effect of space velocity 66
6.4.4 Origin of the "volcano curve" for *m*-cresol conversion 70

7 Conclusions and Recommendations 74

8 References 76

Appendix A: Description of product fractions A-1
Appendix B: Temperature profiles A-2
Appendix C: Further dehydration experiments with n-propanol A-4
Appendix D: Cause of depression in temperature profiles at catalyst bed inlet A-5
Appendix E: Dehydration equilibria and adiabatic temperature drop A-9
Appendix F: Thermodynamic data from functional analysis A-11
Appendix G: Thermodynamic data from group contribution methods A-25
Appendix H: Group contribution method sample calculations A-32
Appendix I: Catalyst drying and activation sequence A-33
Appendix J: Phase calculations for thymol synthesis system A-34
Appendix K: GC methods and apparatus A-35
Appendix L: Peak identification by means of GC/MS A-36
Appendix M: Identification of 1-methylpropyl-3-methylphenol isomers A-38
Appendix N: Thymol synthesis chromatograms A-40
Appendix O: Iso-propanol dehydration sample chromatograms A-47

List of Figures

Figure 1-1: Chemical structure of thymol 1
Figure 2-1: Three-dimensional representation of MFI pore structure with pore dimensions [adapted by Kukard (2008) from Eckroth et al. (1990)]. 6
Figure 2-2: Proposed reaction mechanism for isopropylation of m-cresol with iso-propanol over H-MFI zeolites (Nagooroo, 2012)..... 9
Figure 2-3: Experimental estimation of thermodynamic equilibrium approach for an H-ZSM-5 mediated *m*-cresol/propene alkylation reaction (Fletcher et al., 2001b). 10
Figure 2-4: Isomerisation of thymol and its major position isomers over H-ZSM-5 (Fletcher *et al*., 2002). 11
Figure 2-5: Equilibrium conversion of iso-propanol to water and propene (Nagooroo, 2012). 13
Figure 2-6: *m*-Cresol conversion vs. space velocity obtained during preliminary experiment (Mathews and Tsui, 2007). 13
Figure 2-7: Reaction mechanism for the acid catalysed iso-propylation of *m*-cresol with iso-propanol. 16
Figure 4-1: Schematic of the experimental apparatus employed to conduct the “thymol synthesis” experiments at ambient and elevated pressure. 20
Figure 4-2: Schematic of the modified experimental apparatus employed to conduct the dehydration experiments at ambient pressure. 21
Figure 4-3: Diagrammatic representation of the reactor system. 22
Figure 4-4: Optimised temperature profile generated during commissioning with a depiction of a 5 heating-zone-reactor system. 31
Figure 4-5: Catalyst bed temperature profiles obtained during experiments..... 33
Figure 4-6: Chromatogram with reactor effluent compound groupings. 34
Figure 5-1: Thermodynamic equilibrium conversion of *m*-cresol as a function of temperature. 41
Figure 5-2: Equilibrium distribution of cresylic side chains and remaining olefins as a function of temperature. 42
Figure 5-3: *m*-Cresol conversion as a function of time-on-stream at standard reaction conditions. 43
Figure 5-4: *m*-Cresol conversion with iso-propanol as a function of time-on-stream and effect of varying reaction conditions on catalyst stability. 44

Figure 5-5: *m*-Cresol conversion with di-isopropylether as a function of time-on-stream and effect of varying reaction conditions on catalyst stability. 44
Figure 5-6: *m*-Cresol conversion as a function of space velocity. 46
Figure 5-7: *m*-Cresol conversion vs. space velocity for a range of reaction conditions. 48
Figure 5-8: Yields of the various product fractions vs. space velocity. 50
Figure 5-9: Selectivity of the various product fractions vs. space velocity. 51
Figure 5-10:Thymol and position isomer selectivities vs. space velocity. 52
Figure 5-11:Additional product fractions selectivities vs. space velocity. 52
Figure 5-12:*m*-Cresol conversion and yield of various product fractions vs. pressure 53
Figure 5-13:Selectivity of thymol position isomers and di-isopropylated *m*-cresol obtained as a function of pressure. 54
Figure 5-14:*m*-Cresol conversion with iso-propanol as function of reaction temperature. 55
Figure 5-15:Yields of the various product fractions vs. reaction temperature. 56
Figure 5-16:Selectivity to product fractions vs. reaction temperature. 57
Figure 5-17:Conversion of neat iso-propanol and yields of the various product fractions as a function of space velocity. 58
Figure 5-18:Conversion of iso-propanol and yields of the various product fractions as a function of temperature. 59
Figure 6-1: Arrhenius plot for the equilibrium constant (K_a) obtained from simulations. 60
Figure 6-2: Arrhenius plot for *m*-cresol iso-propylation reaction. 61
Figure 6-3: Thymol selectivity as a function of *m*-cresol conversion 65
Figure 6-4: *m*-Cresol conversion and alkylation conversion vs. temperature. 66
Figure 6-5: Selectivity to “kinetically favoured” and “secondary poducts” vs. *m*-cresol conversion in the “high space velocity” regime. 67
Figure 6-6: Thymol selectivity vs. *m*-cresol conversion in “high space velocity” regime. 67
Figure 6-7: Selectivity to “kinetically favoured” and “secondary poducts” vs. *m*-cresol conversion in “low space velocity” regime. 68
Figure 6-8: Thymol selectivity vs. *m*-cresol conversion in “low space velocity” regime. 68

Figure 6-9: Lengthwise through the catalyst bed in the fixed bed reactor employed for thymol synthesis. 70

Figure C-1: Propene selectivity vs. temperature for dehydration experiments.....A-4

Figure D-1: Temperature profiles obtained at standard reaction conditions.....A-6

Figure D-2: Temperature profiles obtained during experiments A-7

Figure G-1: *m*-Cresol conversion at thermodynamic equilibrium as a function of temperature. A-29

Figure I-1: Catalyst drying and activation sequence (1 bar, 50 ml·min^{-1} N_2).....A-33

Figure J-1: Txy diagrams for IPA/*m*-cresol mixture.....A-34

Figure J-2: Dew point pressure of a propene-water-*m*-cresol-thymol system a function of *m*-cresol conversion. A-34

Figure L-1: Fragmentation pattern of 6-propyl-3-methylphenol (MS NIST, Version 2.0). A-37

Figure L-2: Fragmentation pattern of thymol (MS NIST, Version 2.0). A-37

Figure M-1: Fragmentation pattern of 6-(1-methylpropyl)-3-methylphenol (H-MFI-400, 1 bar, gas phase, 300℃, is o-propanol to *m*-cresol ratio =1:1 and 0.04 $g_{m\text{-cresol}} \cdot g_{cat}^{-1} \cdot hr^{-1}$). A-39

Figure N-1: Sample GCMS Chromatogram for reaction conditions: 300℃, 1 bar, gas phase, iso-propanol to *m*-cresol molar ratio 1:1, 0.04 $g_{m\text{-cresol}} \cdot g_{cat}^{-1} \cdot hr^{-1}$, H-MFI-400. .....A-40

Figure N-2: Sample GCMS Chromatogram for reaction conditions: 300℃, 1 bar, gas phase, IPA to *m*-cresol molar ratio 1:1, 0.04 $g_{m\text{-cresol}} \cdot g_{cat}^{-1} \cdot hr^{-1}$, H-MFI-400. .....A-41

Figure N-3: Sample FID chromatogram (H-MFI-90, iso- propanol:*m*-cresol molar ratio = 1:1, 250℃, 1 bar, gas phase, 1.03 $g_{m\text{-cresol}} \cdot g_{cat}^{-1} \cdot hr^{-1}$, catalyst bed diluted with SiC at a 1:1 (vol.) ratio). A-42

Figure N-4: Sample FID chromatogram of (H-MFI-90, iso- propanol:*m*-cresol molar ratio = 1:1, 325℃, 1 bar, gas phase, 1.03 $g_{m\text{-cresol}} \cdot g_{cat}^{-1} \cdot hr^{-1}$, catalyst bed diluted with SiC at a 1:1 (vol.) ratio). A-43

Figure N-5: First section of FID chromatogram showing grouping of peaks to compound fractions shown in Figure N-4.....A-44

Figure N-6: Sample FID chromatogram (H-MFI-90, iso- propanol:*m*-cresol molar ratio = 1:1, 275℃, 15 bar, trickle bed phase , 0.05 $g_{m\text{-cresol}} \cdot g_{cat}^{-1} \cdot hr^{-1}$, catalyst bed diluted with SiC at a 1:1 (vol.) ratio).....A-45

Figure N-7: Section of FID chromatogram showing grouping of peaks to compound fractions shown in Figure N-6. .....A-46

Figure O-1: Section of FID sample chromatogram (H-MFI-90 at 1 bar, 250℃ in the gas phase, IPA to N_2 molar ratio of 1:1 and 0.57 $g_{iso\text{-}propanol} \cdot g_{cat}^{-1} \cdot hr^{-1}$).....A-47

Figure O-2: Section of FID sample chromatogram (H-MFI-90 at 1 bar, 250℃ in the gas phase, IPA to N_2 molar ratio of 1:1 and 0.57 $g_{iso\text{-}propanol} \cdot g_{cat}^{-1} \cdot hr^{-1}$).....A-48

List of Tables

Table 4-1: H-MFI catalysts tested and their properties 19
Table 4-2: Feedstocks and auxiliary chemicals used and their properties 19
Table 4-3: Impurities in the *m*-cresol feedstock 19
Table 4-4: Details of catalyst charges 26
Table 4-5: Standard experimental conditions applied with the respective feeds 30
Table 4-6: Thymol synthesis product fractions seen at severe conditions 35
Table 6-1: Average side chain length as a function space velocity 73
Table B-1: Temperature controller set points to achieve a 250℃ isothermal zone A-2
Table D-1: Adiabatic temperature drop and heat of IPA dehydration reaction. A-6
Table E-1: Results yielded by the model used to derive the chemical equilibrium composition of the iso-propanol dehydration system A-9
Table E-2: Constants yielding the equilibrium conversion of iso-propanol at 250℃ and 1 bar, iso-propanol was co-fed with N_2 at a 1:1 molar ratio. A-9
Table E-3: Results from the adiabatic model with the feed and product stream specifications. A-10
Table F-1: Pure component values for the respective compounds computed with the PW91 GGA functional A-13
Table F-2: Pure component values for the respective compounds computed with the PW91 GGA functional A-14
Table F-3: Pure component values for the respective compounds computed with the PW91 GGA functional A-15
Table F-4: Pure component values for the respective compounds computed with the HCTH GGA functional A-16
Table F-5: Pure component values for the respective compounds computed with the HCTH GGA functional A-17
Table F-6: Pure component values for the respective compounds computed with the HCTH GGA functional A-18
Table F-7: Pure component values for the respective compounds computed with the RPBE GGA functional A-19
Table F-8: Pure component values for the respective compounds computed with the RPBE GGA functional A-20

Table F-9: Pure component values for the respective compounds computed with the RPBE GGA functional A-21
Table F-10:Pure component values for the respective compounds computed with the PLYB GGA functional.....A-22
Table F-11:Pure component values for the respective compounds computed with the PLYB GGA functional.....A-23
Table F-12:Pure component values for the respective compounds computed with the PLYB GGA functional.....A-24
Table G-1: Estimated pure component physico-chemical and thermodynamic property values for the respective compounds....A-27
Table G-2: Comparison of the normal boiling points estimated A-29
Table G-3: Comparison of the critical temperatures estimated using different group contribution methods A-30
Table G-4: Comparison of the Critical pressures obtained using different group contribution methods compared to experimental values.....A-31
Table K-1: Gas chromatography equipment and methods.....A-35
Table O-1: Sample of compounds identified during dehydration experiment....A-49

List of Equations

Equation 4-1: Calculation of response factor (f_i) 37
Equation 4-2: Calculation of corrected peak area (PAC_i) 37
Equation 4-3: Calculation of mol proportional peak area (PAM_i) 37
Equation 4-4: Calculation of *m*-cresol conversion ($X_{m\text{-}cresol}$) 37
Equation 4-5: Calculation of *m*-cresol alkylation conversion ($X_{m\text{-}cresol,\ alkylation}$) 37
Equation 4-6: Calculation of *molar selectivity* (S_i) 38
Equation 4-7: Calculation of component yield (Y_i) 38
Equation 4-8: Calculation of average carbon no. in side chains ($N_{Avg\ C\ in\ side\ chains}$) .. 38
Equation 4-9: Thymol synthesis thermodynamic equilibrium constant (K_a) 38
Equation 4-10: Calculation of mass selectivity (S_i) for the dehydration exp. 39
Equation H-1: Calculation of critical temperature, T_c (Lydersen, 1955) A-32
Equation H-2: Denominator in critical temperature eqn. (Lydersen, 1955) A-32
Equation H-3: Calculation of critical pressure A-32

List of Symbols

$X_{m\text{-}cresol}$	*m*-Cresol conversion
S_{thymol}	Selectivity toward the formation of thymol
$X_{m\text{-}cresol,\ alkylation}$	Conversion of *m*-cresol to alkylated products
PA_i	Peak area of component ***i*** as obtained from data report
f_i	Response factor of component ***i***
PAC_i	Corrected peak area of component ***i***
PAM_i	Mol proportional peak area of component ***i***
C_i	Number of carbon atoms in component ***i***
K_a	Thermodynamic equilibrium constant for the thymol synthesis reaction
$\mathbf{T_b}$	Normal boiling point
$\mathbf{X}_{i,est}$	Parameter **X** estimated, for physical property ***i,*** with the use of group contribution methods e.g. $\mathbf{T_{b,est}}$ which represents the estimated value of $\mathbf{T_b}$
$\mathbf{X}_{i,exp}$	Parameter **X** measured, for physical property ***i*** experimentally e.g. $\mathbf{T_{b,exp}}$ which represents the experimentally measured value of $\mathbf{T_b}$ as obtained from literature
$\mathbf{T_c}$	Critical temperature
$\mathbf{P_c}$	Critical pressure
$\boldsymbol{\theta}$	Constant used in the calculation of T_c in the modified Guldberg rule
$\mathbf{M_r}$	Molecular mass
$\mathbf{\Delta H_f°_{est}}$	Standard Enthalpy of formation (estimated)
$\mathbf{\Delta G_f°_{est}}$	Standard Gibbs energy of formation (estimated)
Sg	Specific gravity

Glossary

EXPERIMENTAL PRODUCT FRACTIONS	
Fraction	**Description**
Lights	Di-and Trimethyl-phenols Ethyl-methyl-phenols Isopropyl-phenols n-Propyl-phenols Methyl-isopropyl-phenols with the methyl group not in the 3 position
C-10	Other compounds eluding in the same time frame (11.0-12.4 minutes) as the mono-isopropylated isomers e.g. n-Propylated *m*-Cresol
Σ Isomers	Isopropylated *m*-Cresol isomers: 3-Methyl-2-isopropyl-phenol Thymol 3-Methyl-5-isopropyl-phenol 3-Methyl-4-isopropyl-phenol
Di-propylated	Di-propylated *m*-Cresol (with n-Propyl and iso-Propyl)
Heavies	*m*-Cresol alkylated with side chains consisting of 4-8 carbon atoms (C_{4-8})
Kinetically favoured	Thymol 3-Methyl-2-isopropyl-phenol 3-Methyl-4-isopropyl-phenol Di-isopropylated *m*-Cresol
Secondary products	Heavies C-10 Lights 3-Methyl-5-isopropyl-phenol
THE FOLLOWING APPLIES TO FRACTIONS SIMULATED IN THERMODYNAMIC EQUILIBRIUM CALCULATIONS	
C4 remaining	n-Butenes (cis-2-, trans-2- and 1-Butene)
C3 remaining	Propene
iso-C4 substituents	n-Butenes which have alkylated *m*-Cresol to form secondary butyl substituents
2 x iso-C3 side chains	Propene which has alkylated the m-cresol ring twice to form Di-isopropylated m-cresol compounds
iso-C3 side chains	Propene which has alkylated the *m*-Cresol ring to form Thymol and Thymol position isomers
THE FOLLOWING APPLIES TO ACRONYMS DESIGNATING PRODUCT COMPOSITION IN THERMODYNAMIC CALCULATIONS	
M	*m*-Cresol
P	Propene
W	Water
T	Thymol and thymol isomers
D	Di-isopropylated *m*-Cresol derivatives
I	sec. butylated *m*-Cresol isomers
B	n-Butenes
ALKYLATING AGENT ABREVIATIONS	
IPA	Iso-propanol
DIPE	Di-isopropylether

1 Introduction

Traditionally, thymol (Figure 1-1) has been extracted from plants such as thyme, mint and eucalyptus but, in more recent times, synthetic synthesis of thymol has commenced.

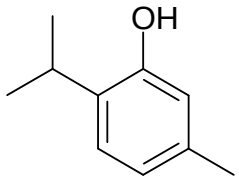

Figure 1-1: Chemical structure of thymol

Synthetic thymol is produced industrially by Symrise, in Germany (formed by a merger of Bayer-AG subsidiary Haarmann & Reimer with the flavour and fragrance maker Dragoco in 2002). In 2003, the global demand for thymol was estimated at 4,500 metric tons per annum (Marais, 2003). At that stage, thymol production costs were approximately $ 3.4/kg with a sales price at $ 9/kg. The relatively large difference between production costs and market price served as an indication of its considerable market value (Fiege, 2003). Reportedly, half of the total thymol synthesised was being hydrogenated to menthol, specifically the L-menthol stereoisomer (Marais, 2003).

Currently Symrise synthesises menthol via this route in collaboration with Lanxess (a German company spun off from Bayer-AG in 2005). The current capacity of this plant is estimated at 3 000 – 3 600 metric tons per annum (McCoy, 2010; Leffingwell, 2010). Therefore, Symrise produces at least 3 000 – 3 600 metric tons of thymol per year and intends to double this amount in response to a recent announcement by BASF of its intent to enter the menthol market. Given the scale of the production capacity of only one of the thymol producers, the current global thymol demand is probably much larger than the previously estimated 4 500 tons per annum and should Symrise's expansion plans materialise, the capacity will be far in excess of 6 000 metric tons per annum.

Menthol is considered the world's top selling aroma chemical on a volume basis (BASF, 2010; McCoy, 2010). In 1998, the global L-menthol demand was put at 12 000 tons per annum (Clark, 1998). In 2007 the combined global demand for both L-menthol and its optical isomer (racemic menthol) was estimated to be 32 000 metric tons per annum (Clark, 2007). Currently, the global demand for L-menthol

alone is estimated to be in excess of 20 000 metric tons per year. With a selling price of approximately $ 19/kg, this world market is worth $ 380 million (Leffingwell, 2010).

Presently India (with a capacity to meet 80%, or 16 000 metric tons, of this demand with natural menthol extracted from the *Mentha arvensis* or *Mentha piperita* mint plants) and China are the major producers of menthol. However, India's dependence on unreliable Monsoons for its fresh water supply causes shortfalls in menthol production and this coupled with speculation by traders, results in threefold price increases at such times (Leffingwell, 2010).

The synthetically produced L-menthol demand is, by most accounts, estimated to increase and these forecasts are supported by the double digit annual increase in demand seen in past years. This growth is exemplified by the sharp increase between 1998 and 2010 described previously (Clark, 1998; Symrise, 2010; McCoy, 2010). In response to this prospect and with the possible aim to replace the unreliable natural L-menthol supply, Tagasako announced its intent to increase production capacity of its plant in Japan's Shizuoka prefecture to 3 000 metric tons per year in 2007. The first phase of this project was recently completed. This has been followed by consecutive announcements by BASF (expected to have production capacity in the range of 3 000 to 5 000 metric tons per year (Leffingwell, 2010; McCoy, 2010) that it would enter the menthol market by constructing the world's largest menthol production plant and that of Symrise (currently the largest menthol producer) of its intent to double its menthol production capacity. Should these intended expansions and construction projects be finalised the total combined production capacity of these 3 producers is projected to be between 12 000 and 15 000 tons per year.

Apart from reaction to menthol, thymol may also be hydrogenated to menthone and converted to chlorothymol and thymol iodide (Ashford, 1994). Other possible applications resulting from thymol's antiseptic properties include antimicrobial activity against bacteria responsible for upper respiratory tract infections, inhibitory activity against *Escherichia coli*, *Salmonella typhimurium* (Helander *et al*., 1998) and also oral bacteria (Dirdy *et al*., 1993; Shapiro, 1996; Botelho, 2000). In addition, thymol has shown activity in protecting low-density lipoproteins (Teissedre and Waterhouse, 2000) and has been reported to show high efficiency as an anti-oxidant, e.g. the triacylglycerols found in sunflower oil (Kruase and Ternes, 1999; Yanishlieva and Marinova, 1999; Milosh *et al*., 2000). Moreover, thymol is also an important intermediate in perfumery.

South Africa is one of the world's largest phenolics producers owing mainly to the coal-to-synfuels industries and to a lesser extent, the steel industry. These phenolic compounds are formed at high temperatures through pyrolysis or cracking of materials such as coal, petroleum or wood and their production exceeds their market demand.

Coal gasification in Lurgi gasifiers (part of the Sasol synfuel refineries-situated in Secunda) is a major phenolics source in South Africa. During this process, phenolics, together with aromatics and hydrocarbons are driven off during pyrolysis at temperatures between 500-650℃. The total yield of phenolics is about 3.2 kg/ton of coal, among which, the cresol fractions have a comparatively high economic value. The market for *m*-cresol, specifically, is rapidly growing as a result of its use in the production of vitamin E, thermally sensitive papers, thymol and derivatives such as menthol, antioxidants, agrochemicals, fragrances etc. (Fiege, 2003).

Reportedly, Sasol is considering to build an additional coal-to-liquids plant in the Free State or Waterberg (Limpopo). This facility is intended to add an additional 80 000 bbl/day to its current 150 000 bbl/day production capacity and will add a corresponding 50% to the South African phenolics production capacity (Webb, 2007).

Along with *m*-cresol, propylating agents such as propene and iso-propanol (IPA) are also produced by Sasol as products and by-products. Thymol may be synthesised by alkylation of the *m*-cresol with the formerly mentioned propylating agents in a process similar to that of Symrise and the upgrading of this domestically available phenolic substrate could increase its value by as much as 300% (Isaacs, 2004; Fletcher, 2004).

The dehydration of propyl ethers to propene would produce less water (1 water molecule per 2 propene molecules) compared to the dehydration of propyl alcohols (2 water molecules per 2 propene molecules) an advantage both in terms of effluent and reactor heat duty. Should their use prove more beneficial in terms of thymol selectivity and *m*-cresol conversion compared to propyl alcohols, it would be possible to manufacture these compounds via a condensation reaction of the propyl alcohol groups for use in the thymol synthesis process (Joseph Antony Raj *et al*., 2005).

Since propene is gaseous, denser than air and highly flammable at ambient conditions, its storage, handling and transportation is costly and requires specific safety measures. Thus, the use of propene presents difficulties for industries located at distances which do not allow transportation by pipeline.

Similarly, propene might not be a suitable propylating agent for use by small or medium sized enterprises which do not have the resources to deal with the aspects associated with its handling, transportation and storage. The use of propene is also associated with oligomerisation which results in deactivation of the catalyst and loss of propene as alkylating agent.

Therefore, to make the thymol syntheses process attractive to small or medium scale chemical enterprises, alternative alkylating agents, which are liquid and less flammable, such as propyl alcohols and dipropyl ethers appear attractive. These compounds offer further advantages as they form water when reacted over an acid catalyst which in turn serves to suppress polymerisation of propene and thereby prolongs catalytic activity (Yadav and Pathre, 2005; Harmer and Qun, 2001).

In summary, the major fraction of thymol produced globally is hydrogenated to menthol. From this menthol raw product stream, L-menthol has to be separated from its chiral isomers. AECI South Africa was granted a patent to separate (-)-menthol from its stereo-isomers using a stereospecific enzyme (Chaplin et al., 2002) and therefore, the technology exists in South Africa that could aid in the purification of a raw menthol product stream. Consequently, the availability of raw materials, a growing demand for both thymol and L-menthol and the value addition potential of a thymol synthesis process appears promising. In addition, the use of *m*-cresol and propyl alcohols could be implemented in small-to-medium enterprises as thymol is a typical small- or medium-volume chemical. Finally, such an enterprise could contribute to employment opportunities, import replacements, exports and foreign investment and, consequently, research aimed at a domestic thymol synthesis process appears attractive.

2 Literature review

2.1 Identification of H-MFI as most suitable catalyst

Extensive literature reviews have also been conducted previously by researchers to identify suitable catalysts for the synthesis of thymol via the alkylation of *m*-cresol.

Friedel-Crafts type alkylation catalysts and mineral acids employed in acid catalysed alkylation reactions are synonymous with poor atom efficiency, enhanced tar formation, generation of waste salts, corrosion and pollution. As a result these catalytic systems are no longer considered viable process options (Yadav and Pathre, 2005).

In a literature review conducted by Fletcher and co-workers (2003), several catalytic routes were considered, including those reported by Fiege (2003), Umamaheswari (2002), Grabowska *et al.* (2001a), Grabowska *et al.* (2001b), Velu *et al. (*1998), Wimmer *et al.* (1991), Yamanaka (1976), Nitta *et al.* (1974a), Nitta *et al.* (1974b), Yamanka *et al*. (1970b) and Yamanaka *et al.* (1970a). These catalytic routes involved a range of catalysts, alkylating agents (propene and iso-propanol), reaction pressures, temperatures, reagent stoichiometric ratios and space velocities. Although most of these reaction systems generated high thymol yields, factors such as severe reaction conditions and lack of catalyst stability, rendered these catalytic routes not suitable for a modern day thymol synthesis process intended for small enterprises.

Fletcher *et al.* (2003) proceeded to evaluate 3 commercial zeolite catalysts (H-MOR, H-BEA and H-MFI) for *m*-cresol isopropylation with propene. Under mild reaction conditions in the vapour phase (~250℃ and 1-10 bar), MFI with a silica-alumina (SiO_2/Al_2O_3) ratio of 400 exhibited the best performance with respect to activity, selectivity and stability. These observations were attributed, inter-*alia*, to H-MFI's superior shape selective properties.

Although MCM-22 appears also to be a promising catalyst for thymol synthesis (with *m*-cresol and iso-propanol) based on the findings of Moon (2003), in the case of para-selective phenol alkylation, the commercial availability of H-MFI led to its selection as the catalyst of choice for this study.

2.2 Zeolite H-MFI

Zeolite MFI (also known as ZSM-5) was first synthesized by scientists at Mobil Oil Corporation in 1972 and was first employed commercially in 1978 (Eckroth *et al*., 1990). Zeolites such as MFI consist of a three dimensional network of primary building units (SiO_4^{-4} and AlO_4^{-5} tetrahedra bridged by oxygen atoms). The charge imbalance of the AlO_4^{-5} tetrahedron has to be compensated for by a charge balancing cation, e.g. a mobile Na^+ ion. The acid form of MFI is produced by exchanging the Na^+ ions present in the MFI structure for NH_4^+ cations, after which the catalyst is calcined and NH_3 is driven off, forming the protonated MFI zeolite, H-MFI. The protons associated with the zeolite structure form structural hydroxyl groups which act as strong Brønsted acids.

The strength of the Brønsted acid site depends on the SiO_2/Al_2O_3 ratio and the location and distribution of aluminium in the zeolite framework. The strength of an individual acid site increases with increasing SiO_2/Al_2O_3 ratio, whereas the number of acid sites decreases with increasing SiO_2/Al_2O_3 ratio. Therefore, there is an optimum SiO_2/Al_2O_3 ratio for each type of reaction for which activity is maximised (Mikovsky and Marshall, 1976). The pore system of MFI consists of channels formed by puckered 10-membered rings. Straight channels with elliptical openings of 5.1 x 5.5 Å intersect sinusoidal channels (depicted in Figure 2-1) with apertures of 5.4 x 5.6 Å (Weitkamp and Puppe, 1999). In effect the pore system allows three-dimensional diffusion of molecules.

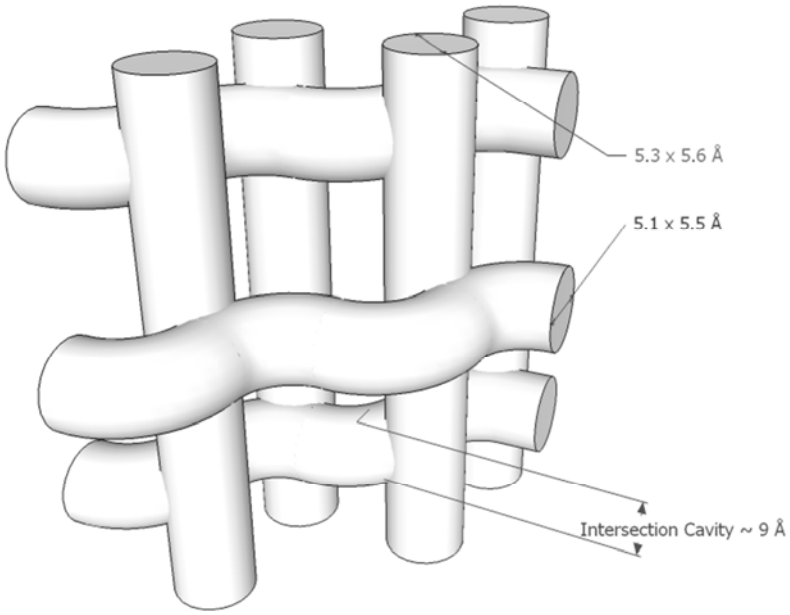

Figure 2-1: Three-dimensional representation of MFI pore structure with pore dimensions [adapted by Kukard (2008) from Eckroth *et al.* (1990)].

2.3 Shape Selectivity of Zeolites

The intra-crystalline channels (micro-pores) of zeolites form molecular sieves. These molecular sieves favour the diffusion or formation of molecules which are less bulky compared to their counterparts within the macro-porous structures of other catalysts. This characteristic of zeolites is referred to as shape selectivity, of which there are three major forms, namely **reactant-, product-** and **restricted transition state selectivity.** Shape selective effects in zeolites are usually predominant when configurational diffusion takes place, i.e. under conditions where kinetic molecular diameters are similar to the diameters of the intra-crystalline pores of the zeolite (Derouane, 1980).

The selective process, in which certain reactants are prevented from entering the pore structure as their effective diameter is larger than the pore openings of the zeolite, is known as **reactant selectivity.**

Product selectivity occurs when the formation of certain product species is favoured above their more bulky counterparts. The less bulky products diffuse out of the pore structure faster and therefore are less likely to react further in contrast to the more bulky products which have a greater probability to be further converted. The high para-xylene selectivity observed during toluene disproportionation or toluene methylation is an example of product selectivity.

Restricted transition state selectivity occurs as a result of certain reaction transition states being unable to form for reasons of space restrictions with the consequence of such products not being formed within the zeolite channel system.

2.4 Zeolite deactivation

Deactivation is a term used to refer to loss of activity of a catalyst with increasing time-on-stream. There are three main sources of deactivation of catalysts, namely sintering, poisoning and coking (Fogler, 1999).

Given the relatively low reaction temperatures in addition to the chemical nature of reagents, sintering and poisoning are the least likely deactivation mechanisms of concern to this study.

Coking is the process by which carbonaceous matter ranging from high molecular mass polymers to hydrogen deficient carbon deposits on the catalyst surface. Hard coke is defined as $(CH_x)_n$ (where $x < 1$)(Fogler, 1999). Considering the restricted transition-state shape-selectivity of the MFI zeolite, the formation of the large polynuclear aromatics required for the formation of hard coke, is unlikely (Csicery, 1986).

Likewise, O'Connor *et al.*, (2003) suggested that the formation of so-called "soft coke" resulting from propene oligomerisation will be the most probable cause of zeolite deactivation observed in the current study. This notion was supported by findings of Wichterlová and Čejka (1993).

2.5 Thymol synthesis with iso-propanol at UCT

In a recent study, thymol synthesis from *m*-cresol and iso-propanol was investigated employing H-MFI zeolites with a range of different SiO_2/Al_2O_3 ratios, crystallite sizes and reaction conditions (Nagooroo, 2012). One of the study foci was the first step in the reaction mechanism of *m*-cresol conversion with iso-propanol.

Two parallel reaction pathways were identified, namely O-alkylation of *m*-cresol with iso-propanol to yield isopropyl-3-tolylether (reaction (a) in Figure 2-2) and dehydration of iso-propanol to yield propene (reaction (b)). Rapid internal rearrangement and transalkylation of the ether with *m*-cresol, resulted in the formation of thymol, 2-isopropyl-3-methyl-phenol and 4-isopropyl-3-methyl-phenol. While the propene formed in reaction (b), almost exclusively alkylated the C-position on the *m*-cresol molecule (C-alkylation / reaction (d)) to form thymol, subsequent conversion to 5-isopropyl-3-methyl-phenol (the thermodynamically favoured isomer) via a 1,2 shift isomerisation reaction (reaction (e)) and further alkylation of the mono-isopropylated products occurred with a second propene molecule (reaction (f)).

The increase in thymol selectivity with decreasing space velocity / increasing *m*-cresol conversion and reaction temperature was attributed to the reaction system's preference for the C-alkylation reaction pathway as opposed to O-alkylation under these conditions. This preference stems from the differences in activation energy for the various reaction routes with the energy barrier for the C-alkylation pathway being the higher of the two routes.

At higher *m*-cresol conversions, i.e. conversions obtained with decreasing space velocity and/or increasing reaction temperature, the selectivity toward the kinetically favoured thymol position isomers (thymol, 2- and 4-isopropyl-3-methyl-phenol) proceeded to pass over a maximum.

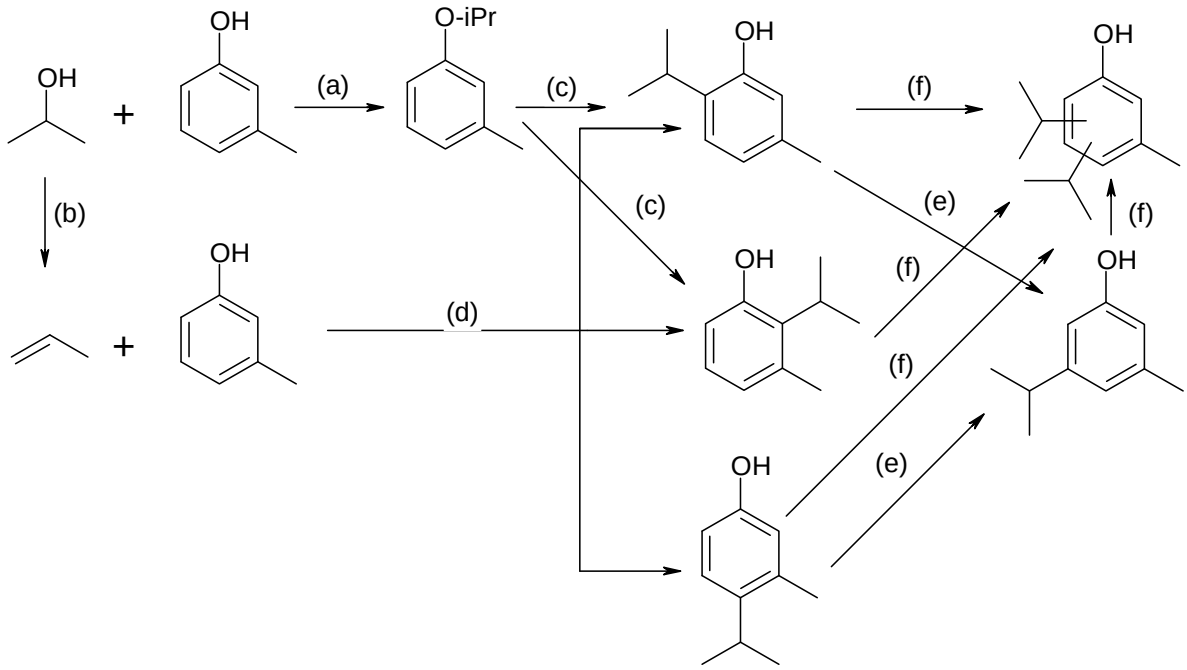

Figure 2-2: Proposed reaction mechanism for isopropylation of m-cresol with iso-propanol over H-MFI zeolites (Nagooroo, 2012).

Results from this study also suggested that the reaction was most likely first order with respect to propene and zero order with respect to *m*-cresol at reaction temperatures of interest to this study. Analogously, the reaction system with methanol and phenol over H-ZSM-5 (at 200℃ and low phenol conversion), showed reaction orders; first and- zero with regard to methanol and phenol, respectively. This result was attributed to capillary condensation which caused a high excess of phenol (constant phenol concentration) in close proximity to the acid sites, irrespective of the phenol concentration in the gas phase (Marczewski *et al.,* 1996).

2.6 Influence of thermodynamic equilibrium in thymol synthesis

2.6.1 *m*-Cresol conversion limitation during thymol synthesis

In the aforementioned research involving H-MFI mediated *m*-cresol alkylation with propene (Fletcher *et al.* 2001b; Fletcher *et al.,* 2003; O' Connor *et al.*, 2003), *m*-cresol conversion and, consequently, thymol yield (Figure 2-3) was found to be inhibited in the higher temperature range (above 250℃) investigated. This finding was attributed to the effect of thermodynamic limitations.

As shown by the upper edge of the data array in Figure 2-3 (obtained at the lowermost space velocity employed), thymol yield increased with temperature in the lower temperature range (temperatures below 250℃- right branch of the data series). With a further increase in temperature (left branch of the series), the decline in thymol yield was interpreted as an indication of thermodynamic limitations (depicted by the dashed line).

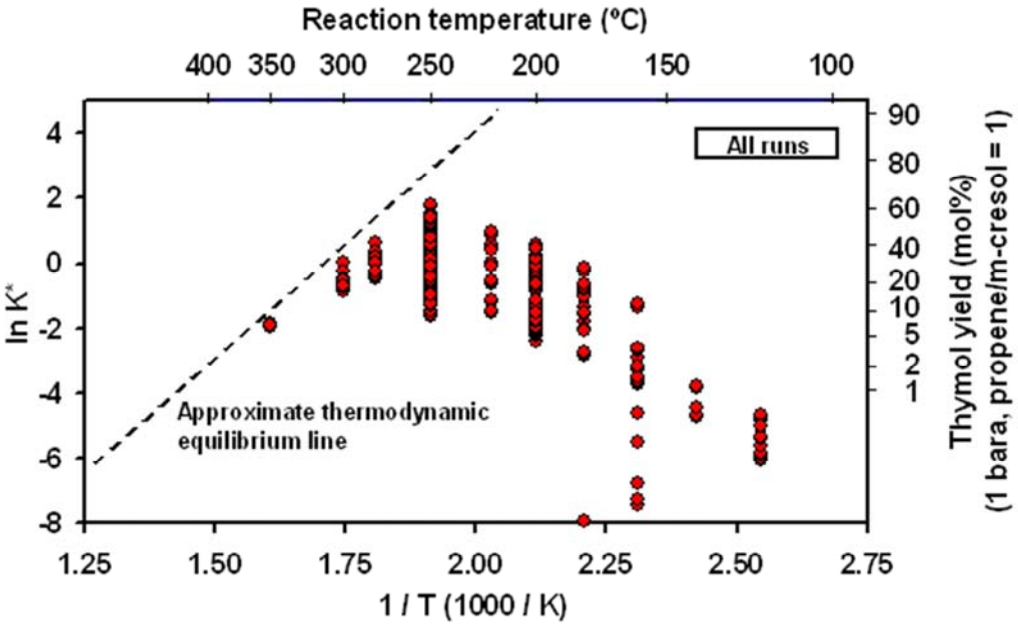

Figure 2-3: Experimental estimation of thermodynamic equilibrium approach for an H-ZSM-5 mediated m-cresol/propene alkylation reaction (Fletcher *et al*., 2001b).

2.6.2 Equilibrium distribution of thymol position isomers

Fletcher *et al.* (2002) investigated the thermodynamic equilibrium distribution of the thymol position isomers in reactions mediated by H-ZSM-5 over a range of reaction temperatures. The results of this investigation are shown in Figure 2-4 note that the fraction of the 2-isopropyl-3-methyl-phenol isomer, although present in the final product, was negligible which allowed representation of the results in the form of a ternary diagram. For the purposes of the investigation, two different feed mixtures were employed in separate experiments. These feed mixtures are represented by the white circles in the middle of the bottom- and right edge of the aforementioned ternary diagram, respectively.

In spite of the differences in feed compositions, the resultant product distributions converged toward the region comprising mostly 5-isopropyl-3-methyl-phenol, some thymol and a small amount of 4-isopropyl-3-methyl-phenol with traces of 2-isopropyl-3-methyl-phenol. The approximate equilibrium distribution of the three position isomers in the temperature range of 200 - 300℃ was estimated from the experimental results to be approximately 75% 5-isopropyl-3-methyl-phenol, 20% thymol and 5% 4-isopropyl-3-methyl-phenol.

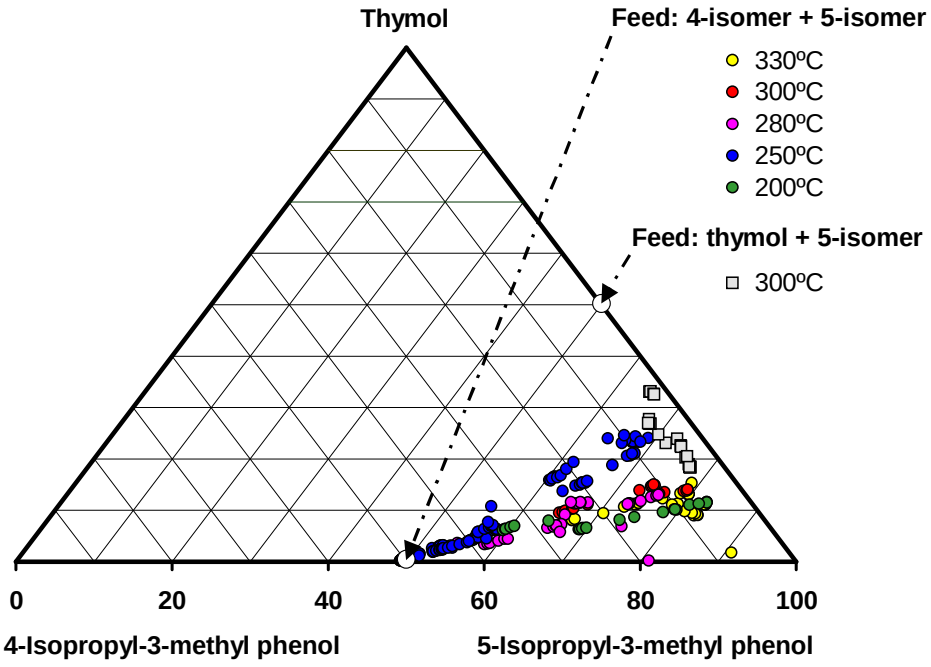

Figure 2-4: Isomerisation of thymol and its major position isomers over H-ZSM-5 (Fletcher *et al*., 2002).

These results can be attributed to the mesomeric effect, by which the lone electron pairs of the oxygen atom of the *m*-cresol hydroxyl group are delocalised into the aromatic nucleus via π orbitals, thus activating *m*-cresol in the para- and ortho positions (with respect to the hydroxyl group) for electrophilic attack by a carbenium ion (Sykes, 1986).

The electrophilic attack of the secondary carbenium (propyl) ion (see the reaction mechanism schematic in Section 2.9) on 3-methyl-phenol in the 2-position and the 4-position, resulting in the formation of 2-isopropyl-3-methyl-phenol and 4-isopropyl-5-methyl-phenol, respectively, is more sterically hindered than the attack of the secondary carbenium ion in the 6-position resulting in the formation of thymol (2-isopropyl-5-methyl-phenol). Hence, thymol is the kinetically favoured isomer of *m*-cresol isopropylation. The miniscule content of 2-isopropyl-3-methyl-phenol in the final product compared to the other thymol position isomers was attributed to the fact that it's the most sterically hindered isomer of the four (Fletcher *et al.*, 2002).

3-Isopropyl-5-methylphenol is the thermodynamically favoured isomer as it has higher stability compared to the other isomers. This increased stability arises from the fact that the inductive effect of the propyl and methyl groups in the meta-positions does not prevent delocalisation of the lone pair electrons on the hydroxyl group into the aromatic system to the same extent as would be the case for these substituents in the para and ortho-positions.

2.6.3 Thermodynamic equilibrium for iso-propanol dehydration

Nagooroo (2012) simulated the thermodynamic equilibrium for the dehydration of iso-propanol to form water and propene. The results of this simulation are shown in Figure 2-5.

The Aspen Plus User Interface, Aspen Technology, Inc. (2006) software package was employed for the simulation under conditions of 200 - 300℃ and 1.5 - 10 bar.

A significant thermodynamic driving force for the dehydration of iso-propanol was revealed by the extent of the iso-propanol equilibrium conversion over the range of conditions explored.

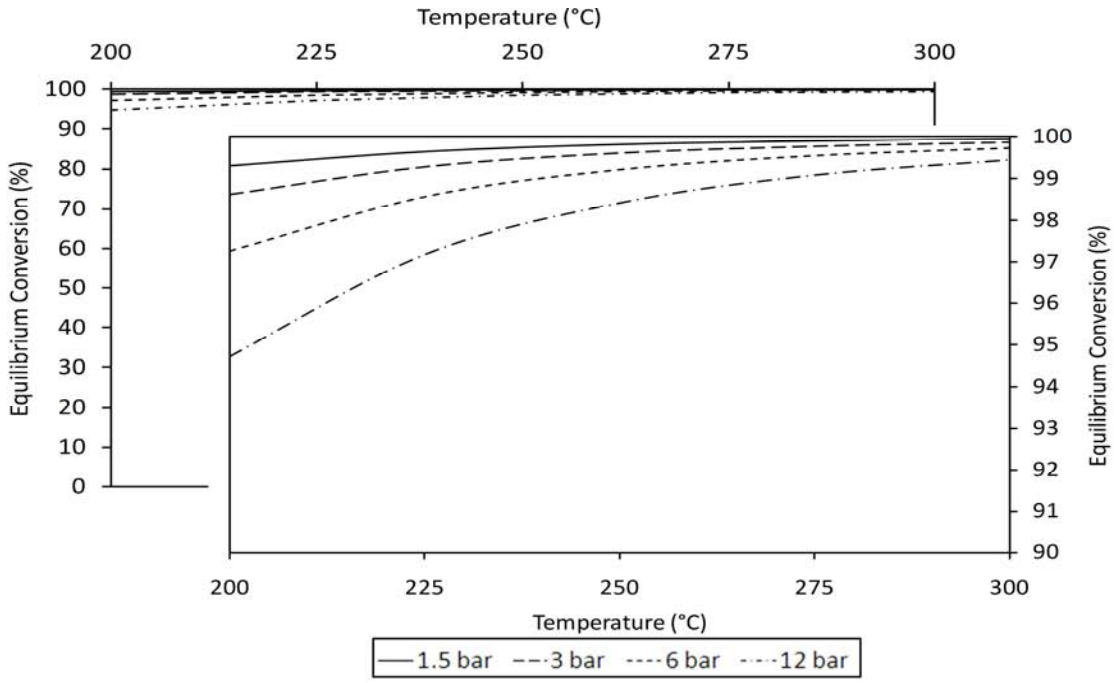

Figure 2-5: Equilibrium conversion of iso-propanol to water and propene (Nagooroo, 2012).

2.7 Preliminary experimental results

Preliminary experiments were carried out by Mathews and Tsui (2007), co-supervised by the author of this study, in an attempt to identify suitable conditions for the thymol synthesis reaction with iso-propanol and *m*-cresol. The experimental results are displayed in Figure 2-6.

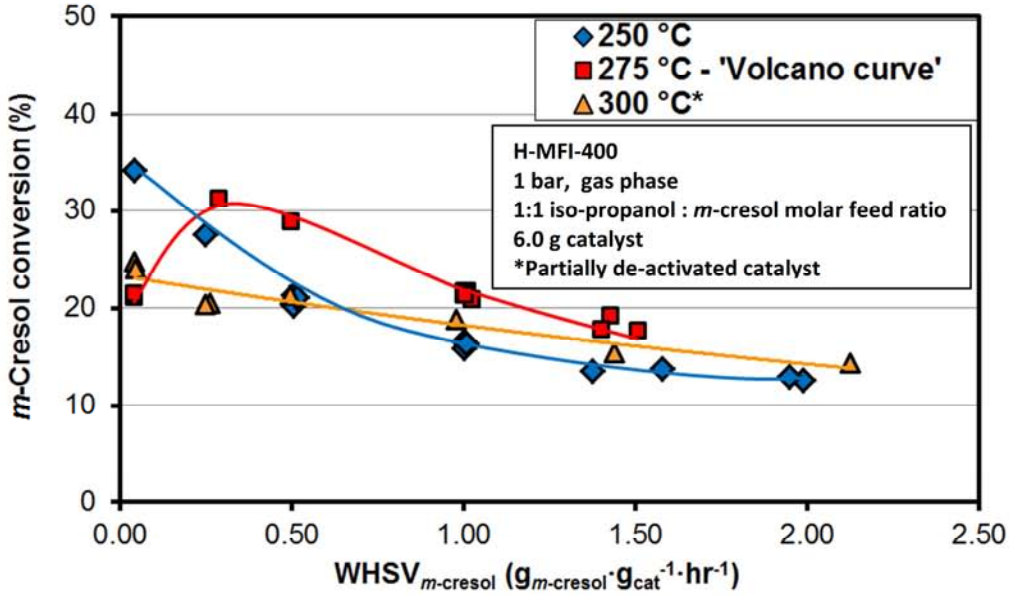

Figure 2-6: *m*-Cresol conversion vs. space velocity obtained during preliminary experiment (Mathews and Tsui, 2007).

It should be noted that the results corresponding to 300 ℃ were obtained over a catalyst that had suffered appreciable deactivation. Hence, the level of activity observed is somewhat lower than that corresponding to 275 ℃.

In contrast to the trends observed for 250 and 300 ℃, the trend shown at 275 ℃ (viewed in the direction of decreasing space velocity) showed conversion to first increase and then, counter-intuitively to pass over a maximum and subsequently decline at the lower most space velocities, thereby forming a so-called “volcano curve” with respect to space velocity.

The authors concluded that this decline in *m*-cresol conversion at low space velocity was due to significant catalyst deactivation and, therefore, did not investigate this apparent anomaly further. However, no explanation was offered for the corresponding decrease in thymol selectivity with decreasing space velocity. Should catalyst deactivation have been the sole cause of the observed decline in *m*-cresol conversion, one would have expected a different trend in thymol selectivity. Consequently, a re-investigation of this anomaly was considered necessary to gain further insight into the reaction pathway for thymol synthesis from *m*-cresol and iso-propanol.

2.8 Equilibrium limitations in phenolic conversions

The findings of the previous studies related to thymol synthesis along with the preliminary results of this study allude to the complexity of the system with respect to reaction pathway. These findings also suggest that thermodynamic limitations might be responsible for the peculiar *m*-cresol conversion trend at low space velocity (Figure 2-6).

The absence of measured thymol thermodynamic data frustrated attempts to conduct a full thermodynamic analysis of the reaction system. Therefore the influence of the thermodynamic equilibria is sought by comparison to experimental findings of analogous systems in which phenolic rings/substituted phenolic rings are alkylated with alcohols/olefins or are converted via transalkylation reactions with xylenols.

2.8.1 Isomerisation of cresol

In the acid catalysed isomerisation of cresols (Böhringer, 2009) the major reaction, initially, was the 1,2-shift migration of the methyl group around the ring. Side reactions such as disproportionation, i.e. the transalkylation of a methyl group to form a phenol and a xylenol molecule were comparatively slow with total selectivity of less than 5%. However, when approaching the thermodynamic equilibrium distribution of the cresol isomer and, in particular, after reaching the thermodynamic equilibrium, the isomerisation reactions effectively came to a halt. Consequently, the former side reactions dominated the reaction system, consuming the cresols. Evidence of this was seen in the steep increase of transalkylation product yields and selectivities in addition to a decline of cresol isomer yields and selectivities once equilibrium conversion of the feed cresol isomer was reached.

2.8.2 Transalkylation between phenol and xylenol

Similar limitations to those observed for cresol isomerisation (Section 2.8.1), were observed in the transalkylation of xylenols with phenol (Moeketsi, 2007). The major initial reaction in this system was that of methyl group transfer from xylenol to phenol molecules resulting in cresol formation and, consequently, increasing phenol conversion with decreasing space velocity. However, at very low space velocities, the phenol conversion decreased with decreasing space velocity. In the resultant product mixture, increasing percentages of higher methylated phenols (tri-methyl, tetra-methyl and penta-methyl phenol) were observed, with decreasing space velocities in particular, once the xylenol / phenol / cresol system approached thermodynamic equilibrium. These higher methylated phenols were formed via secondary and tertiary reactions by, for instance, the transfer of methyl groups from the primary cresol product onto remaining xylenol molecules, thereby re-forming phenol, such that the net phenol conversion decreased with decreasing space velocity in the said low space velocity regime.

2.8.3 Alkylation of phenol with iso-propanol

Phenol alkylation with iso-propanol catalysed by zeolite $H_{0.85}Na_{0.15}Y$ with a SiO_2:Al_2O_3 ratio of 4.5 has been reported (Areshidze et al., 1974). All experiments were conducted in the vapour phase at atmospheric pressure and with a phenol-to-alcohol molar ratio of 1:1. Phenol conversion decreased with increasing temperature in the range 270 to 300℃ (at a LHSV of 0.4 hr^{-1}), i.e. a maximum phenol conversion was achieved at 270℃ .

2.9 Reaction mechanism for *m*-cresol isopropylation

Figure 2-7 shows the acid catalysed reaction scheme in which iso-propanol alkylates *m*-cresol to form thymol over a zeolite catalyst. Iso-propanol is dehydrated to form a secondary carbenium ion which attacks *m*-cresol in the least sterically hindered ortho-position. Finally, a proton is extracted from the thymol intermediate to form thymol.

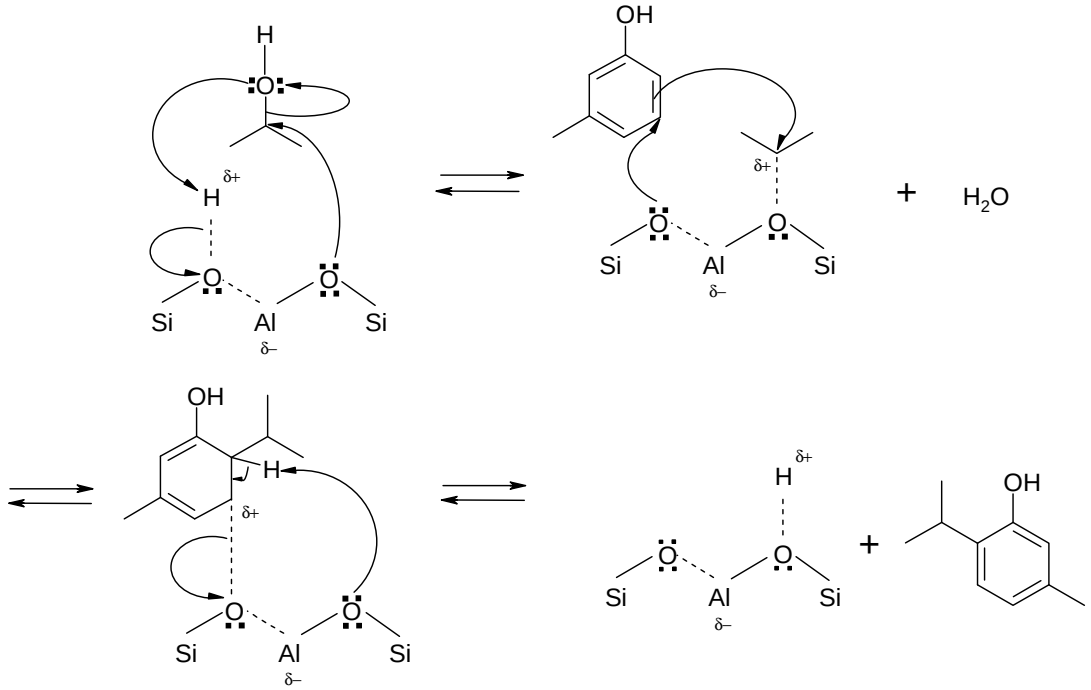

Figure 2-7: Reaction mechanism for the acid catalysed iso-propylation of *m*-cresol with iso-propanol.

2.10 Acid Catalysed Propylation of Aromatic Compounds

Other than the studies mentioned thus far (Fletcher *et al*., 2003; O'Connor *et al*., 2003; Nagooroo, 2012), literature which alludes to the specific reaction system and mechanism responsible for the seeming anomaly observed by Mathews and Tsui (2007) (discussed earlier in Section 2.7) was not found for the specific reaction system. Therefore, what follows below explores analogous reaction systems, such as the acid catalysed alkylation of phenols and other aromatic compounds with iso-propanol and isopropylating agents carrying halides as leaving groups (over Friedel-Crafts type catalysts, mineral acids, zeolites and various forms of alumina).

In the analogies considered, some as early as 1891 (Heise, 1891), phenolic and aromatic substrates were mainly mono-, di- and tri-isopropylated (Heise, 1891; Sowa *et al.*, 1935; Calcott *et al.*, 1939; Stroh *et al.,* 1957; Turova-Pollak *et al*., 1960; Gakh *et al.,* 1966; Korenskii *et al*., 1968; Klemm and Taylor, 1980a; Klemm and Taylor, 1980b; Pillai and Pillai, 1993; Wichterlová and Čejka, 1993; Pillai, 1996). The extent, to which the multi-propylated compounds formed, depended on the shape selective constraints offered by the respective catalysts employed.

Oligomerisation of the propene (formed by dehydration of iso-propanol) and subsequent oligomer cracking resulting in an olefin pool, was observed in reactions involving conversion of iso-propanol and toluene over H-Mordenite and H-Y (Wichterlová and Čejka, 1993).

Both S_N1 and S_N2 reaction mechanisms were observed in these studies. No charge migration for either of these respective reaction mechanism types was reported along the backbone of the carbenium ion or skeletal isomerisation of the alkyl group residing on the ring, under relatively mild reaction conditions.

Formation of n-propylated substrates was only observed at higher temperatures and n-propyl to iso-propyl ratios increased with increasing temperature in reaction systems catalysed by alumina (above 300ºC) (Klemm and Taylor, 1980b) and with H-Mordenite and H-Y (Wichterlová and Čejka, 1993). Klemm and Taylor (1980b) attributed this to subsiding relative differences in stabilisation energy between the primary and secondary carbenium ions (formed during an S_N1 type reaction mechanism) with increasing temperature.

3 Objectives of study

3.1 Aim of the study

It will be endeavoured to identify an operating window in which optimal thymol yield can be achieved.

3.2 Special study objectives

In addressing the study's aim, the following objectives have been set:

- To establish whether *m*-cresol conversion and consequently thymol yield are thermodynamically constrained at elevated temperatures.
- Establishing to what extent the reaction route diverges when thermodynamic limits are approached.

3.3 Hypothesis

In light of the findings of the literature review, the author hypothesizes as follows:

The reason for the counter intuitive decline in *m*-cresol conversion with decreasing space velocity (seen in the "volcano curve" presented in Section 2.7) is the increase in ratio of the average carbon number of the cresylic-ring- substituents to actual cresylic rings as residence time in the reactor increases. Therefore the system becomes irreversibly depleted of iso-propylation agent. This occurs amid a considerable thermodynamic driving force for the said reaction.

3.4 Key questions

The following questions need to be addressed which have arisen from the review of literature:

- Will iso-propanol dehydrate completely under the reaction conditions employed?
- Will differences in thymol selectivities emanate from differences in reaction pathways and mechanisms?
- Will the isopropyl alkylating agents dehydrate rapidly to propene which in turn alkylates the phenolic ring?
- Is the *m*-cresol conversion to thymol thermodynamically limited at elevated temperatures?

4 Experimental

4.1 Catalysts

Both acid zeolite catalysts of the MFI (ZSM-5) type employed were obtained from Clariant (formerly Süd-Chemie) and are commercially available. The properties of these catalysts are given in Table 4-1.

Table 4-1: H-MFI catalysts tested and their properties

Sample Code	Material Form	Size	SiO_2/Al_2O_3 Molar Ratio*	Channel Size (Å)**	Channel Shape**
H-MFI-90	Extrudates***	1/16"	90	5.1 x 5.5 5.3 x 5.6	Sinusoidal Straight
H-MFI-400	Extrudates***	1/16"	400		

* As reported by manufacturer (general product designation/sample code)
** Baerlocher *et al.,* 2001
*** With alumina binder comprising 20% of extrudate mass (Fletcher et al., 2003)

4.2 Feed stocks and other materials used

The feedstocks and other chemicals employed in this study (presented in Table 4-2) were of commercially available quality and were used without further purification.

Table 4-2: Feedstocks and auxiliary chemicals used and their properties

Material/chemical	Purity (%)*	Manufacturer	Use
m-Cresol	>99	Riedel-de Haën	Feedstock
iso-Propanol	>99.9	Merck	Feedstock
Di-isopropylether	>99.9%	Riedel-de Haën	Feedstock
Nitrogen	>99.999	Messer Fedgas	Catalyst drying, activation and pressurisation of system
Hydrogen	>99.999	Messer Fedgas	To pressurise for leak testing
Silicon carbide (930-1035 µm)	--	Colbern	Packing in the preheater/evaporator zone of the reactor, diluent in the catalyst bed and as support packing

* Purity as reported by industrial manufacturer

GC analyses of the *m*-cresol feedstock showed that it contained small amounts of the position isomers of which *p*-cresol comprised the largest portion (Table 4-3).

Table 4-3: Impurities in the *m*-cresol feedstock

Component	Abundance (mol-%)
m-Cresol	99.3
p-Cresol	0.6
o-Cresol	0.1

4.3 Experimental apparatus

The same catalyst testing equipment and procedures as employed by Nagooroo (2012) was used for the thymol synthesis experiments conducted in this study. A schematic layout of this test unit as employed for thymol synthesis reactions is provided in Figure 4-1. This test unit was adapted for on-line gas chromatography for use in the dehydration experiments and is shown schematically in Figure 4-2.

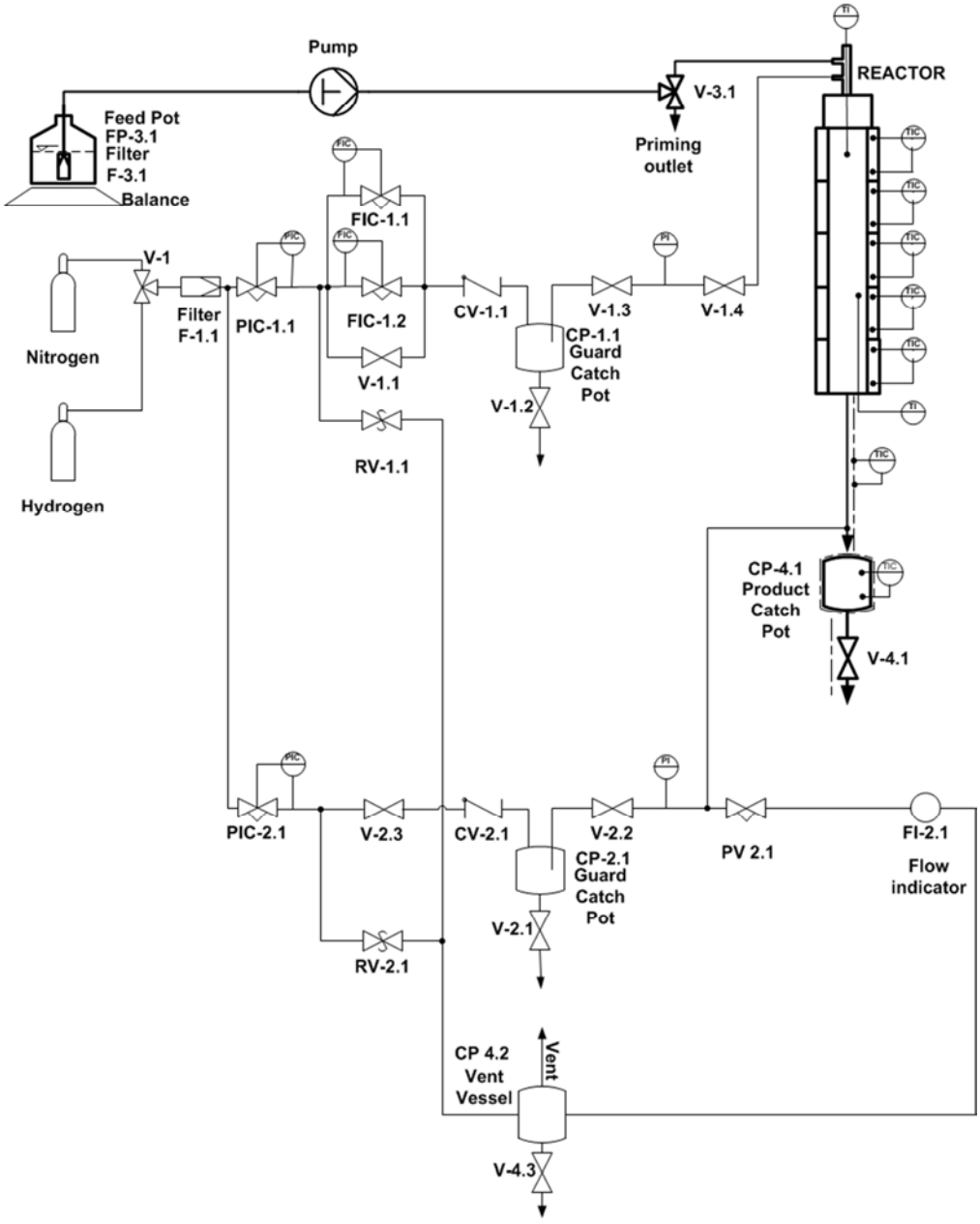

Figure 4-1: Schematic of the experimental apparatus employed to conduct the "thymol synthesis" experiments at ambient and elevated pressure.

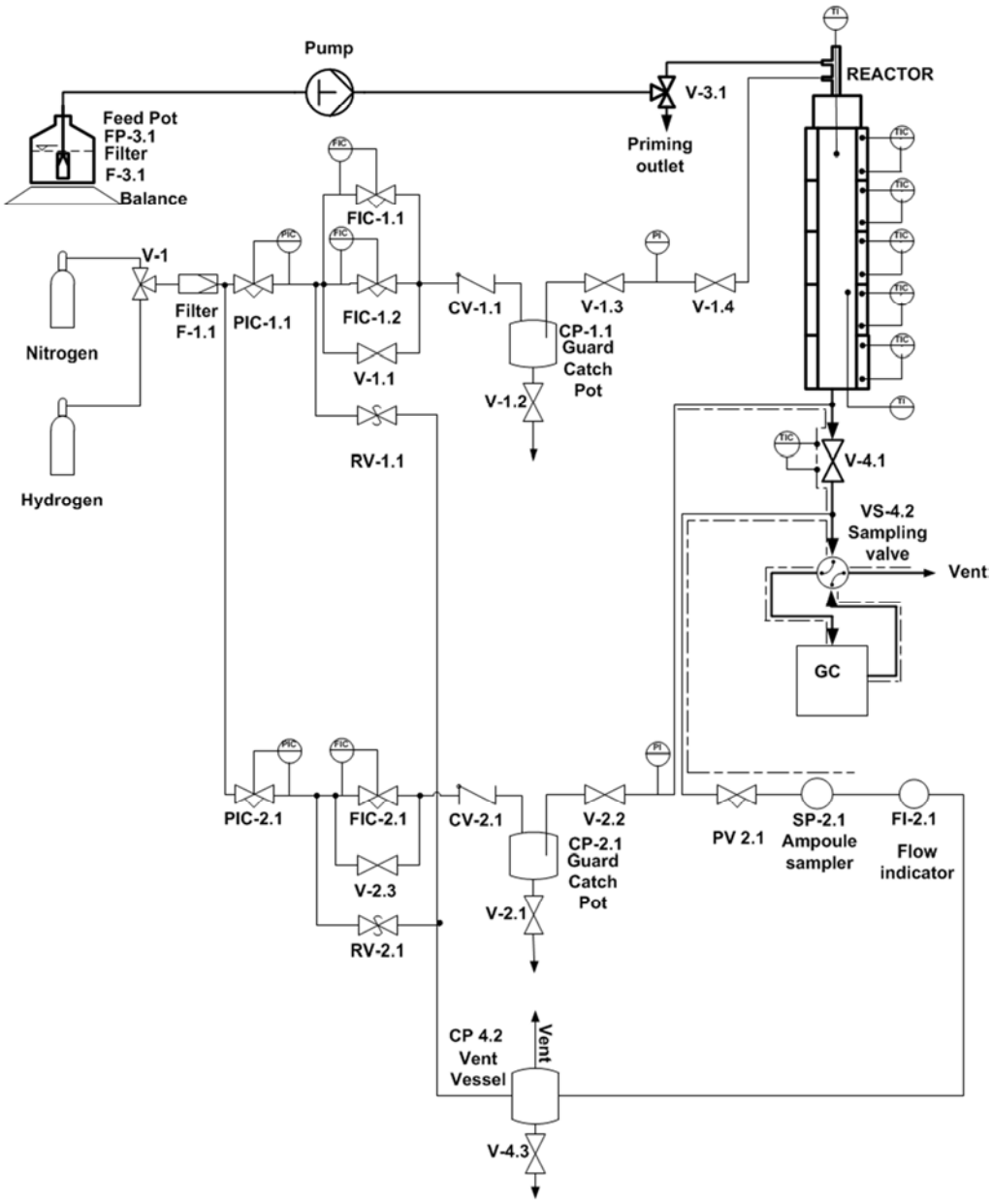

Figure 4-2: Schematic of the modified experimental apparatus employed to conduct the dehydration experiments at ambient pressure.

4.3.1 Reactor and reactor heating systems

Reactions were carried out in a bench scale, tubular fixed bed plug flow reactor. The reactor consisted of a 316L grade stainless steel reactor tube with an external and internal diameter and length of 19 mm, 16 mm and 730 mm respectively. It was equipped with a central thermo-well with an internal diameter of 1.7 mm allowing a thermocouple (with an external diameter of 1.6mm) to measure the bed temperature along the length of the reactor inside this thermo well. The reactor was held in a brass heating block (650 x 60 x 60 mm) of adequate “thermal mass” to facilitate isothermal reactor conditions.

Heating bands (each equipped with a thermocouple) supplied heat to the reactor indirectly via the heating block. For details on the maintenance of isothermal reactor conditions, see Section 4.4.10.

A schematic of the reactor system is depicted in Figure 4-3., showing four distinct zones inside the reactor. Silicon carbide (SiC) is employed as inert packing material in the preheater or evaporator zone (in the reactor's uppermost section). A temperature gradient is established (refer to Section 4.4.10 for details), such that the point of initial contact between the liquid feed and SiC packing is maintained below the liquid's boiling point. The temperature reading at the inlet was provided by a stationary thermocouple.

The catalyst bed was diluted with SiC and resided in the isothermal region of the system (sandwiched between the inert packing layers). In later experiments, this bed consisted of two zones instead of one. A higher SiC-to-catalyst dilution ratio was employed in zone X as compared to zone Y (refer to Section 4.4.10 for details).

The temperature profile along the length of the reactor was obtained with a thermocouple by insertion into the central thermo-well. Futhermore, the heating-system was insulated from its surroundings to minimise heat loss.

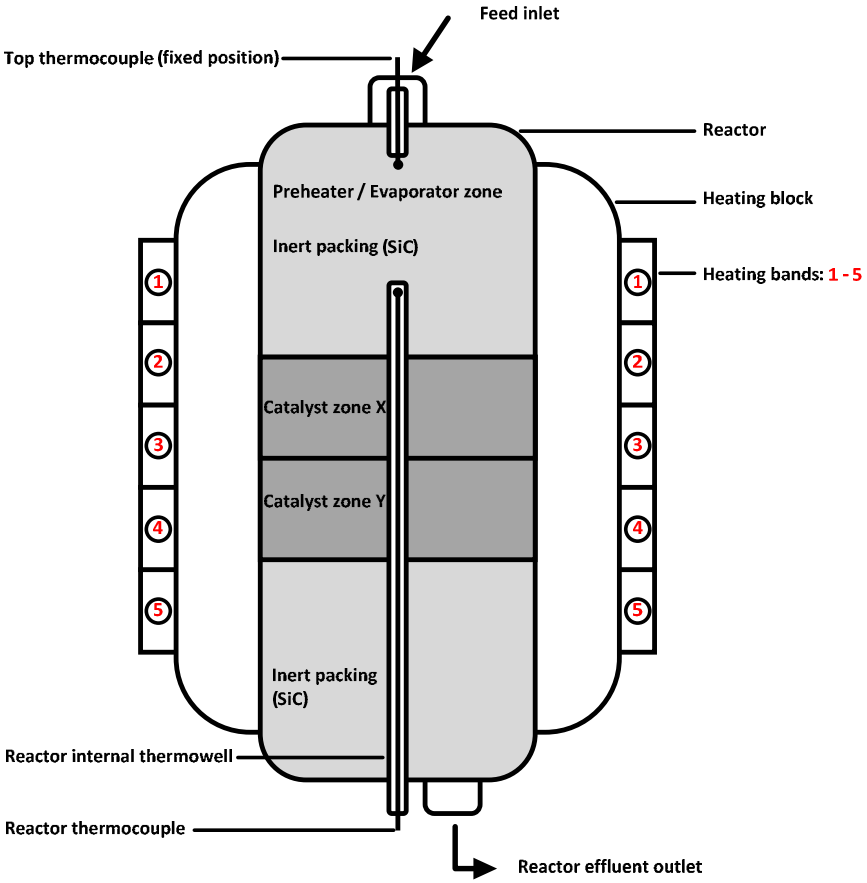

Figure 4-3: Diagrammatic representation of the reactor system.

4.3.2 Liquid feed delivery

m-Cresol and the respective alkylating agents were charged to the feed pot, a 5 L glass bottle (device FP-3.1 in Figure 4-2) and mixed. The feed pot was placed on a balance from which readings were taken periodically to check the feed mass flow rate to the system and to confirm accurate operation of the feed pump.

The feed was pumped to the reactor by a metering pump (HPLC pump, Series I, marketed by Lab Alliance -) which had a flow range of 0.01 to 10 ml/min and could be adjusted in increments of 0.01 ml/min.

4.3.3 Gas supplies

Gaseous nitrogen and hydrogen was obtained from the reticulated gas supply system at 80 bar and 60 bar respectively. These gasses were employed to inertise the experimental apparatus, conduct pressure testing, as carrier and diluent gas, and for reaction pressure control.

Pressure regulators (PIC-1.1 and PIC-2.1 in Figure 4-2) were used along with bypass valves (V-1.1 and V-2.3 in Figure 4-2) for pressure testing of the various sections of the experimental apparatus. Nitrogen was employed for the first round of pressure tests and subsequently hydrogen for the latter.

Furthermore, nitrogen was metered with mass flow controllers (FIC-1.1 and FIC-1.2 in Figure 4-2) for pre-experimental inertisation of testing apparatus catalyst pre-treatment / drying, feed dilution and post experimental flushing. FIC-1.2 was employed for low flow rates and FIC-1.1 for the higher range. Adequate nitrogen flow rate was established with FIC-2.1 for reactor effluent dilution.

Guard catchpots (CP-1.1 and CP-2.1 in Figure 4-2) were checked daily for liquid which would have indicated system blockages.

4.3.4 Pressure control

Pressure control was established and maintained with the use of nitrogen gas which was introduced as a back pressure regulating gas, downstream from the reactor effluent port and before throttle valve PV-2.1 (Figure 4-1).

The reaction pressure was set by adjustment of pressure regulator PIC-2.1 and opening valve V-2.3. Throttle valve PV-2.1 (equipped with a regulating stem) was set

such that the volumetric flow rate of the gas stream being vented through PV-2.1 was slightly higher than that of reactor effluent and diluent gasses (olefin and water vapours) from the reactor system. For this purpose, a flow indication device was fitted after PV-2.1.

4.3.5 Sampling

4.3.5.1 Thymol product sampling (for off-line analysis)

Unconverted feed and product was captured in sample catchpot CP-4.1 (see Figure 4-1). The product line to CP-4.1 and the catchpot itself were heated to 45℃ to prevent the solidification of the higher phenolic derivatives present in the product stream.

After exiting the reactor, the effluent stream was air cooled and partially condensed. The condensed fraction contained all of the phenolic compounds.

The sample catchpot also served to separate the gaseous fraction in the reactor effluent from the liquid. The catchpot had two outlets namely: a constantly open outlet for the gasses at the top and a drain outlet for the liquid at the bottom (valve V-4.1).

The effluent gasses and the pressure control gas (Section 4.3.4) were expelled through the throttle valve, PV-2.1, to the vent vessel from where these gasses were vented.

Liquid samples were withdrawn from the sample catchpot through valve V-4.1 for off-line analysis. For sampling, valve V-4.1 was opened only slightly in order to prevent a pressure drop in the system although care was also taken to drain all the liquid out of the catchpot. The guard catchpots were checked daily for liquid (which would have indicated a blockage in the system).

4.3.5.2 Iso-propanol dehydration product sampling (for on-line analysis)

To ensure analysis of the complete reaction product as a gaseous reactor effluent, lines and components between the reactor and GC were heated to 120℃. In addition, nitrogen (at a 50:1 volume ratio with respect to reactor effluent gasses) was introduced as a diluent gas.

Post dilution, the reactor effluent was split into two streams; the Gas Chromatograph (GC) feed line and the vent line. Throttle valve PV-2.1 was used to establish the flow of the respective streams. In this mode, PV-2.1 served as a flow control valve instead of a pressure control valve as all the dehydration experiments were conducted at ambient pressure.

In the normal position, the stream to sampling valve VS-4.2 passed through a sample loop present in the valve and thereafter flowed to the vent. In order to analyse this stream with the GC, VS-4.2 was switched so as to allow the carrier gas of the GC to entrain the sample present in the sample loop. After 10 seconds of flushing the sample loop, VS-4.2 was switched back to the normal position.

4.3.5.3 Iso-propanol dehydration product sampling (for off-line analysis)

The following procedure describes the process by which samples were extracted from the system for offline analysis (Schulz *et al*., 1984). Evacuated glass ampoules (with approximately 1.5 ml internal volume) equipped with a capillary extending from one end (ca. length: 100 mm, outer diameter: 1 mm), were used to encapsulate these samples.

During sampling, the capillary side was inserted through the ampoule sampler (SP-2.1) septum and its tip broken off so as to drain a sample into the ampoule. Subsequently the capillary was sealed using a butane torch.

4.4 Procedures

The following gives a brief description of the procedures followed operating the experimental test unit. A more detailed description was given by Nagooroo (2012).

4.4.1 Loading of the reactor

Table 4-4 provides the details of catalyst charges with which the reactor was loaded for the respective experiments conducted in this study.

Table 4-4: Details of catalyst charges

Catalyst type	Shape	Catalyst amount (g)	Zeolite amount (g)[a]	Diluted with SiC (vol/vol)[b]	Total volume (mL)	Length of Cat bed (mm)[c]	Feed[h]
H-MFI-400[d]	Extrudates[e]	6.0	4.8	1:1	18.7	100	iso-propanol/ *m*-cresol
H-MFI-90	Extrudates[e]	5.8	4.7	1:1	18.7	100	di-isopropylether/ *m*-cresol
H-MFI-90	Extrudates[e]	13.8	11.0	1:1	44.9	240	iso-propanol/ nitrogen
H-MFI-90	Extrudates[e]	5.87	4.70	1:1	18.7	100	iso-propanol/ *m*-cresol
H-MFI-90	Extrudates[e]	13.42	10.73	1:1	42.1	225	di-isopropylether/ nitrogen
H-MFI-90	Extrudates[e]	17.8[f]	14.26	1:5[f]	70.5	377	iso-propanol/ *m*-cresol

[a] Assuming 20 wt% binder (Fletcher *et al*., 2003)
[b] Size range: 930-1035 µm
[c] Internal diameter of reactor tube - 15.75mm
[d] Results from preliminary experiments (Mathews and Tsui, 2007).
[e] Diameter: 1/16"
[f] Mass contained in zone x - 30% , mass contained in zone y - 70%
[g] Dilution ratio for zone x given, dilution ratio in zone y, 1:1
[h] Refer to Table 4-5 for feed composition

4.4.2 Pressure testing

The experimental test unit was pressurised to 16 bar N_2 (excluding the product line to the online GC for the iso-propanol dehydration experiments). The isolation of the experimental apparatus was achieved by closing valves PV-2.1 (thymol synthesis apparatus, see Figure 4-1) and V-4.1 (iso-propanol dehydration version, see Figure 4-2). The respective sections of the apparatus (each section equipped with a pressure gauge) were isolated from the rest of the test unit, by closing valves V-1.3, V-2.2 and V-3.1. Thereafter, V-1.1 was opened (thereby bypassing mass flow controllers FIC-1.1 and FIC-1.2) and the pressure was slowly increased by manipulation of pressure regulator PIC-1.1. For the thymol synthesis experiments, pressure was increased using PIC-2.1 in addition to PIC-1.1. Care was taken not to unsettle the catalyst bed with excessively high upward gas flows when PIC-2.1 was used. The system was isolated from the N_2 gas supply and monitored for leaks.

For small leaks and when the system was found to be leak tight with N_2, the system was repressurised with H_2. A thermal conductivity gas leak detector was used to locate leaks at the connection points. Leaky fittings were tightened and retested. Once all connections were examined, H_2 supply was shut off by closing valve V-1. The pressure of the apparatus was monitored over a 4 hour period and at the end of this period, if no pressure decrease occurred, the apparatus was deemed leak tight. The apparatus was depressurised, H_2 was vented from the system, the N_2 supply was opened (valve V-1) and the catalyst drying-and-activation sequence was initiated.

4.4.3 Catalyst drying and activation

Prior to the introduction of feed, the catalyst was dried and freed from adsorbed materials by passing N_2 over the catalyst bed. This was carried out at atmospheric pressure and a flow rate of 50 $ml \cdot min^{-1}$, metered by mass flow controller FIC-1.1. While drying, product catch pot valve V-4.1 was opened and a container was placed under it to capture any residual liquid from previous experiments. With the iso-propanol dehydration experiments, throttle valve PV-2.1 was opened fully so as to allow the N_2 stream along with the entrained materials to pass directly into the vent vessel instead of flowing through the GC supply lines.

The temperature sequence employed during drying and activation of the catalyst is shown in *Appendix I* (Figure I-1). Heating occurred at a rate of 1℃/min. The sequence entailed heating the bed up to 90℃, 100℃ and 110℃, respectively, and pausing for an hour at each of these temperatures in order to slowly remove absorbed moisture. Thereafter the temperature was elevated to 390℃ and maintained for 6 hours before cooling the bed down to standard reaction temperature (e.g. 250℃).

4.4.4 Start-up procedure: thymol synthesis experiments

After the catalyst drying and activation sequence was completed, the following procedure was followed to commence with catalyst testing:

1. The controller setpoints of the respective heating zones were adjusted to the values determined with nitrogen flow during the commissioning phase of the experimental apparatus (see *0*, Table B-1).
2. Nitrogen supply to the reactor was stopped by setting the flow through MFC-1.1 to zero and thereafter closing valve V-1.4 and shutting off the nitrogen supply with pressure regulator PIC-1.1.
3. Valve V-4.1 was closed.
4. The moveable thermocouple was positioned at the top end of the catalyst bed.
5. The apparatus was primed with liquid feed. For this purpose, the liquid feed pump was run at maximum flow rate (“prime” mode) whilst observing the temperature at the top end of the catalyst bed.
6. As soon as a sharp increase in the catalyst bed temperature was observed, the pump rate was adjusted to the “standard condition” flow rate (shown in Table 4-5).
7. The mass shown on the feed pot balance display was recorded and a stop watch was started to record time-on-stream.
8. Once the catalyst bed temperature had reached steady state, a temperature profile was measured.
9. The set points of the controllers were adjusted such that the closest approach to an isothermal zone was attained over the catalyst bed (see Section 4.4.10 for this procedure). The temperature profile was continuously monitored and adjustments were made to counteract the effects of changes in reaction conditions and catalytic activity due to, for instance, catalyst deactivation.

4.4.5 Start-up procedure: iso-propanol dehydration experiments

1. The controller setpoints to the respective heating zones were adjusted to the set points as determined with nitrogen flow during the commissioning phase of the experimental apparatus (see *0*, Table B-1).
2. Nitrogen supply to the reactor was set (to a flow rate that corresponded to a 1:1 molar ratio with respect to the intended iso-propanol flow rate, using mass flow controllers FIC-1.1 or FIC-1.2 (depending on the required flow rate as FIC-1.1 controlled accurately in the range 20 $ml \cdot min^{-1}$ – 480 ml/min and FIC-1.2 controlled accurately in the range 1 - 19 $ml \cdot min^{-1}$).
3. The nitrogen diluent gas flow rate was set 50 times higher (molar) than that of the nitrogen feed to the reactor using mass flow controller FIC-2.1.
4. Proceed as per steps: **4 – 9** in the previous start up procedure (Section 4.4.4).
10. The on-line sampling sequence was initiated (Section 1.1.1.1).
11. The off-line sampling sequence was initiated (Section 4.3.5.3).

4.4.6 Increasing system pressure: thymol synthesis experiments

The experimental apparatus was pressurised from ambient pressure (refer to Figure 4-1) as follows:

1. Pressure regulator PIC-2.1 was closed off.
2. Throttle valve PV-2.1 was opened.
3. Valve V-2.3 was opening slowly thereby venting all pressurised nitrogen from the back pressure gas supply line.
4. Throttle valve PV-2.1 was closed.
5. Pressure regulator PIC-2.1 was opened slightly so that there were no rapid pressure increases in the system.
6. Once the required pressure was reached, throttle valve PV-2.1 was set such that the volumetric flow rate of the gas stream being vented through PV-2.1, was slightly higher than that of product gasses (especially propene and water vapour) from the reactor system.

When pressure was increased from a pressure higher than ambient, it was done starting from point **4** in the above sequence.

4.4.7 Standard conditions employed for experiments

Table 4-5 presents the standard conditions at which experiments were initiated. Catalyst activity was allowed to reach quasi steady state, which usually was around 50 hrs. on stream, before conditions were altered. Product sample composition was monitored until constancy was reached, such that samples representative of the reaction conditions could be attained.

Table 4-5: Standard experimental conditions applied with the respective feeds

	Thymol synthesis with		Dehydration of	
	Iso-propanol	Di-isopropylether	Iso-propanol	Di-isopropylether
Temperature (℃)	250	250	250	250
Pressure (bar)	1	1	1	1
Phase	gaseous	gaseous	gaseous	gaseous
Isopropyl group:*m*-cresol ratio	1	1	-	-
Molar ratio to *m*-cresol	1:1	0.5:1	1:1	0.5:1
Feed partial pressures (bar)				
- *m*-Cresol	0.5	0.5	-	-
- alkylating agent	0.5	0.25	0.5	0.25
- Nitrogen	-	-	0.5	0.5
WHSV $(g_{m\text{-cresol}} \cdot g_{cat}^{-1} \cdot hr^{-1})$	1.03	1.03	-	-
WHSV$(g_{\text{alkylating agentl}} \cdot g_{cat}^{-1} \cdot hr^{-1})$	1.03	0.49	0.57	0.49

4.4.8 Shut-down procedure for thymol synthesis experiments

After completion of each set of experiments the following procedure was carried out:

1. The feed pump was switched
2. The temperature controllers were switched off
3. Valve V-4.1 was closed
4. The nitrogen pressure control gas supply to the apparatus was closed off.
5. In order to completely vent the system of nitrogen, regulating valve PV 2.1 was opened
6. Nitrogen flow to the top of the reactor was established by ensuring that valve V-1.1 was in the correct nitrogen-supply position. PIC-1.1 was adjusted to 5 bar. N_2 flow of 20 ml/min was set through mass flow controller FIC-1.2, closing bypass valve, V-1.2 and also opening valves V-1.3 and V-1.4.
7. The reactor was then allowed to cool overnight before being dismounted and unloaded.

4.4.9 Shut-down procedure dehydration experiments

Once dehydration experiments were completed, the following sequence was initiated:

1. Proceed as per steps **1 & 2** in the previous start up procedure (Section 4.4.8).
3. Nitrogen flow to the top of the reactor was set to 20 ml/min (mass flow controller FIC-1.2)
4. The diluent gas flow was set to 20 ml/min (mass flow controller FIC-2.1)
5. The reactor was then allowed to cool overnight before being dismounted and unloaded.

4.4.10 Setup of an isothermal profile over the catalyst bed

During commissioning under flow of N_2 over silicon carbide (SiC), the reactor achieved the long axial isothermal zone shown in Figure 4-4. The plot depicts the requisite, low temperature at the reactor entrance (see Section 4.3.1) and the isothermal zone achieved at 250℃ with optimal temp erature controller settings of the individual heating bands / heating zones (each equipped with its own thermocouple). The X-axis depicts the distance from the liquid-feed-introduction point to the end of the reactor bed.

Table B-1 (*0*) column "N_2" lists the controller set points required to attain this temperature profile, along with the set points employed in the generation of the other profiles also shown in this appendix.

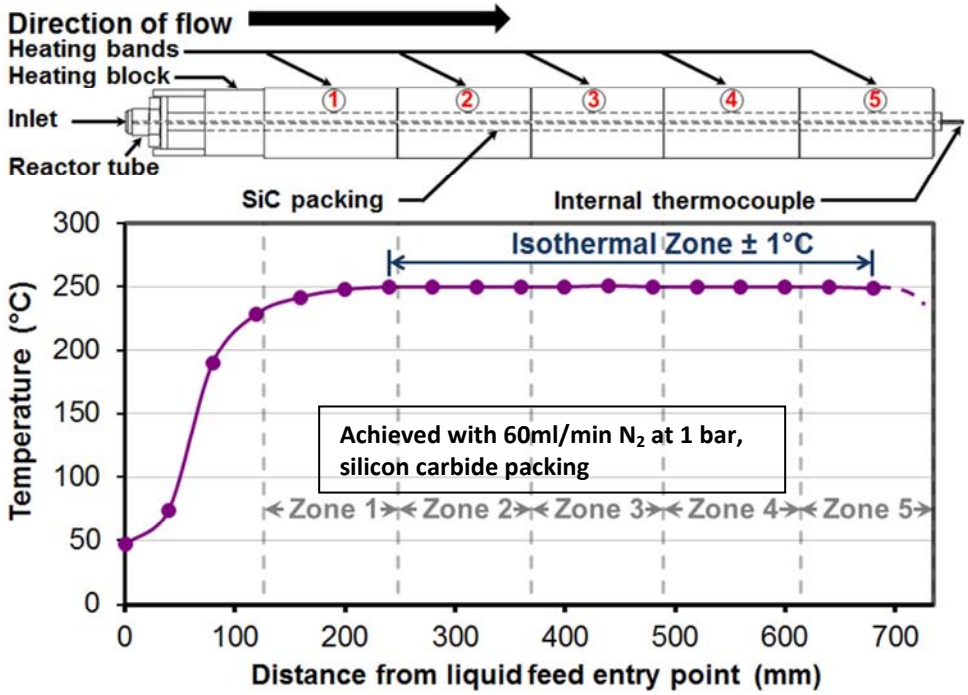

Figure 4-4: Optimised temperature profile generated during commissioning with a depiction of a 5 heating-zone-reactor system.

Figure 4-5 shows the optimised temperature profiles obtained during experiments in which reagents were reacted over the catalyst bed. The beginning of the respective catalyst beds are indicated by the zero position on the x-axis.

In contrast to the curve shown in Figure 4-4, the latter mentioned plots show a characteristic temperature depression in the region of initial contact between reagents and catalyst.

This depression can be attributed to the endothermic dehydration of iso-propanol to propene and water (see *Appendix D*, Table D-1 for the calculated heat of reaction). This depression was observed in all experiments irrespective of reagent feed or reactor conditions, though the extent of the depression was influenced by these parameters (refer to *Appendix D*, Figure D-1).

In an attempt to negate this depression or at least minimise the extent of the effect of this depression on the experimental results, the temperature controller set points were adjusted so as to maximise the length of the isothermal zone of the catalyst bed downstream from the temperature depression zone whilst minimising the temperature depression in the initial contact zone. This philosophy was adapted as the dehydration of the alcohol or ether occurs rapidly compared to the cresylic ring alkylation. Therefore, the cresylic ring alkylation is thought to occur in the isothermal zone for the greater part. By maximising the length of the isothermal zone downstream from the temperature depression zone, the effect the temperature depression has on ring alkylation is minimised.

In a further attempt to alleviate the extent of the depression, the SiC:catalyst dilution ratio was increased five fold to 5:1 (vol.) in the initial section (2.5 g) of the catalyst bed (17.8 g total mass). The position of this bed is demarcated by the red dotted lines in Figure 4-5.

Considering that a 3 fold increase in reactant feed rate was used (as compared to the lower catalyst loading experiment – 5.9 g), the increased dilution served to alleviate the magnitude of the temperature depression resulting from the iso-propanol dehydration reaction. This conclusion was drawn as a similar extent of temperature depression was observed as with the lower catalyst loading. In addition, the temperature profile prior to the bed was not depressed as with the lower catalyst loading experiment.

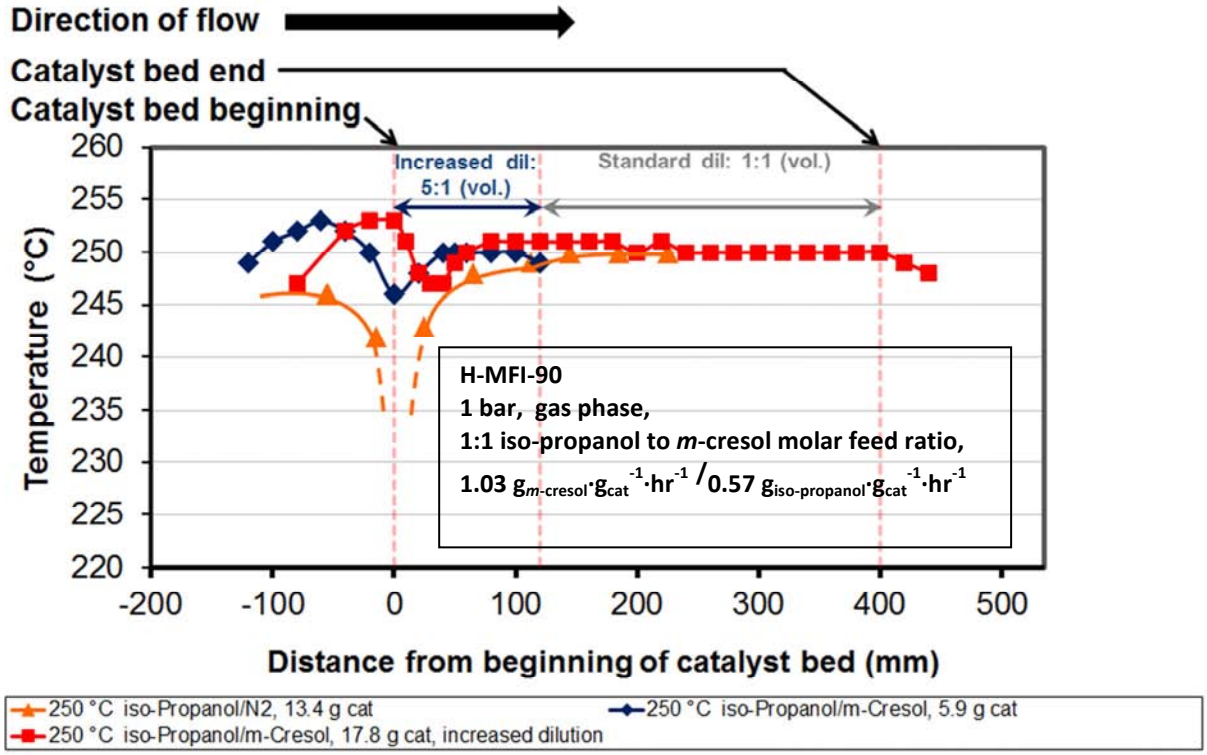

Figure 4-5: Catalyst bed temperature profiles obtained during experiments.

4.5 Product analysis

All product analysis was conducted via Gas Chromatography (GC) for purposes of both quantitative and qualitative interpretation. Table K-1 (*Appendix K, pg. A-35*) lists the details of the GC methods and apparatus employed in the respective sets of experiments. Gas Chromatography Mass Spectral (GC/MS) analysis was employed for identification of compounds formed during thymol synthesis and iso-propanol dehydration reactions.

Sample chromatograms for qualitative and quantitative analyses are presented in *Appendix N (pg. A-40*).

4.5.1 Identification of compounds

Model compounds (if available) for the various products expected to be present in the reactor effluent, were used for peak identification in gas chromatograms. Both individual compounds and spiked product samples were injected.

In cases where the model compounds were not available, peak identification was performed using GC/MS. The mass spectra of these unidentified compounds were compared to the NIST mass spectrum data bank. If a close matching mass spectrum

was not found in this data bank, the spectrum of the unidentified compound was interpreted. For examples of how the mass spectra of compounds were interpreted, please refer to *Appendix L and Appendix M (pg. A-36 and A-38* respectively*)*.

It should be noted that throughout this study IUPAC rules were not strictly followed in the naming of compounds. Instead, phenolic compounds were named such that the methyl group of the original *m*-cresol molecule is always in the 3-position on the phenolic ring.

4.5.2 Groupings of fractions for thymol synthesis experiments

Thymol synthesis reactor effluents obtained at severe conditions (temperatures > 275 ℃, low space velocities at < 0.5 $g_{m\text{-cresol}} \cdot g_{cat}^{-1} \cdot hr^{-1}$) yielded product fractions not seen under milder conditions. Compounds found in the reactor effluent were grouped together as fractions as shown in Figure 4-6. For the full chromatogram, showing the compounds preceding the fractions shown here, refer to Figure N-4 and Figure N-5 *(Appendix N, pg. A-43 and A-44)*.

Table 4-6 provides a list of types of compounds identified in each of these fractions (refer to a sample GC/MS chromatograms in Figure N-1 and Figure N-2, *Appendix N, pg. A-40*).

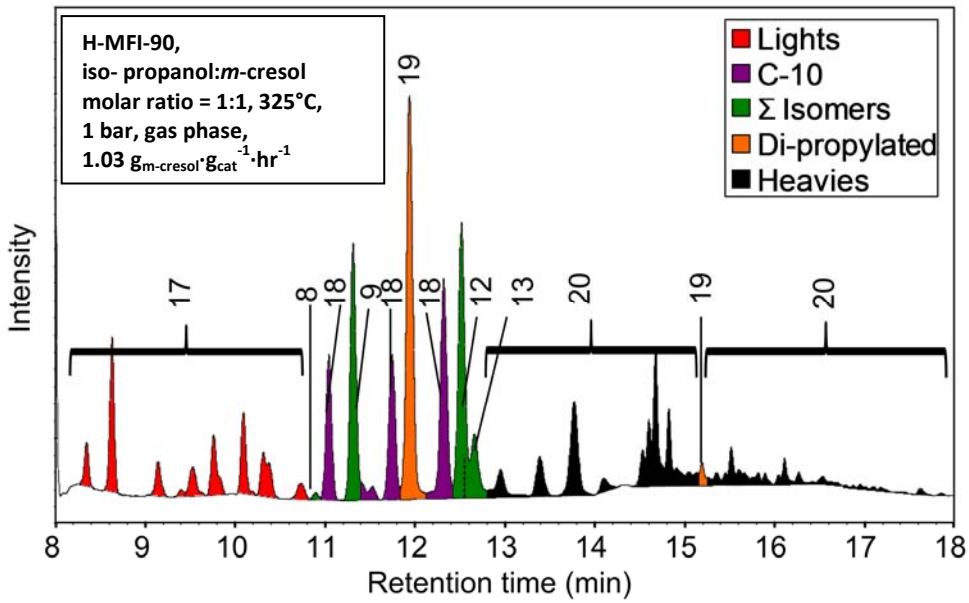

Figure 4-6: Chromatogram with reactor effluent compound groupings.

Table 4-6: Thymol synthesis product fractions seen at severe conditions

Peak No.	Fraction	Description	$N_{C\ in\ side\ chains}$*
17	Lights	Di-and Trimethyl-phenols Ethyl-methyl-phenols Isopropyl-phenols n-Propyl-phenols Methyl-isopropyl-phenols with the methyl group not in the 3 position	2
18	C-10	Other compounds eluding in the same time frame (ca,11-12.4 min) as the mono-isopropylated isomers e.g. n-Propylated *m*-Cresol	3
8 9 12 13	Σ Isomers	Isopropylated *m*-cresol isomers: 3-Methyl-2-isopropyl-phenol Thymol 3-Methyl-5-isopropyl-phenol 3-Methyl-4-isopropyl-phenol	3
19	Di-propylated	Di-propylated *m*-cresol (with n-Propyl and iso-Propyl)	6
20	Heavies	*m*-Cresol alkylated with side chains with total carbon numbers ranging from 4 to 8	6

* Total number of carbon atoms residing on the cresylic ring (an avg. estimated for the fraction) This number was employed in the calculation of the average number of carbon atoms in the side chains

For data analysis, the compounds of a certain fraction were lumped and dealt with as a single compound. For instance, the "C-10" fraction was treated as a compound with carbon number of 10. The Lights and Heavies fractions were treated as compounds with carbon numbers of 9 and 13 respectively. These carbon numbers were assigned based on the average carbon number of the particular fraction.

A sample chromatogram with identified compounds corresponding to the iso-propanol dehydration experiments is presented in *Appendix O (pg. A-47)*.

4.6 Data evaluation

Conversions, yields and selectivities were calculated as measures of catalyst performance. In the case of thymol synthesis, these parameters were calculated on molar basis, i.e. on the basis of a phenolic ring balance in which all phenolic compounds were treated as mono-cyclic species. Olefins and unconverted alkylating agents were not taken into account. Only isopropyl-3-tolyl ether and species with retention times higher than that of isopropyl-3-tolyl ether were considered in these calculations.

4.6.1 Response factors and corrected peak areas for the thymol synthesis experiments

The CG Flame Ionisation Detector (FID) produces a signal that is proportional to the actual concentration of carbon in the flame. The signal integrator gives raw sample data reports with individual peak areas ($\boldsymbol{PA_i}$). These peak areas represent the integral of the intensity of the FID signal as a function of time. Therefore, the peak area is a measure the amount of carbon which eluted with compound ***i***. However, each carbon atom will give a response which depends on its environment. For carbon atoms bonded to other carbon or hydrogen atoms, the FID intensity is unaffected. However, when a carbon atom is bonded to an oxygen atom with a single bond, the resultant signal intensity is halved (approximately).

Hence, the peak areas as obtained from the sample data reports are corrected for the peak areas corresponding to molecules containing oxygen atoms.

If one regards the response of a carbon atom bonded to another carbon or hydrogen atom as **1**, the response given by a carbon atom bonded to an oxygen atom with a single bond would be **0.55**, whereas a carbon atom single bonded to two oxygen atoms or double bonded to one oxygen atom gives no response i.e. **0** (Callanan and van Steen, 1999). Consequently, the peak area ($\boldsymbol{PA_i}$) was multiplied by the average response factor ($\boldsymbol{f_i}$) for a particular molecule to obtain the “corrected peak area” ($\boldsymbol{PAC_i}$). Corrected peak area was calculated according to Equation 4-2.

Equation 4-1 shows the calculation of the response factor ($\boldsymbol{f_i}$) of compound ***i***. In this equation $\boldsymbol{C_i}$ represents the number of carbon atoms in the molecule / carbon number species, $\boldsymbol{a_i}$ the number of carbon atoms bonded only to carbon and/or hydrogen and $\boldsymbol{b_i}$ the number of carbon atoms single bonded to oxygen.

Equation 4-1: Calculation of response factor (f_i)

$$f_i = \frac{C_i}{a_i + b_i \cdot 0.55}$$

Equation 4-2: Calculation of corrected peak area (PAC_i)

$$PAC_i = PA_i \times f_i$$

4.6.2 Molar calculations

Corrected peak areas ($\boldsymbol{PAC_i}$) were converted to mol proportional peak areas ($\boldsymbol{PAM_i}$) by division of $\boldsymbol{PAC_i}$ by the carbon number of the molecule as shown in Equation 4-3.

Equation 4-3: Calculation of mol proportional peak area (PAM_i)

$$PAM_i = \frac{PAC_i}{C_i}$$

4.6.3 Conversion

For the "thymol synthesis" experiments, two types of conversion were calculated, viz. "*m*-cresol conversion" ($\boldsymbol{X_{m\text{-}cresol}}$ - Equation 4-4) and "*m*-cresol alkylation conversion" ($\boldsymbol{X_{m\text{-}cresol,\ alkylation}}$ - Equation 4-5). The *m*-cresol conversion is calculated by dividing the mol proportional peak area of *m*-cresol by the sum of the mol proportional peak areas in the product (including that of the unconverted *m*-cresol) and subtracting this ratio from 1.

Equation 4-4: Calculation of *m*-cresol conversion ($X_{m\text{-}cresol}$)

$$X_{m-Cresol} = 100\% \times \left(1 - \frac{PAM_{m-Cresol}}{\sum_{i=1}^{n} PAM_i}\right)$$

$\boldsymbol{X_{m\text{-}cresol,\ alkylation}}$ refers to the part of *m*-cresol which was converted via alkylation reactions i.e. as shown in Equation 4-5, the segment of *m*-cresol converted via isomerisation to position isomers is excluded from this value. This exclusion is signified by the subtraction of the yields of the *m*-cresol position isomers ($\boldsymbol{Y_{o\text{-}cresol}}$ and $\boldsymbol{Y_{p\text{-}cresol}}$ – see Equation 4-7 for the calculation of these parameters) from $\boldsymbol{X_{m\text{-}cresol}}$.

Equation 4-5: Calculation of *m*-cresol alkylation conversion ($X_{m\text{-}cresol,\ alkylation}$)

$$X_{m-cresol,\ alkylation} = X_{m-cresol} - \left(Y_{o-cresol} + Y_{p-cresol}\right)$$

4.6.4 Selectivity

The molar selectivity toward the formation of a specific component (***i***) was expressed as the amount of the components formed (***PAM$_i$***) divided by the total amount of components formed / *m*-cresol conversion (***X$_{m\text{-}cresol}$***).

Equation 4-6: Calculation of *molar selectivity* (*S$_i$*)

$$S_i = \frac{\frac{PAM_i}{\sum_{i=1}^{n} PAM_i}}{X_{m-Cresol}} \times 100\%$$

4.6.5 Yield

The molar yield of a certain product (***Y$_i$***) is obtained by multiplying the molar *m*-cresol conversion (***X$_{m\text{-}cresol}$***) and the selectivity of the particular product (***S$_i$***) as shown in Equation 4-7.

Equation 4-7: Calculation of component yield (*Y$_i$*)

$$Y_i = X_{m-cresol} \times S_i$$

4.6.6 Average number of carbon atoms in side chains

The average number of carbons in the alkyl substituents of the product compounds (***N$_{Avg\ C\ in\ side\ chains}$***) was calculated by dividing the sum of the product of the side chain length, (***N$_{C\ in\ side\ chains,\ j}$***) and the yield of the specific product fraction (***Y$_j$***) by the sum of the yields of the various product fractions (as shown in Equation 4-8). Table 4-6 (Section 4.5.2) lists the carbon numbers of the product fractions taken into account. Note that the original cresylic methyl group was not counted as part of ***N$_{C\ in\ side\ chains,\ j}$***.

Equation 4-8: Calculation of average carbon no. in side chains (*N$_{Avg\ C\ in\ side\ chains}$*)

$$N_{Avg\ C\ in\ side\ chains} = \frac{\sum_{j=1}^{5}\left(N_{C\ in\ side\ chains,j} \times Y_j\right)}{\sum_{j=1}^{5} Y_j}$$

4.6.7 Thymol synthesis thermodynamic equilibrium constant

The thermodynamic equilibrium constant (K_a) for the thymol synthesis reaction with propene and *m*-cresol (considering water formed by dehydration of iso-propanol as a diluent), is given by Equation 4-9.

Equation 4-9: Thymol synthesis thermodynamic equilibrium constant (K_a)

$$K_a = \frac{X_{m-cresol} \times S_{thymol} \times (3 - 2 \times X_{m-cresol} + X_{m-cresol} \times S_{thymol})}{(1 - X_{m-cresol})^2}$$

4.6.8 Selectivity of Alkylating agent dehydration experiment

Selectivities corresponding to the "dehydration experiment" series were calculated on a carbon weight percentage base and not on a molar basis as with the "thymol synthesis experiment" series. In all cases these, the alcohol or ether dehydration reactions went to completion. Therefore, the selectivity of the respective product fractions was calculated as the peak area of the specific compound/fraction over the sum of the peak areas of all the product fractions as shown in Equation 4-10

Equation 4-10: Calculation of mass selectivity (S_i) for the dehydration exp.

$$S_i = \frac{PA_i}{\sum_{i=1}^{n} PA_i}$$

4.7 Obtaining thermodynamic data

No measured thermodynamic data was found in the literature for the phenolic derivatives of *m*-cresol produced in this study. Therefore, molecular modelling and group contribution methods were used to generate the required thermodynamic data for calculating thermodynamic equilibrium product distributions. For details regarding the use of these respective estimation techniques, refer to *Appendix F and Appendix G (A-11 and A-25)*.

The thermodynamic and other data generated in this manner (such as standard enthalpy of formation and Gibbs free energy of formation) together with specific gravity, molecular weight, structural information, pure component physico-chemical data (such as normal boiling point, critical temperature and critical pressure) were used in the Aspen Plus software simulation package (Aspen Technology, Inc. 2006) to compute the thermodynamic equilibrium distribution of compounds. This software package offered a variety of group contribution methods which could be employed to calculate the ideal gas heat capacity of these compounds. As recommended by the package, the BensonR8 option was used to generate the ideal gas heat capacities. This method corresponds to that described by Benson and co-workers (Benson and Buss, 1958; Benson, 1968; Benson *et al.,* 1969) and was released with the 8th version of Aspen Plus (2006). The UNIFAC and IDEAL property methods were employed to calculate other parameters required for the simulations.

5 Results

In the following chapter, iso-propanol and di-isopropylether are usually referred to as IPA and DIPE, in particular, in figures and tables. A fold-out list of such abbreviations is given in *Appendix A (pg. A-1)*.

5.1 Theoretical considerations – thermodynamic equilibrium limitations

No experimentally determined thermodynamic data was available at the outset of this study for the various isopropylated derivatives of *m*-cresol formed. These derivatives include thymol itself, the various position isomers of thymol, the di-isopropylated isomers, or the *m*-cresol derived compounds found, with higher alkyl groups. Therefore, this data was estimated using mathematical simulations. Various methods were tested against a control group of phenolic compounds for which measured values were available (see *Appendix G, pg. A-25*). Based on the accuracy with which it predicted the parameters for this control group and recommendations from literature (Daubert and Thomas, 1999), the Constantinou and Gani 2nd order group contribution method was selected as the technique of choice for the estimation of all the thermodynamic data used in this study. However, the limitation of this technique is that it does not differentiate between position isomers of the cresol derivatives.

The curves in Figure 5-1 represent *m*-cresol equilibrium conversions for iso-propanol as the co-feed (but completely decomposed to propene and water under the conditions considered and therefore iso-propanol was not included in the reactor feed). The curves differ according to the specific product distributions considered (indicated by the acronyms - see the key). Experimental results have shown that a pool of higher olefins forms from propene at relatively high reaction severity.

Acronyms containing the letters “I-B” indicate that an equilibrium pool of propene and olefins with higher carbon numbers that had formed from propene were also considered for this estimation (limited to the form of n-C_4 olefins together with the sec. butylated products resulting from the alkylation of *m*-cresol with these n-C_4 olefins in order to indicate trends and orders of magnitude).

In all scenarios, equilibrium conversion declines with increasing temperature (in the range of interest to this study: 250 - 325°C). The start of the downward sloping branches of the curves (at around 200°C) indicates the transition from trickle phase to gas phase with increasing temperature. Consequently, in cases where the product

fraction had a higher average boiling point, this phase transition occurred at slightly higher temperatures as compared to instances with lower boiling points.

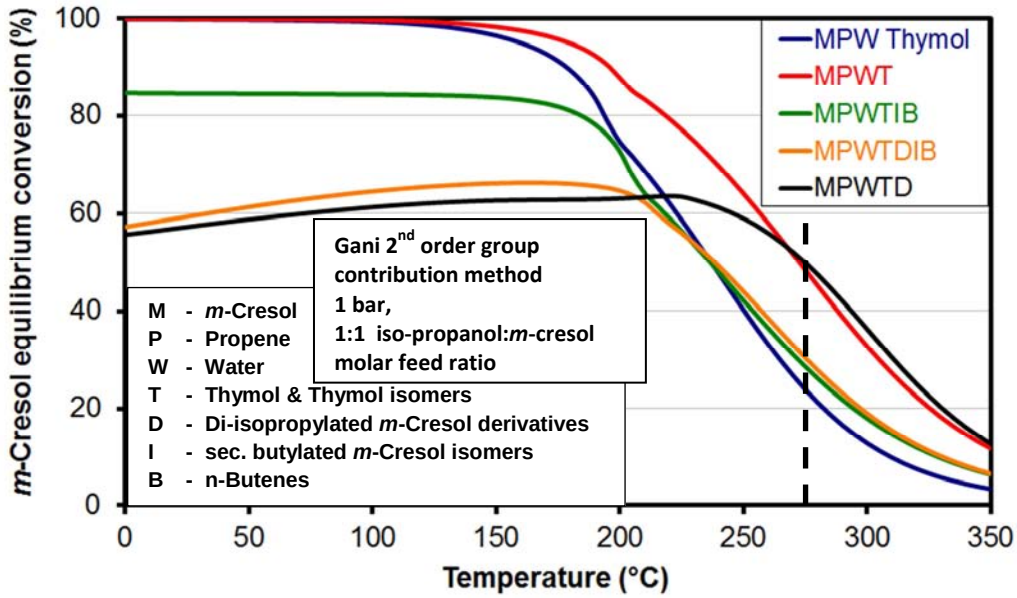

Figure 5-1: Thermodynamic equilibrium conversion of *m*-cresol as a function of temperature.

Refer to Appendix A (blue page) for a fold out detailing the components considered in the thermodynamic calculations.

Figure 5-1 indicates that 100% conversion of *m*-cresol (at lower temperatures) is only possible if di-isopropylation or conversion of propene to higher olefins (simulated as C_4-olefins) and the corresponding higher alkylated and *m*-cresol derivatives, does not take place. This is indicated by the curves MPW **Thymol** and **MPWT**. Once di-isopropylation and/or formation of higher olefins and higher *m*-cresol alkylation products are taken into account, the maximum *m*-cresol equilibrium conversion is significantly below 100%.

At the reaction conditions of 275℃ and 1 bar (see Figure 5-1) equilibrium conversion to thymol (MPW Thymol) is 24% and to thymol plus position isomers (MPWT) is 48%.

Figure 5-2 shows the effect of temperature on the distribution of side chains and remaining olefins for the **MPWTDIB** mixture. Alkyl substituents considered in the model are C_3 side chains (either mono- or di-isopropylated) and C_4 side chains in the form of sec. butyl groups (mono-butylated)**.** Unreacted olefins are referred to as **C_3 olefins remaining** and **C_4 olefins remaining (only n-C_4 olefins)**.

According to Figure 5-2, at temperatures below 175°C, there are only trace amounts of free propene and butenes present in the equilibrated mixture. Under these

conditions, these compounds are mainly present (in the model) as iso-C_3 and sec. C_4 substituents on the *m*-cresol rings. With increasing temperature, the amounts of propene and butenes increase, with the butenes being the major constituents of the olefin fraction. The change in curve shape at around 200℃ indicates the transition from trickle phase to gas phase with increasing temperature.

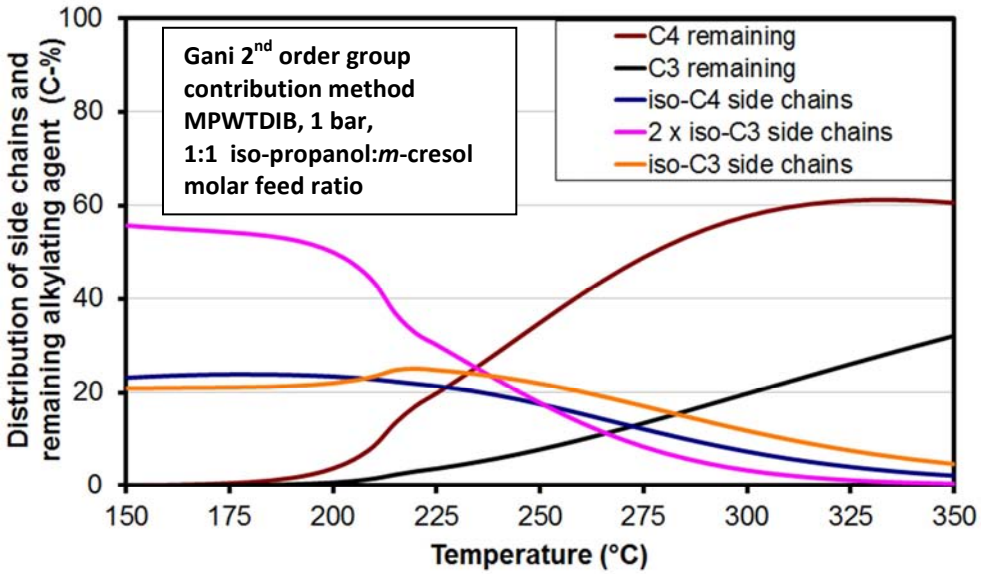

Figure 5-2: Equilibrium distribution of cresylic side chains and remaining olefins as a function of temperature.

Refer to Appendix A (blue page) for a fold out detailing the components considered in the thermodynamic calculations.

5.2 Initial experimental findings

5.2.1 Quasi-steady state data

The hold-up in the experimental apparatus (particularly in the lines downstream from the reactor where liquid condenses out of the gaseous/vaporous reactor effluent and also inside the product catchpot) results in back mixing and consequently, delays in reactor effluent egress. Hence, after changing reaction conditions, samples collected during the transition state (i.e. samples neither representative for the previous, nor the actual reactor conditions) were disregarded and only representative samples obtained during the so called quasi-steady state of practically constant composition (see Section 1.1.1), were considered for evaluation. Accordingly, only data points corresponding to these individual quasi-steady state samples were plotted.

5.2.2 Catalyst stability vs. time-on-stream

To monitor and quantify catalyst deactivation, all experiments were initiated at reference standard reaction conditions (1 bar, 250°C, gas phase, iso-propyl group to *m*-cresol molar ratio = 1:1, 1.03 $g_{m\text{-cresol}} \cdot g_{cat}^{-1} \cdot hr^{-1}$). These conditions were also reverted back to after a number or series of reaction parameter variations and before termination of the individual experimental runs.

Examples of such data are presented in Figure 5-3, Figure 5-4 and Figure 5-5 for systems with co-fed propene, di-isopropylether and iso-propanol, respectively. A rapid decline of *m*-cresol conversion was observed for all alkylating agents employed over an initial ca. 50-100 hour period on stream. The decline was less severe over the ensuing 50-100 hours on stream, after which the rate of decline became comparatively low. This period of very slow decline in activity with time-on-stream is referred to as the 'quasi-steady state'. The associated rate of deactivation was found to be slow enough, such that the effects of and trends obtained by variation of parameters (determined during short periods of time-on-stream of typically around 120 hours) were hardly affected by progressing deactivation. Therefore, parameter variation was only conducted once product composition had stabilised, which typically needed about 4 hours on stream. Product composition was monitored until found steady, such that samples representative of these conditions could be obtained. Results for propene conversion have been taken from a previous study (Fletcher *et al.*, 2003).

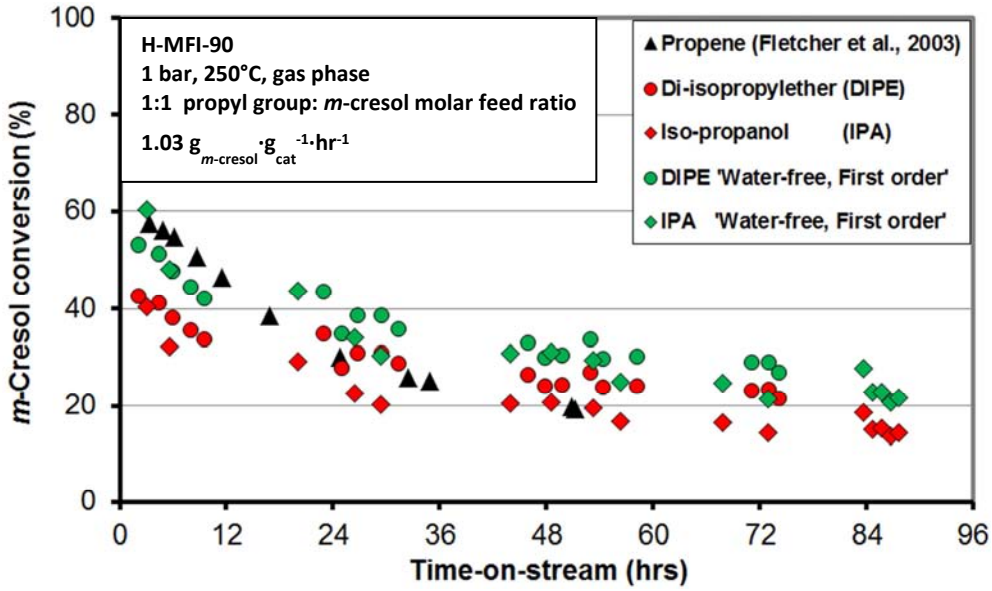

Figure 5-3: *m*-Cresol conversion as a function of time-on-stream at standard reaction conditions.

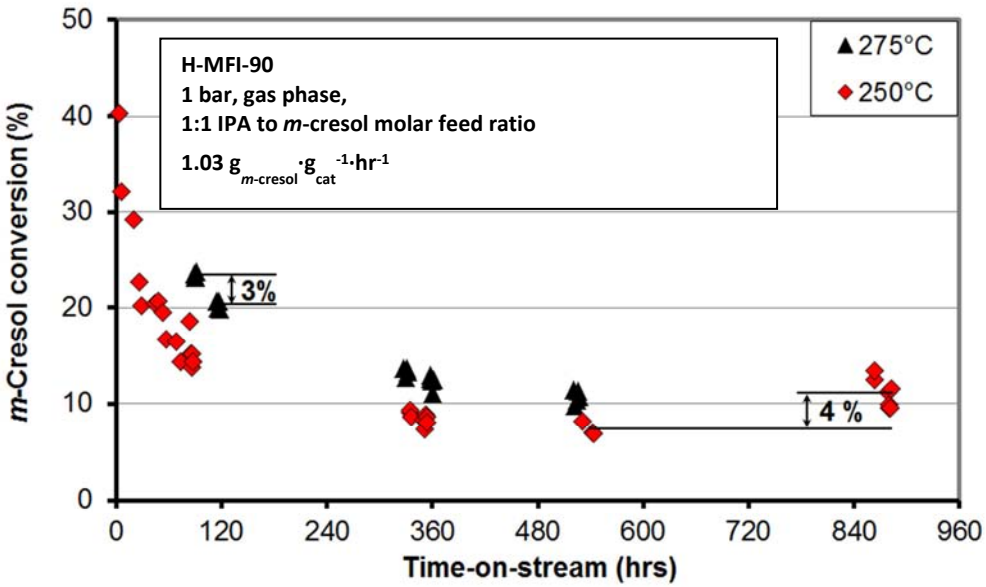

Figure 5-4: *m*-Cresol conversion with iso-propanol as a function of time-on-stream and effect of varying reaction conditions on catalyst stability.

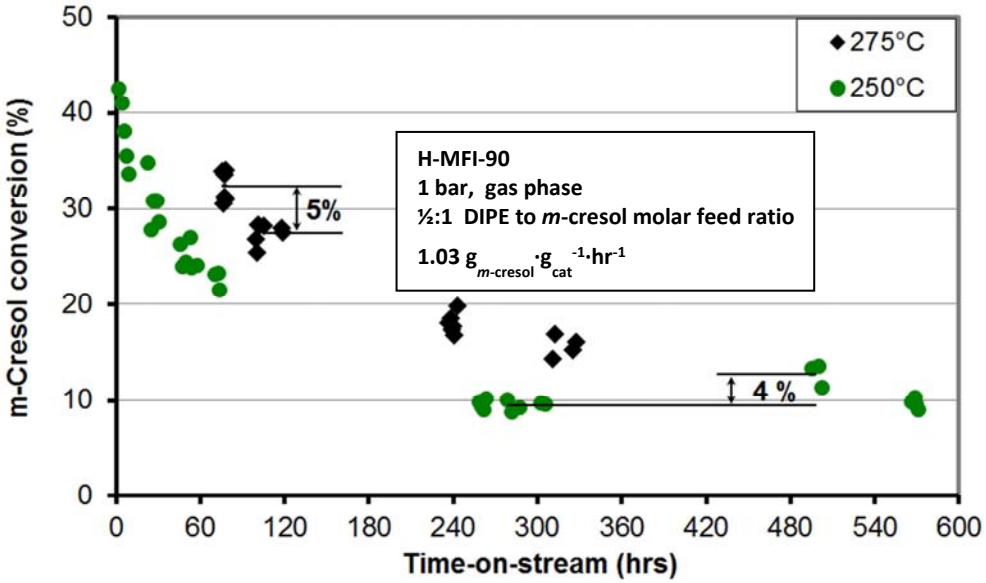

Figure 5-5: *m*-Cresol conversion with di-isopropylether as a function of time-on-stream and effect of varying reaction conditions on catalyst stability.

Initially, *m*-cresol conversion achieved with di-isopropylether and iso-propanol as the alkylating agents was lower than that achieved with propene. However, the rate of deactivation was slower. Therefore, *m*-cresol conversion for the formerly mentioned alkylating agents surpassed that of propene after around 50 hrs. on stream.

Post-experiment discharged catalyst extrudates, were observed as blackened compared to the light coloured extrudates initially charged, for all alkylating agents employed.

5.2.3 Effect of reaction conditions on catalyst stability

The time-on-stream data for experiments with iso-propanol and di-isopropylether are shown in Figure 5-4 and Figure 5-5, respectively. This data corresponds to that represented in Figure 5-3 (corresponding to standard conditions only). Data is presented for 250℃ and 275℃ for standard feed and WHSV. The periods (>100h) in which no data is presented, correspond to different reaction conditions. Marginal catalyst deactivation was observed continually (following the initial rapid catalyst deactivation period) over the time frames presented. The extent of this catalyst deactivation reflects that observed during previous studies under similar reaction conditions (Nagooroo, 2012).

A relatively rapid loss of catalyst activity was observed during the 90 -120 and 80 - 110 hours period corresponding to iso-propanol and di-isopropylether co-feeds (275ºC, standard feed and WHSV), respectively. Losses of 3 percentage points and 5 percentage points in *m*-cresol conversion, within 1 day is attributed to the fast deactivation of the catalyst at the higher temperatures (300 and 325℃) applied during this time frame as well as the 'aggressive' activity of the fresh catalyst. Accelerated deactivation at high temperature was also found in former studies (Nagooroo, 2012; Fletcher *et al.*, 2003).

After 530 and 260 hrs. for the iso-propanol and di-isopropylether runs, respectively, space velocities were varied (15 bar, 275℃, isopro pyl group to *m*-cresol molar ratio = 1:1). The pressure increase caused a phase change from vaporous to trickle phase. Subsequently, *m*-cresol conversion (at the standard reference condition) was found to have recovered by 4 percentage points compared to the activity obtained at the same condition before the space velocity series was carried out.

5.2.4 Exclusion of external mass transfer limitations

The exclusion of artificial effects, such as external mass transfer limitations is necessary to prove experimental integrity. These specific limitations are of particular concern to systems employing low linear velocity (such as laboratory scale reactors). The variation of catalyst loading with concomitant change in volumetric feed rate equates to variation of the linear velocity of the reaction mixture over the catalyst bed.

In this study, the absence of external mass transfer limitations was tested over two different changes of the H-MFI-90 catalyst (at 275°C, 15 bar, iso-propanol:*m*-cresol

molar ratio =1:1 and a range of space velocities). Results are shown in Figure 5-6. The first was conducted with a catalyst loading of 5.87 g [diluted with SiC 1:1 (vol. ratio)] and the latter with a catalyst loading of 17.82 g, i.e. at three times the linear velocity. For the higher catalyst loading, the upper layer of the bed was diluted at a 5:1 SiC:catalyst vol. ratio with the rest of the bed at 1:1 (vol. ratio)

The higher catalyst bed dilution was employed to negate the effect whereby the rapid initial iso-propanol dehydration influences the temperature profile (see Section 4.4.10).

Over the range of space velocities, the *m*-cresol conversion data points corresponding to the respective experiments mimicked one another quite closely. This applied even at the lower most space velocities, i.e. at the lower most linear velocity. Therefore, external mass transfer control is not influencing overall performance for the tests of this study.

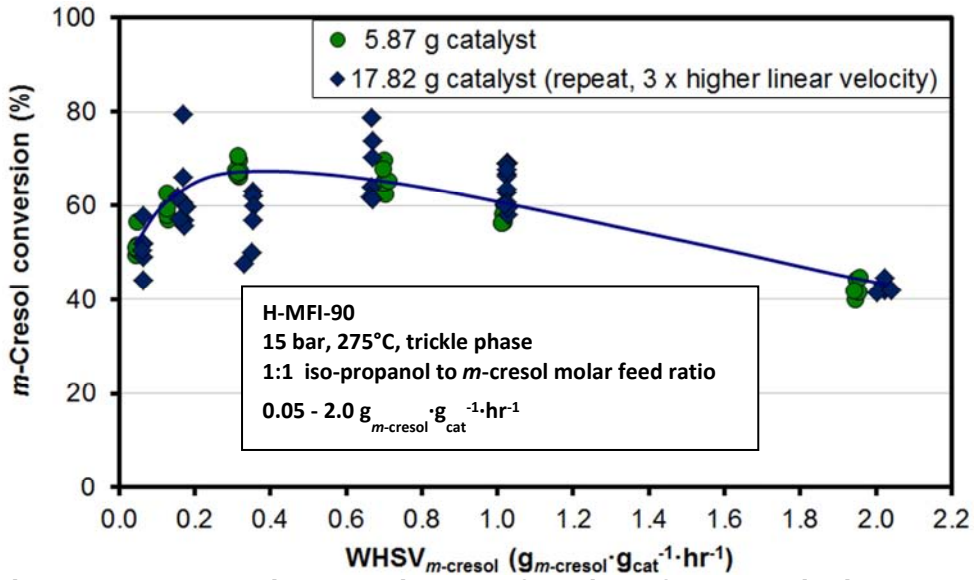

Figure 5-6: *m*-Cresol conversion as a function of space velocity.

5.2.5 Repeatability and data scatter

Repeatability is equally indispensable in the validation of experimental results. The outcome of the experiments described in Section 5.2.4 also serves to check for repeatability. It is evident that the result obtained from the two different experimental campaigns (see Figure 5-6) are comparable, in terms of repeatability. However, data scatter appeared to be significant.

Data points represent the individual samples data during quasi-steady state operation at the respective reaction condition settings. This was not found to be the result of catalyst deactivation as data distribution did not show a correlation with respect to time over the experimental periods employed for variation of the space velocity. With the return to previously employed condition settings, resultant data points still lay within the range of standard deviation determined with the said initially obtained data distribution.

5.3 Thymol synthesis

5.3.1 Alkylating agents vs. reaction rate and catalyst stability

Figure 5-3 to Figure 5-6 show the following ranking for the different alkylation agents with regard to conversion achieved (which is equivalent to reaction rate), over the fresh catalyst:

Propene > di-isopropylether > iso-propanol

These figures also show the ranking for the different alkylation agents in terms of their effect on catalyst deactivation or as follows (propene showing the most adverse effect on catalyst deactivation):

Propene > di-isopropylether ≈ iso-propanol

5.3.2 Variation of space velocity

Space velocity was varied in a series of experiments (also at different pressures) to identify suitable conditions for the thymol synthesis reaction.

Figure 5-7 shows conversion vs. space velocity plots obtained in this study together with the 3 experiments (conducted at 250℃, 275℃ a nd 300℃) from Mathews and Tsui (2007) (presented in Section 2.7). Results correspond to reaction systems catalysed by H-MFI-90 and H-MFI-400 over a range of reaction conditions. The figure also shows lines of estimated *m*-cresol equilibrium conversions for specific reaction mixtures that comprise propene, *m*-cresol and thymol (with an equimolar amount of water present with respect to the original percentage of iso-propanol). These estimates are presented for a range of temperatures and pressures (see Section 5.7 for details concerning the estimation of these values). Calculations consider that iso-propanol and di-isopropylether are very rapidly dehydrated in the reaction system, so that only propene is left as the effective alkylating agent (refer to Section 2.6.3).

For ease of reference, the conversion - WHSV curve was divided into two branches (separated by the black dashed lines in the figures) namely: the “high space velocity” and “low space velocity” branch, respectively. In the “high space velocity branches” of the curves, *m*-cresol conversion increased, as expected, with decreasing space velocity but did not reach equilibrium conversion.

In the “low space velocity branches” of the curves, all curves obtained at 275℃ mimicked a peculiar downward slope of *m*-cresol conversion with further decreasing space velocity (except for the curve obtained for the partially deactivated H-MFI-90 catalyst at 1 bar). The reaction mechanism responsible for this unusual shape and counterintuitive decline of conversion and thymol selectivity is discussed in Section 6.4.4.

Equilibrium conversions were calculated as described in Section 5.1 (see dashed line in Figure 5-1). Please note that the designation “**partially deactivated**” refers to catalyst systems which are considered partially deactivated (as a result of exposure to severe conditions). These systems still have considerable catalytic activity, however are deactivated to a greater extent as compared to the preliminary results corresponding to the “volcano curve” (Curve “**IPA, 275℃, 1 bar, H-MFI-400 (Matthews and Tsui, 2007)**”) presented initially in Section 2.7.

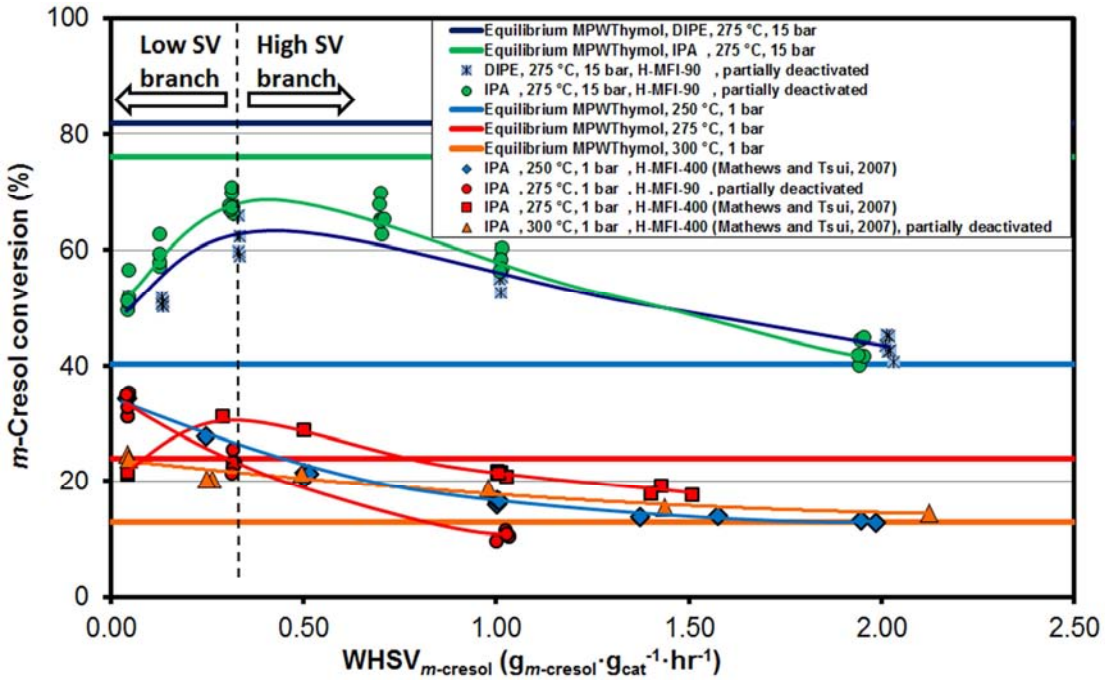

Figure 5-7: *m*-Cresol conversion vs. space velocity for a range of reaction conditions.

Refer to Appendix A (blue page) for a fold out detailing the components considered in the thermodynamic calculations.

Figure 5-8 and Figure 5-9 show how the yields and selectivities of the major products and lumped product fractions varied when space velocity was reduced for the reaction of *m*-cresol with iso-propanol mediated by H-MFI-90. Results show that space velocity has a substantial effect on the selectivity of these product fractions in the low space velocity branch of the curves. Similar trends with respect to conversion and product selectivity were observed in the experiment which employed di-isopropylether as alkylating agent under the same reaction conditions. Selectivity results from the reaction of *m*-cresol with iso-propanol mediated by H-MFI-90 are shown in Figure 5-10 and Figure 5-11 (selectivities).

A breakdown of each of the components found in the respective lumped fractions is given in Figure 4-6. For convenience, *Appendix A also* provides a fold out (blue page) detailing these product fractions.

It should be noted that equilibrium conversion of *m*-cresol (to thymol only) is close to 80% at 15 bar and 275 ℃. In Figure 5-8, the decline in total yields of thymol (30 mol-%), thymol and thymol position isomers (20 mol-%) and di-propylated compounds (10 mol-%) with decreasing space velocity, is accompanied by an increase in the yields of ”Heavies” (10 mol-%), “C_{10}” (3 mol-%) and “Lights” (2 mol-%) (at WHSV < 0.5 $g_{m\text{-cresol}} \cdot g_{cat}^{-1} \cdot hr^{-1}$). The difference reflects the ‘loss’ in *m*-cresol conversion at low space velocity.

The space velocity series carried out by Mathews and Tsui (2007), yielding the initial “volcano curve” (Section 2.7) was conducted over H-MFI-400 (see curve: “**IPA, 275℃, 1 bar, H-MFI-400 (Matthews and Tsui, 2007)**” in Figure 5-7, corresponding to IPA to *m*-cresol molar ratio = 1:1, 275℃, 1 bar, gas phase), over a relatively fresh catalyst. Whereas, the series corresponding to results shown in Figure 5-10 and Figure 5-11 was conducted at the same reaction conditions, but over a comparatively deactivated H-MFI-90 catalyst (It had been exposed to temperatures up to 325℃, pressures up to 15 bar and was on stream for 14 days as opposed to the H-MFI-400 system, which had been on stream for 4 days, and had been exposed mild conditions only). The experiment with H-MFI-90, achieved maximum conversion at the lower most space velocity.

This conversion was at a similar level as the result obtained by Matthews and Tsui (2007) at the equal reaction conditions. Yet, it did not show the characteristic decline

in conversion at the very low space velocities. However, similar trends in selectivities were observed as with the experiments at higher pressure (Figure 5-9).

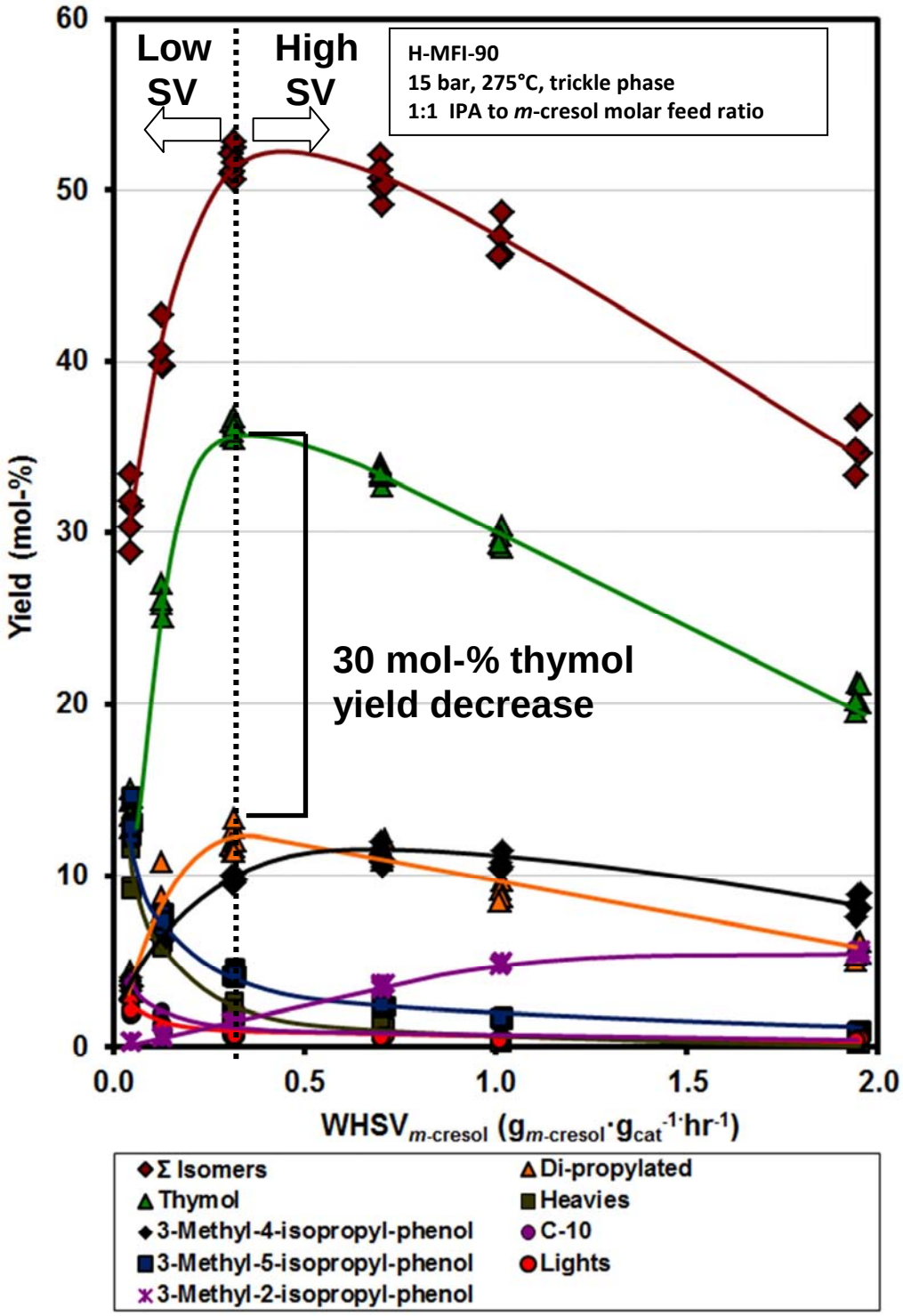

Figure 5-8: Yields of the various product fractions vs. space velocity.

Refer to Appendix A (blue page) for a fold out detailing the various product fractions.

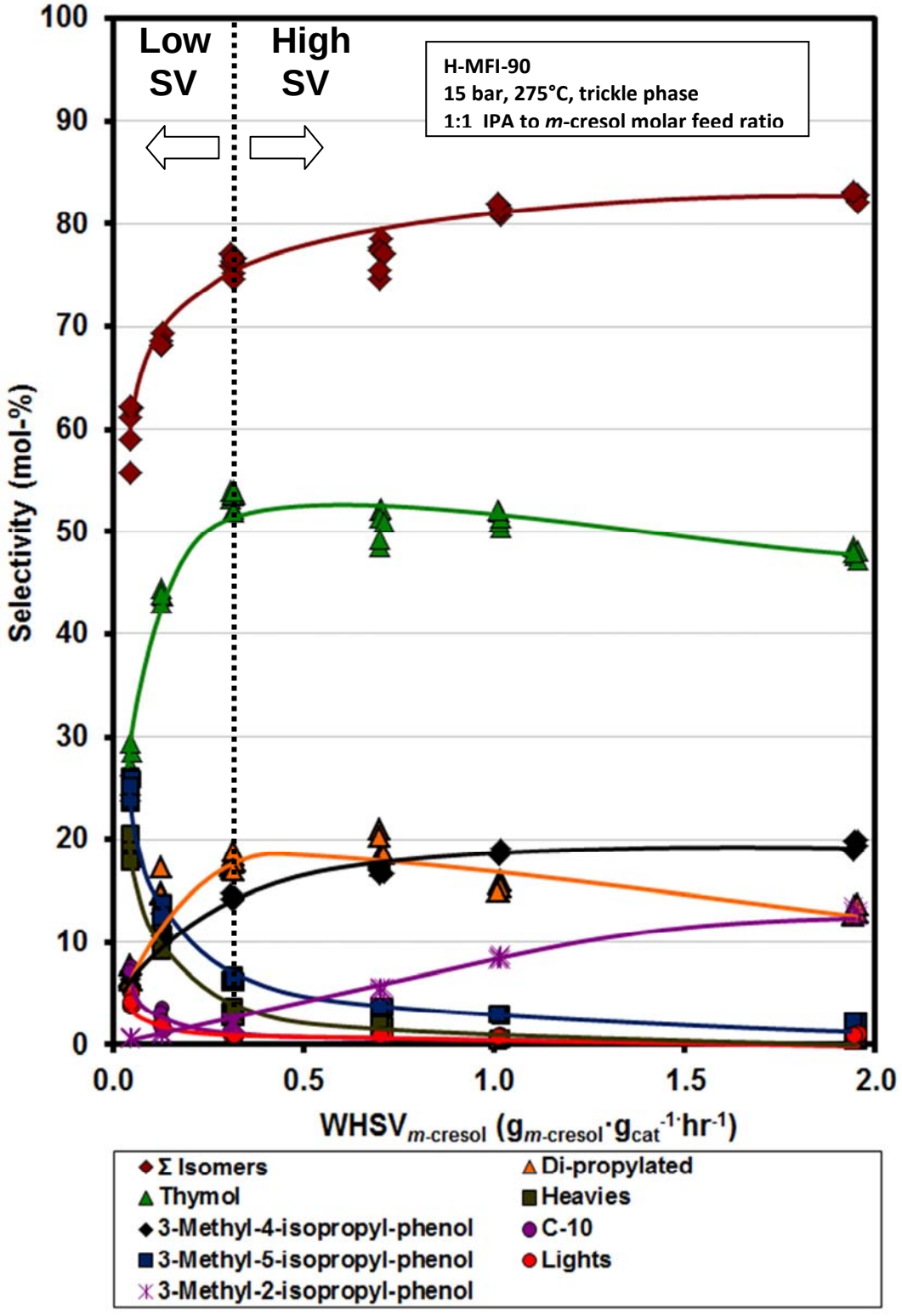

Figure 5-9: Selectivity of the various product fractions vs. space velocity.

Refer to Appendix A (blue page) for a fold out detailing the various product fractions.

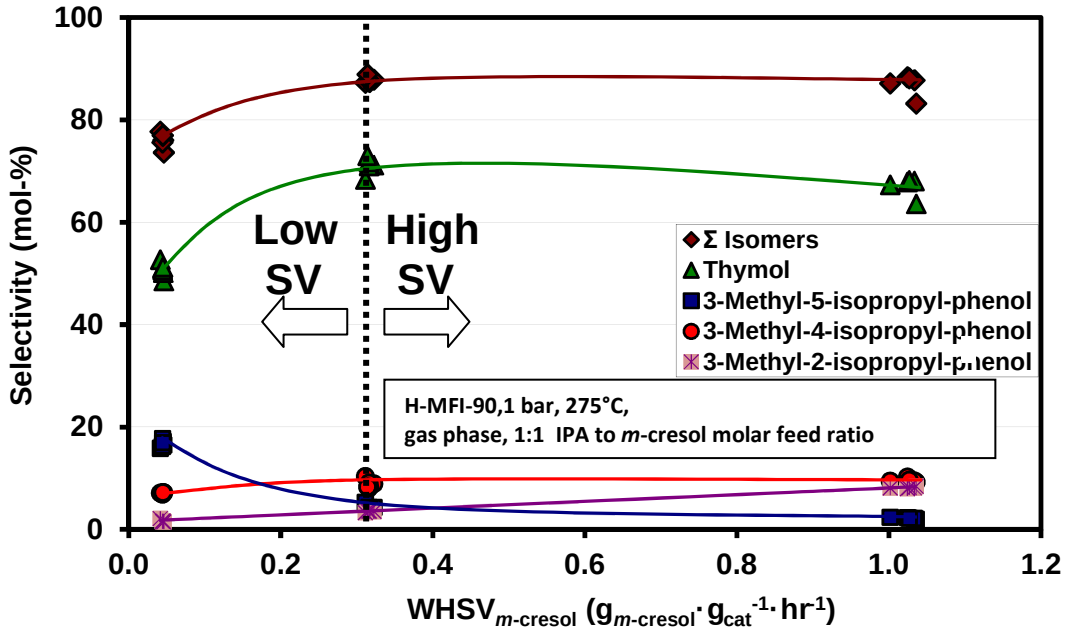

Figure 5-10: Thymol and position isomer selectivities vs. space velocity.

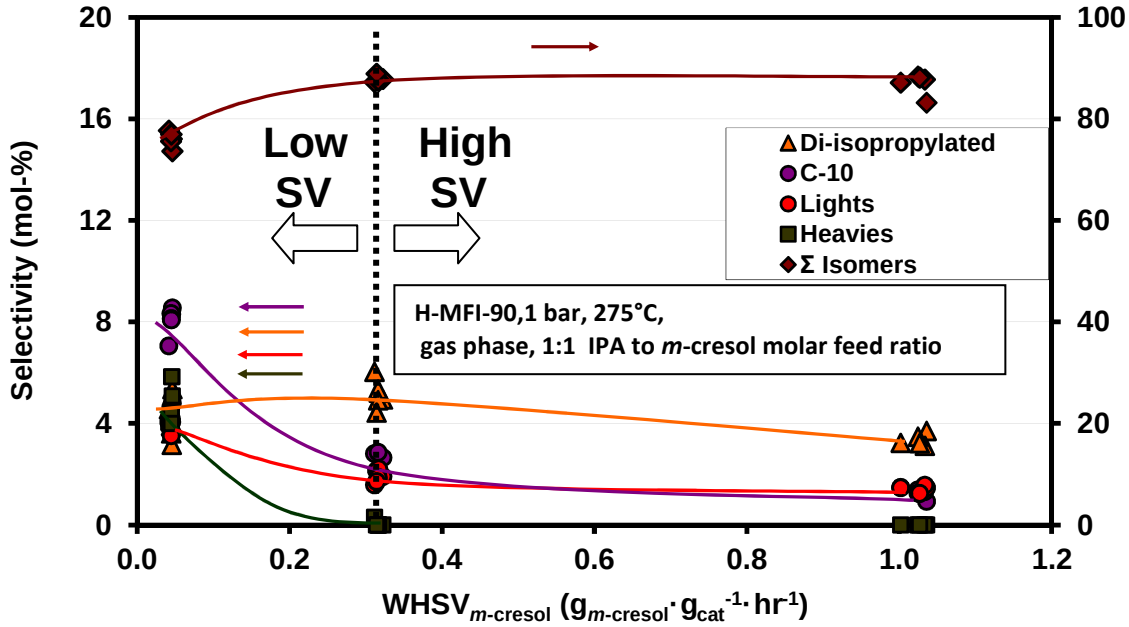

Figure 5-11: Additional product fractions selectivities vs. space velocity.

Refer to Appendix A (blue page) for a fold out detailing the various product fractions.

Runs at 1 bar over H-MFI-400 (Figure 5-7) and temperatures other than 275℃, did also not show the turnaround of conversions with decreasing space velocity within the range of space velocities covered. Conversion at the high temperature of 300℃ was limited by very low *m*-cresol equilibrium conversion (an estimated value, taking only the thymol synthesis reaction into account) while at the low temperature of 250℃ the catalyst lacked activity.

5.3.3 Variation of reaction pressure

Figure 5-12 and Figure 5-13 depict the effect of increasing pressure on *m*-cresol conversion, product yields and selectivities respectively. *m*-Cresol conversion, thymol -and thymol isomer yields showed a logarithmic relationship with respect to pressure. Thymol selectivity decreased as *m*-cresol conversion increased and system selectivity shifted to secondary products like the di-isopropylated *m*-cresols. However in contrast to the effect of increasing conversion due to decreasing space velocity (see Figure 5-9, high space velocity branch), increasing conversion due to increasing pressure translated into decreased selectivity toward thymol. Concomitantly, increases in selectivity toward 3-methyl-4-isopropyl-phenol and 3-methyl-2-isopropyl-phenol with a decrease in the selectivity toward the 3-methyl-5-isopropyl-phenol isomer were observed.

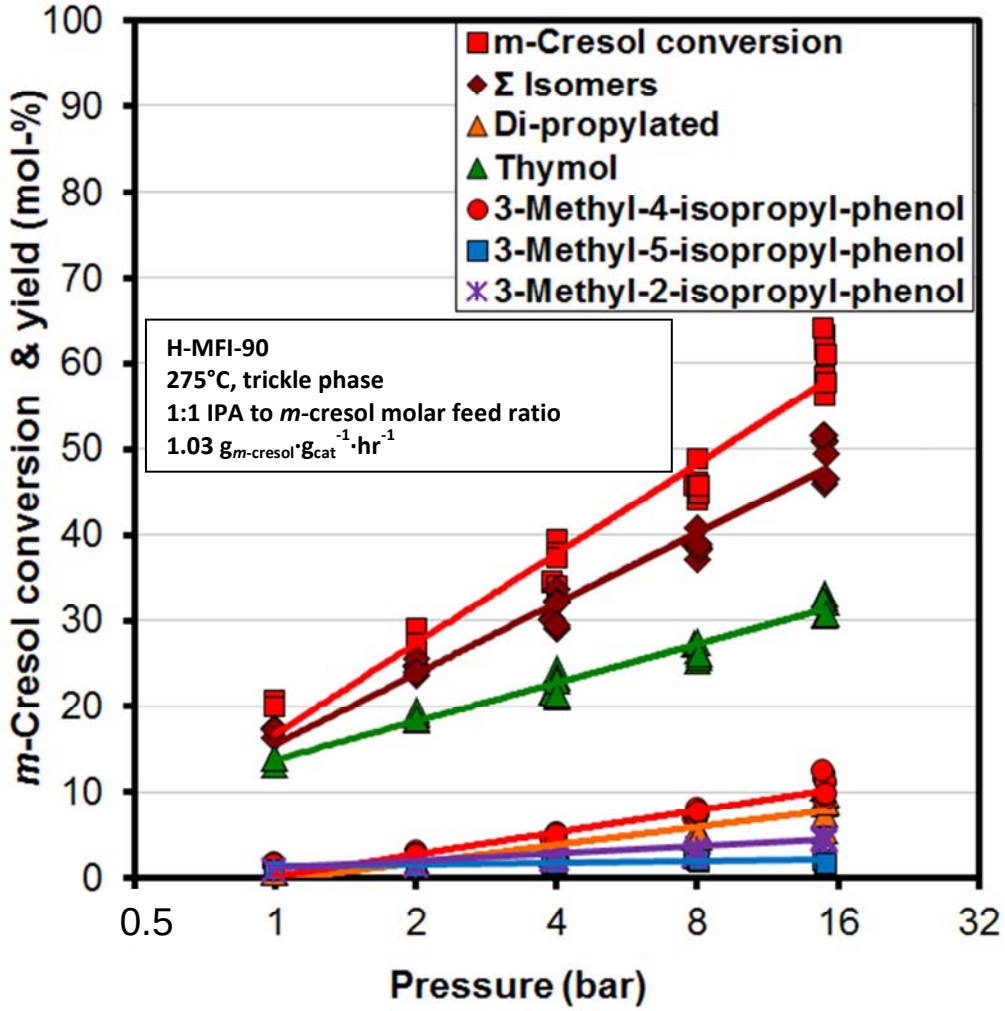

Figure 5-12: *m*-Cresol conversion and yield of various product fractions vs. pressure (Note the logarithmic scale of the x-axis).

Refer to Appendix A (blue page) for a fold out detailing the various product fractions.

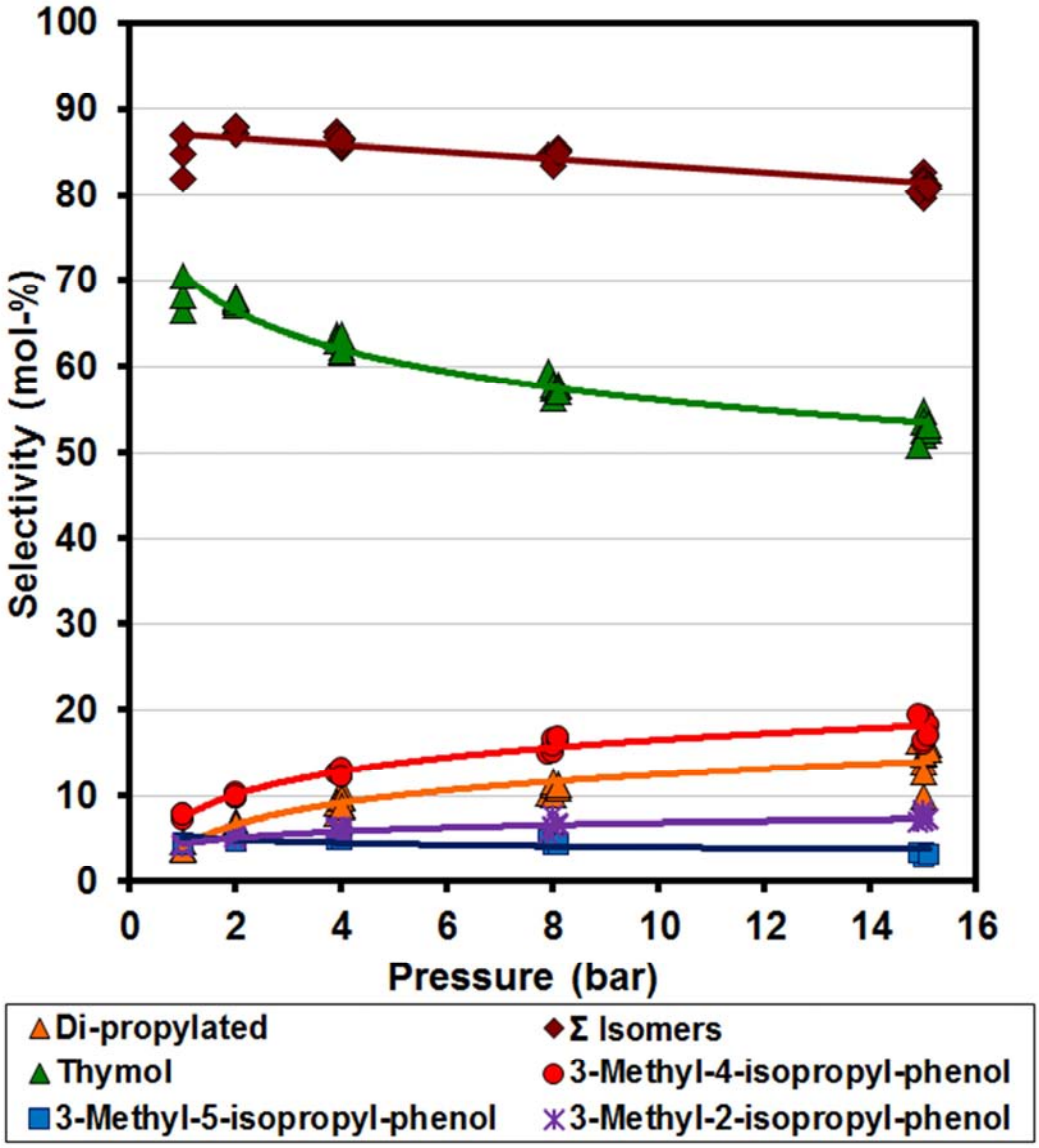

Figure 5-13: Selectivity of thymol position isomers and di-isopropylated *m*-cresol obtained as a function of pressure.

Refer to Appendix A (blue page) for a fold out detailing the various product fractions.

5.3.4 Variation of reaction temperature

Figure 5-14 shows *m*-cresol conversion as a function of temperature for reaction systems mediated by H-MFI-90 and H-MFI-400.

The curve shows a moderate increase in *m*-cresol conversion with increasing reaction temperature above 275℃ and Figure 5-15 shows an increasing percentage of the *m*-cresol undergoing isomerisation to *o*- and *p*-cresol.

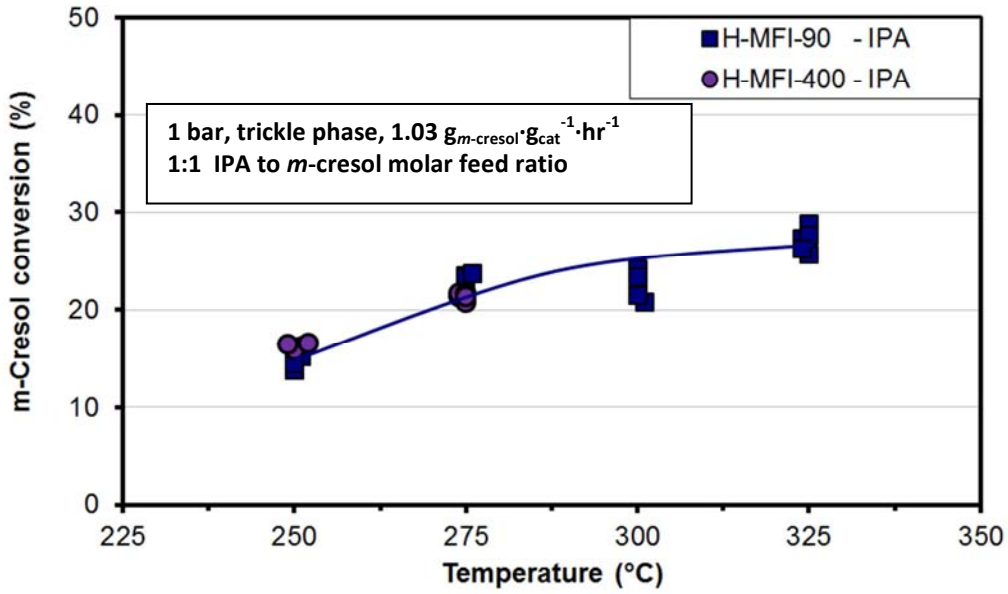

Figure 5-14: *m*-Cresol conversion with iso-propanol as function of reaction temperature.

The same types of compounds observed at 275℃ at the lowest space velocity (see yields of the respective product fractions as a function of space velocity in Figure 5-8) were observed at temperatures above 275℃, as depicted by the yields and selectivities of the respective product fractions in Figure 5-15 and Figure 5-16 respectively. However, the formation of *o*-cresol, *p*-cresol and compounds other than isopropylated *m*-cresol was not as pronounced in the low reaction temperature/ low space velocity product.

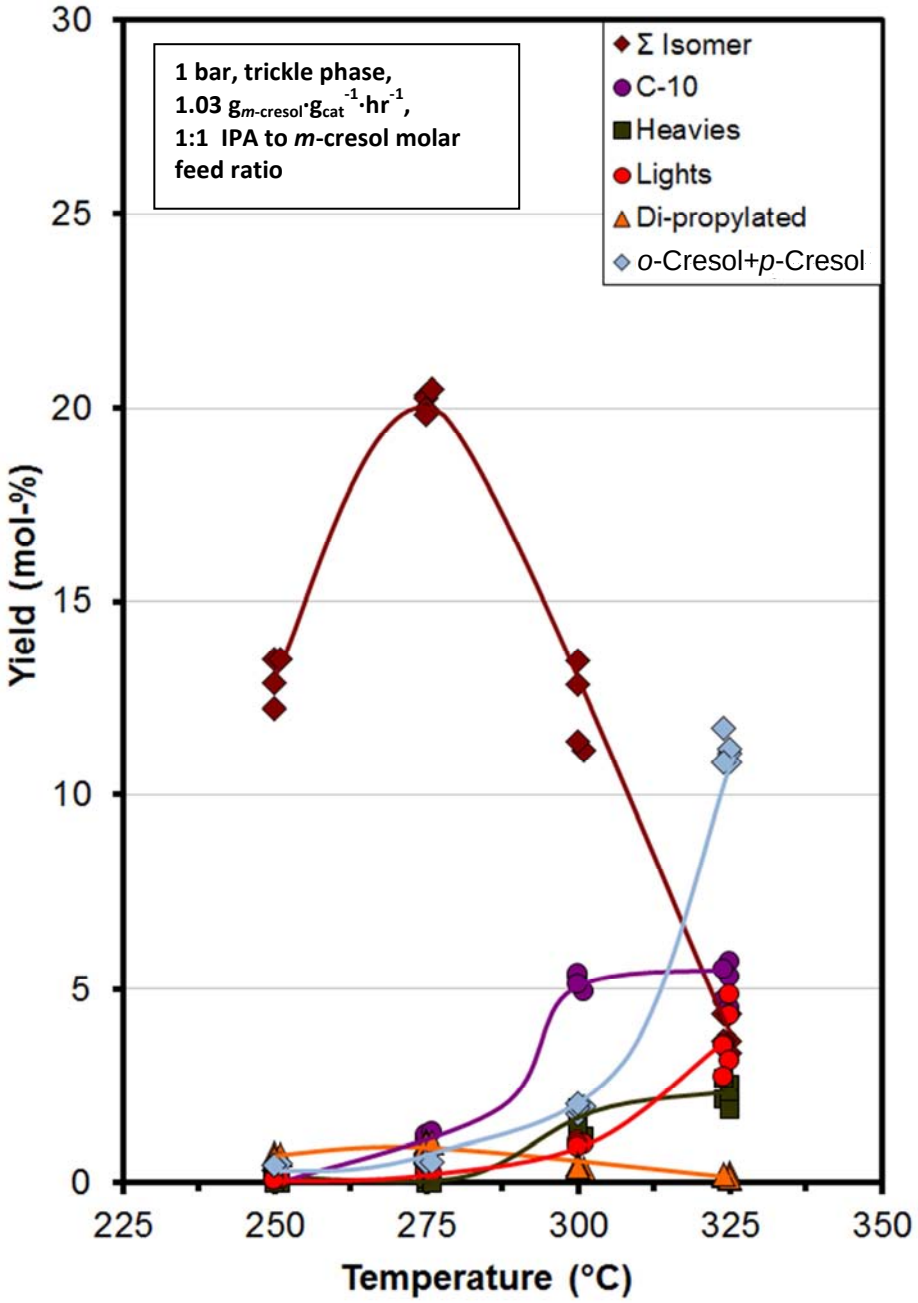

Figure 5-15: Yields of the various product fractions vs. reaction temperature.

Refer to Appendix A (blue page) for a fold out detailing the various product fractions.

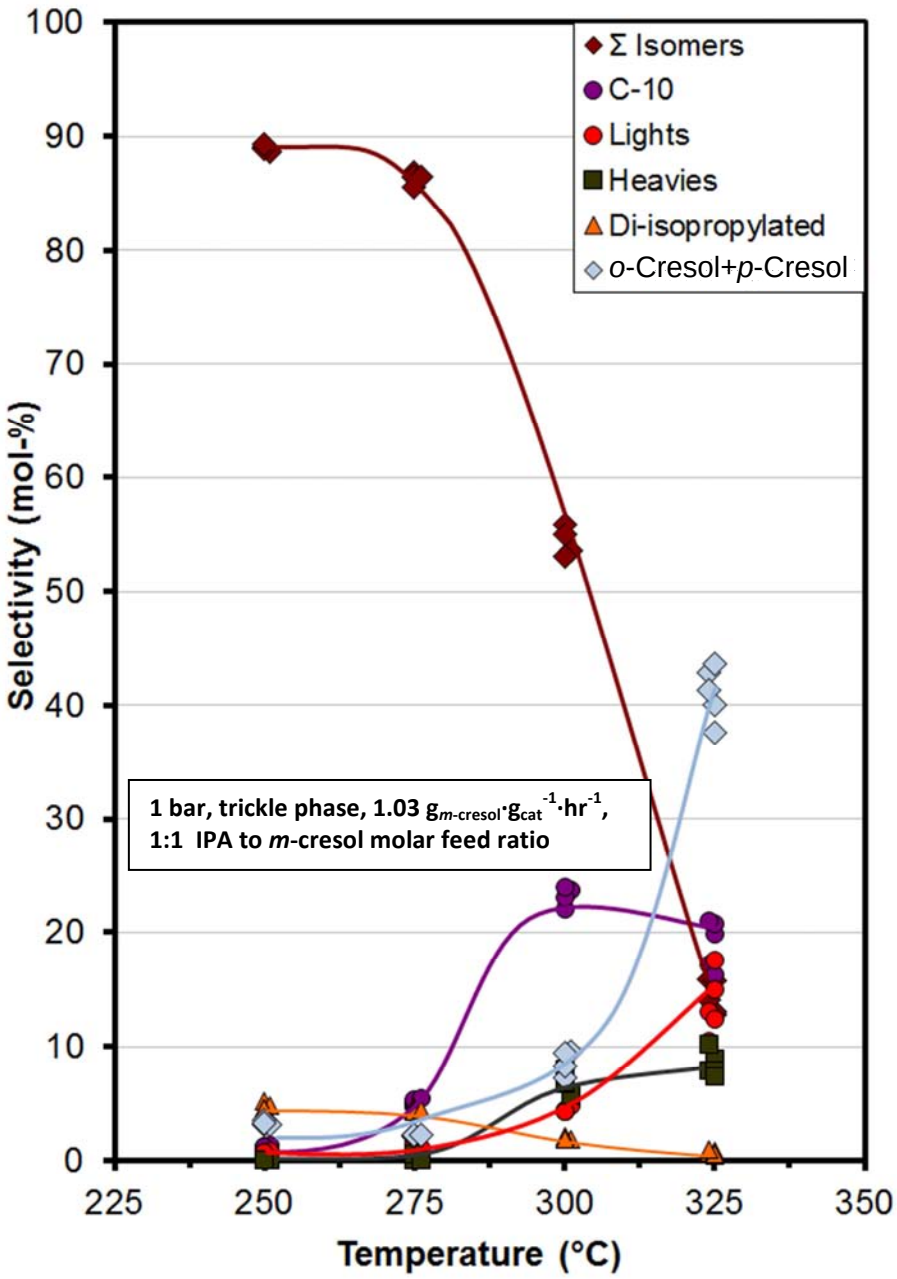

Figure 5-16: Selectivity to product fractions vs. reaction temperature.

Refer to Appendix A (blue page) for a fold out detailing the various product fractions.

5.4 Dehydration of iso-propanol

In determining the origin of individual side chains on the alkylated *m*-cresol species of carbon numbers >3, iso-propanol was converted over one of the catalysts used for thymol synthesis. Dehydration of the iso-propanol was rapid and complete under all the conditions applied, while most of the primarily formed propene reacted further to higher compounds.

5.4.1 Variation of space velocity

To simulate an *m*-cresol containing feed at 1 bar total pressure, iso-propanol (diluted with nitrogen at a partial pressure of 0.5 bar in order to compensate for the absence of *m*-cresol) was converted over zeolite H-MFI-90 at 275ºC while varying space velocity. Figure 5-17 shows the results of this experiment. As indicated by the secondary x-axis in Figure 5-17, the range of iso-propanol WHSV, was varied corresponding to the range of *m*-cresol space velocities employed in the thymol synthesis experiments.

The yield of propene is small in comparison to the yield of higher olefins (C_{4+}) and other product fractions. The higher olefins dominated the product distribution at the high space velocities, but the percentage decreased sharply with decreasing space velocity in favour of the fraction consisting of cyclo-olefins, cyclo-paraffins and paraffins which increased steadily with decreasing space velocity but which also started declining at very low space velocities in favour of aromatic compounds. Aromatics were only observed at very low space velocities below 0.2 $g_{iso\text{-}propanol} \cdot g_{cat}^{-1} \cdot hr^{-1}$, but yields increased steeply with further decreasing space velocity.

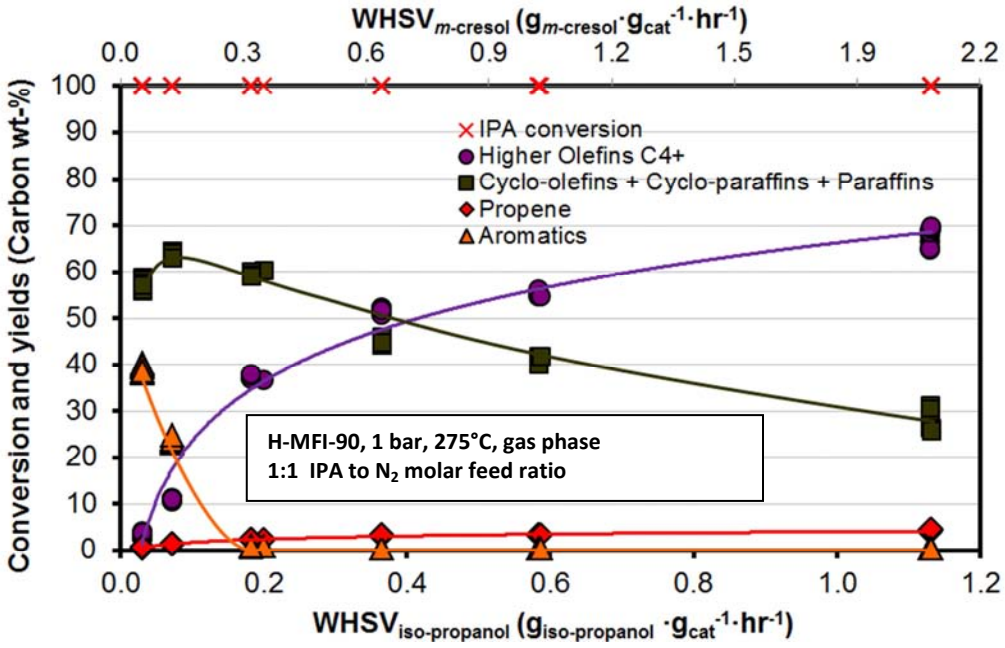

Figure 5-17: Conversion of neat iso-propanol and yields of the various product fractions as a function of space velocity.

5.4.2 Temperature series

The same feed as charged for the space velocity series was converted at 1 bar total pressure and a space velocity of 0.57 $g_{iso\text{-}propanol} \cdot g_{cat}^{-1} \cdot hr^{-1}$ whilst varying reaction temperature.

Figure 5-18 presents the findings of this experiment. Propene yield was small relative to that of the higher olefins (C_{4+}) and other product fractions. The higher olefins dominated the product distribution at low temperatures but the yield of this fraction decreased markedly with increasing temperature.

The fraction consisting of cyclo-olefins, cyclo-paraffins and paraffins increased distinctly with temperature up to 300℃ after which it started declining with further increasing temperature in favour of aromatic compounds. Aromatics were only observed at temperatures higher than 275℃, but yie lds increased considerably with increasing temperature.

The composition of the product fraction obtained from converting neat di-isopropylether showed similar trends (to that presented here for iso-propanol) with respect to temperature.

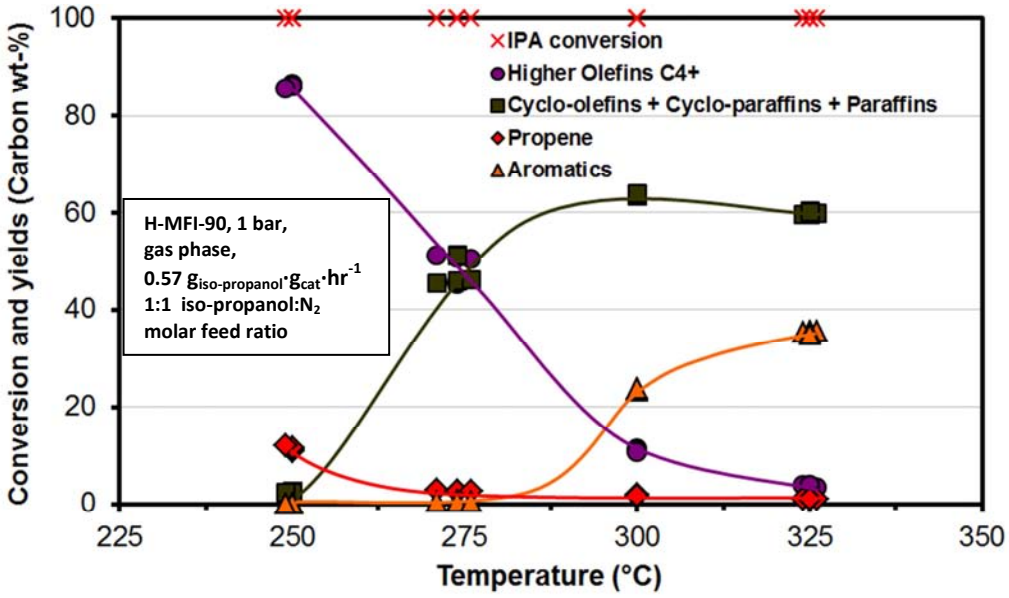

Figure 5-18: Conversion of iso-propanol and yields of the various product fractions as a function of temperature.

6 Discussion

6.1 Thermodynamic limitations relevant to this study

Thermodynamic calculations conducted previously (Nagooroo, 2012) essentially showed that the dehydration of iso-propanol would be completed at reaction conditions pertinent to this study (Section 2.6.3). Hence, only propene, *m*-cresol and thymol were considered in the thermodynamic equilibrium product distribution simulations presented in Figure 6-1 and water was treated as an inert diluent.

Figure 6-1 shows the Arrhenius plot of equilibrium constants for actual experimental results obtained by Fletcher *et al*. (2001b) presented in Figure 2-3, Section 2.6.1 (only the upper edge of the array) and results corresponding to the thermodynamic calculations conducted in this study. Equilibrium constants were calculated from *m*-cresol conversions obtained from results for both cases.

The proximity of the simulated data points to experimental data (left branch), indicate sufficient accuracy of these thermodynamic calculations.

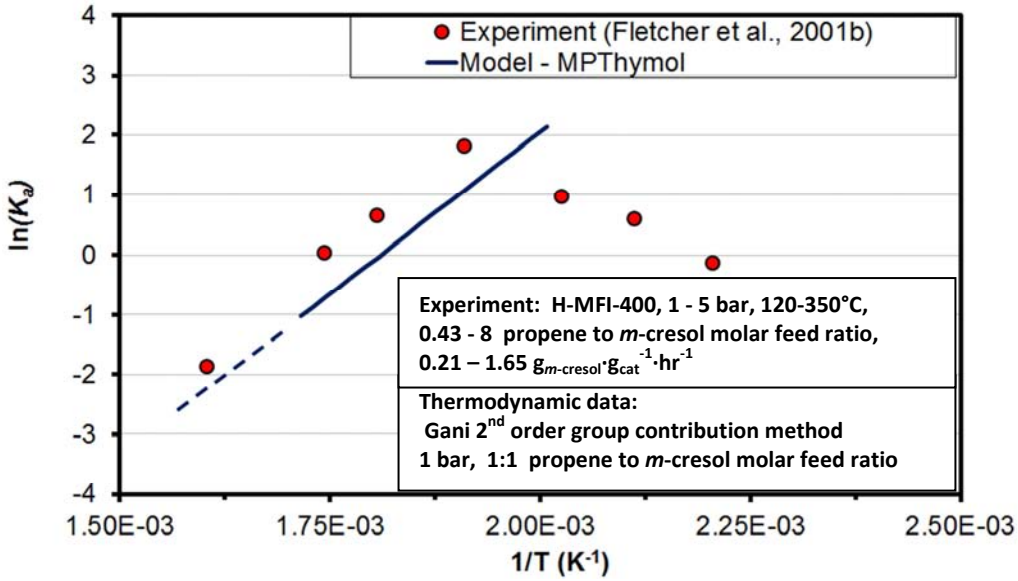

Figure 6-1: Arrhenius plot for the equilibrium constant (K_a) obtained from simulations.

Refer to Appendix A (blue page) for a fold out detailing the components considered in the thermodynamic calculations.

Figure 6-2 presents an Arrhenius plot of *m*-cresol equilibrium conversions (assuming that $X_{m\text{-}cresol}$ is proportional to the reaction rate constant – k at the low conversions presented here) obtained from the said thermodynamic simulations for a range of product distributions considered. Experimentally obtained data points are also displayed in this plot.

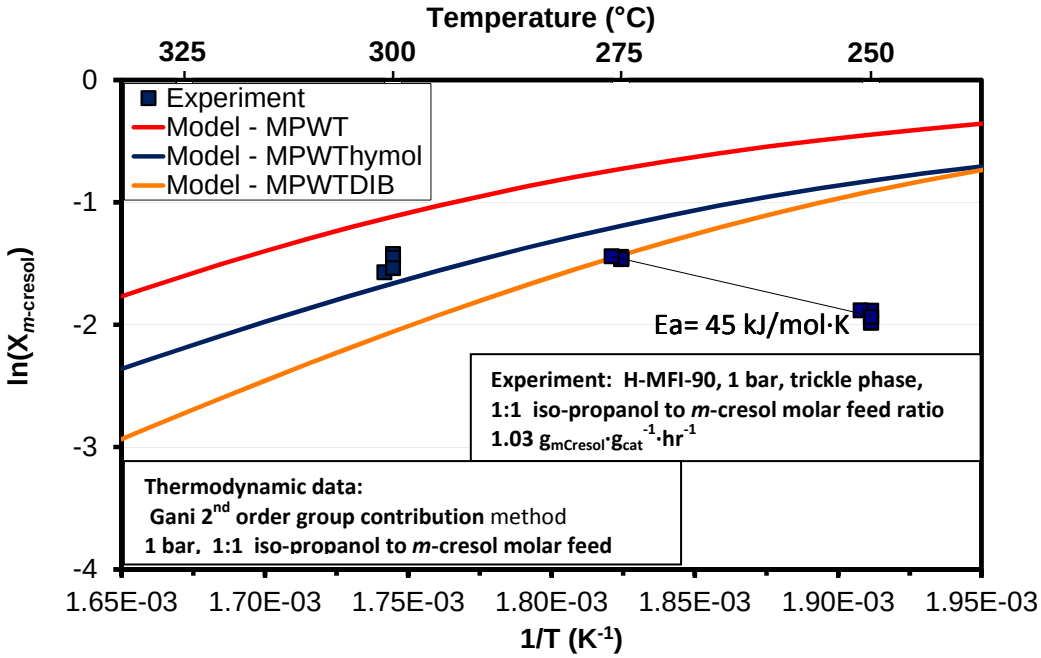

Figure 6-2: Arrhenius plot for *m*-cresol iso-propylation reaction.

Refer to Appendix A (blue page) for a fold out detailing the components considered in the thermodynamic calculations.

Consider firstly the position of simulated curve: **MPWThymol** (*m*-cresol, propene, water and thymol). This curve only takes into account a single alkylation product, namely thymol. The reaction system in which the other thymol position isomers are included in addition- **MPWT** (*m*-cresol, propene, water, thymol and thymol isomers), shows an *m*-cresol equilibrium conversion higher than that for a single isomer only. With further inclusion of butenes, secondary butylated *m*-cresol derivatives and the di-isopropylated *m*-cresol isomers (**MPWTDIB**), there is a reduction in the equilibrium *m*-cresol conversion so that the **MPWTDIB** curve is positioned, below the formerly mentioned **MPWThymol** and **MPWT** curves**.**

The proximity of the experimental data points obtained at 325℃ to the equilibrium conversion curves indicate the approach to thermodynamic equilibrium involving propene, water, *m*-cresol and thymol only (**MPWThymol**). These data points are somewhat higher than the said curve as a result of by-product formation. From these results, one could extrapolate that with inclusion of additional products (i.e. other than *m*-cresol mono-iso-propylated compounds present with more than 3 carbon atoms per *m*-cresol molecule), the equilibrium conversion decreases.

From the theoretical and experimental results, above the conclusion can be drawn that *m*-cresol conversion at elevated temperature (> 275 °C) is subject to

thermodynamic limitations, and these limitations become increasingly inhibiting when compounds other than thymol and its position isomers are formed (i.e. higher alkylated *m*-cresol derivatives). This reveals a significant thermodynamic driving force for the depletion of potential alkylating species by increasing average carbon numbers in the olefin pool, which effectively results in fewer moles of alkylating agent available for reaction with the unreacted *m*-cresol (see Figure 5-2 in Section 5.1).

6.2 Integrity of experimental results

Figure 5-6 shows the results of two space velocity series, each over fresh catalyst charges at equal reaction condition settings and the overlapping data indicates sufficient reproducibility of the experimental procedures.

Similarly, the equal levels of conversion presented in Figure 5-6 corresponding to a 3 - fold difference in linear velocity, indicate that the system is not governed by external mass transfer control. This finding is supported by an approximate activation energy of at least 45 kJ/mol·K, estimated from the experimental data points at 250℃ and 275℃ (Figure 6-2).

In a subsequent study, the absence of internal mass transfer limitations for this particular reaction and catalyst system was verified using the catalyst in extrudate form as delivered (Table 4-1) and in fine milled form (from the extrudates 0.3 – 1 mm) (Shakankale and Thompson, 2012).

Time-on-stream performance shows that the water-free, propene system suffers more rapid deactivation as compared to the systems where water is present. Water appears to alleviate the effect of catalyst deactivation in *m*-cresol iso-propylation over acid zeolite catalysts (see Figure 5-3). Furthermore, recovery in catalytic activity was observed after experiments had been conducted at elevated pressures of 15 bar, when the reaction system is in trickle phase, both in the case of iso-propanol and di-isopropylether (with reference to Section 1.1.1, Figure 5-4 and Figure 5-5). It is therefore suggested that the higher pressure trickle phase conditions could have allowed for a washing effect by which components which caused catalyst deactivation (soft coke) were dissolved and removed, thereby promoting catalyst regeneration. Indeed, the first samples collected after switching to 15 bar reaction pressure were dark in colour consistent with the presence of ‘soft-coke’ species. Samples collected after about 6 hours post-pressure- increase were coloured similar to pre-pressure-increase samples, suggesting that that ‘soft-coke’ deposited under gaseous conditions had been mostly removed within this period under trickle phase.

6.3 Conversion of iso-propanol

The steep temperature decline and equally steep subsequent temperature increase, right at the beginning of the bed (refer to Section 4.4.10, Figure 4-5) is indicative of a rapid iso-propanol dehydration reaction. Furthermore, no iso-propanol was seen in the reactor effluent, even at the least severe conditions applied, i.e. conditions effecting the lowest *m*-cresol conversion such as the lowest temperature and highest space velocity employed. In addition, in previous research involving the same reaction system at milder conditions, the iso-propanol dehydration reaction was reported to proceed much faster than the *m*-cresol alkylation with iso-propanol (Nagooroo, 2012). Therefore, at the comparatively severe reaction conditions applied to this study, direct conversion of *m*-cresol with iso-propanol is unlikely and, the alkylation system observed in this study is thought to involve only *m*-cresol, propene and water.

Both the space velocity (Figure 5-17) and temperature (Figure 5-18) series of dehydration experiments showed that a pool of higher olefins (C_{4+}) formed from the initially introduced iso-propanol with only very small yields of propene. This was observed at reaction conditions equal to those applied for the target reaction (reaction temperature, iso-propanol feed partial pressure and space velocity) but with *m*-cresol substituted by nitrogen. With increasing reaction severity, this olefinic pool was continually converted to other compound fractions as shown in the aforesaid figures. The formation of such a 'pool' of interconverting olefinic species is a typical reaction of olefins over acid zeolite and other solid acid catalysts (O'Connor, 2008; Sealy *et al.,* 1994; van Niekerk, 1996; Garwood, 1983).

In the thymol synthesis experiments at "high" space velocities (above 0.2 $g_{iso\text{-}propanol} \bullet g_{cat}^{-1} \bullet hr^{-1}$ or 0.3 $g_{m\text{-}cresol} \bullet g_{cat}^{-1} \bullet hr^{-1}$), most of the originally formed propene was present in the reactor effluent either as cresylic ring substituents in the liquid fraction or propene in the vapour fraction. At lower space velocities, lower propene yields were observed. Side reactions in which higher olefins (C_{4+}) are formed which also alkylate *m*-cresol, were also seen. This result was in contrast to the far lower propene yields observed in the space velocity experiment at equivalent reaction conditions shown in Figure 5-17. The reaction pathway for propene suggested by the dehydration experiments is therefore representative of the side reactions of propene occurring in alkylation experiments (with m-cresol present), however, these reactions occur at a slower rate in the alkylation systems.

6.4 Thymol synthesis

6.4.1 Effect of pressure and water

The logarithmic response *m*-cresol conversion with increasing pressure (Figure 5-12), points to a reaction order close to 1 in respect of total pressure, as has been reported by others for such systems (Nagooroo, 2012). Moreover, at low time-on-stream, when catalyst deactivation is minimal, systems with iso-propanol and di-isopropylether as alkylating agents show lower initial *m*-cresol conversion than is the case for propene (Figure 5-3), quite possibly reflecting a lower effective reactant (propene) partial pressure. Upon complete dehydration of iso-propanol and di-isopropylether, water constitutes 33% and 20% respectively of the propene/water/-*m*-cresol reaction mixture, while in the case of a propene feed the reaction mixture is water-free. To allow for a comparison, the resulting differences in the effective propene and *m*-cresol partial pressures (of the said water containing alkylating agents, reported in Section 4.4.7, Table 4-5) were accounted for by manipulation of experimental results to simulate the absence of water. The computed results-'**Water-free, First order**' for both IPA and DIPE closely resemble the propene data series at low time on stream values (see curves in Figure 5-3). Therefore, the lower initial *m*-cresol conversion in the case of IPA and DIPE feeds can be ascribed to an artificial effect by which the presence of water lowers reactant (propene) partial pressure, resulting in a reduced reaction rate and conversion.

The above findings seem also to suggest that the presence of water vapour has no direct effect on catalyst activity, yet extended time-on-stream performance shows that the water-free propene system suffers more rapid deactivation as compared to the systems where water is present such that water appears to moderate the extent of catalyst deactivation in *m*-cresol iso-propylation over the zeolite catalyst.

Furthermore, a limited recovery in catalytic activity was observed for experiments in which the system was operated at elevated pressures (15 bar) and where a trickle phase regime exists for both iso-propanol and di-isopropylether alkylating agents (Section 1.1.1). It is likely, therefore, that the higher pressure trickle phase conditions induce a solvent washing whereby species which caused catalyst deactivation (soft coke) are removed under purely vapour phase conditions. Indeed, the first liquid samples collected after the pressure induced trickle-phase, were dark in colour, as

opposed to the generally straw coloured liquids derived from vapour phase conditions.

Given that the data presented in Figure 5-12 (Section 5.3.3) is derived from systems sufficiently far from thermodynamic equilibrium, it appears that the variation of total pressure and the concomitant change of water vapour pressure, have hardly any direct effect on thymol selectivity. This is consistent with other claims that pressure influences thymol selectivity mostly indirectly through its influence on reaction kinetics and overall *m*-cresol conversion level (Nagooroo, 2012).

6.4.2 Effect of temperature

It was found that, unlike the effect of pressure, increasing temperature not only results in increased conversion and thymol yields but also directly influences selectivity to the various product fractions (in addition to the indirect effect via changing conversion), in particular at reaction temperatures below 275℃.

Figure 6-3 shows increasing thymol selectivity with respect to increasing reaction temperature in the range 250℃ - 275℃, at high spa ce velocity. According to Nagooroo (2012) this increase in thymol selectivity results from a shift in the reaction pathway, with a decreasing contribution via the isopropyl-3-tolylether route (O-alkylation) and an increasing contribution via the *m*-cresol propylation route (C-alkylation) - see Section 2.5 for review of reaction mechanisms.

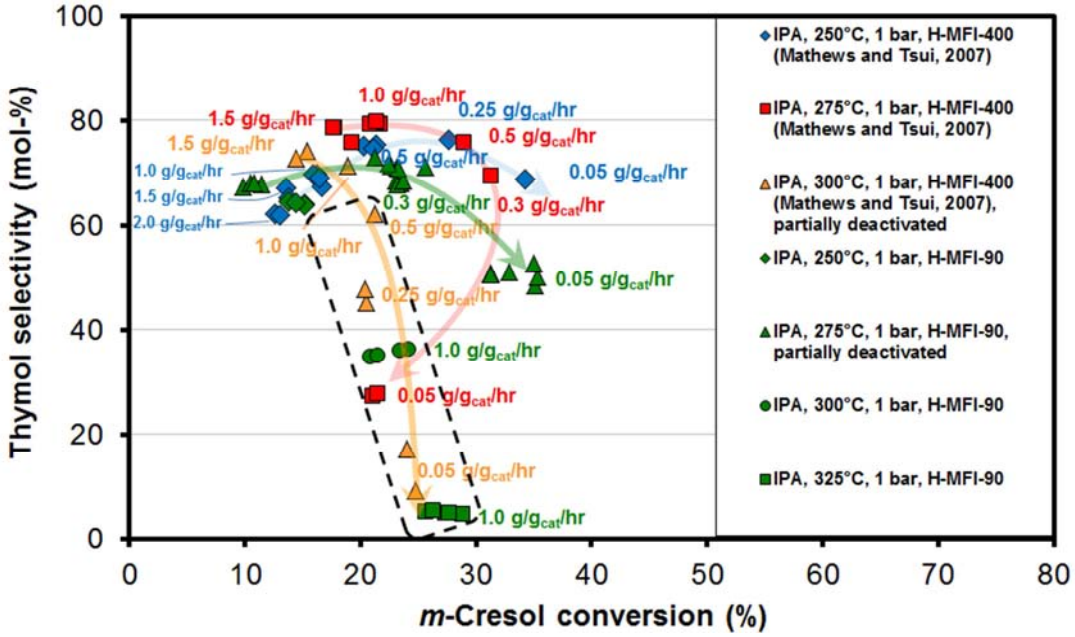

Figure 6-3: Thymol selectivity as a function of *m*-cresol conversion

With further increasing temperature above 275℃, thymol selectivity decreases sharply whilst a marginal increase in *m*-cresol conversion was observed. In addition, under these (severe) conditions, other products including cresol isomers, cresol-cresol transalkylation products (xylenols and phenol), n-propylated *m*-cresol and *m*-cresol alkylated with higher olefins (C_{4+}), appear increasingly in the reaction product.

To indicate the extent of the *m*-cresol isomerisation, the *m*-cresol alkylation conversion is plotted alongside the *m*-cresol conversion as a function of temperature in Figure 6-4. It is seen that negligible *m*-cresol isomerisation takes place at temperatures below 275℃. Above 275℃, even though *m*-cresol conversion increases only marginally, a substantial amount of *m*-cresol is consumed in isomerisation reactions such that the number of cresol rings alkylated with C_{3+} actually decreases with increasing temperature (above 275℃).

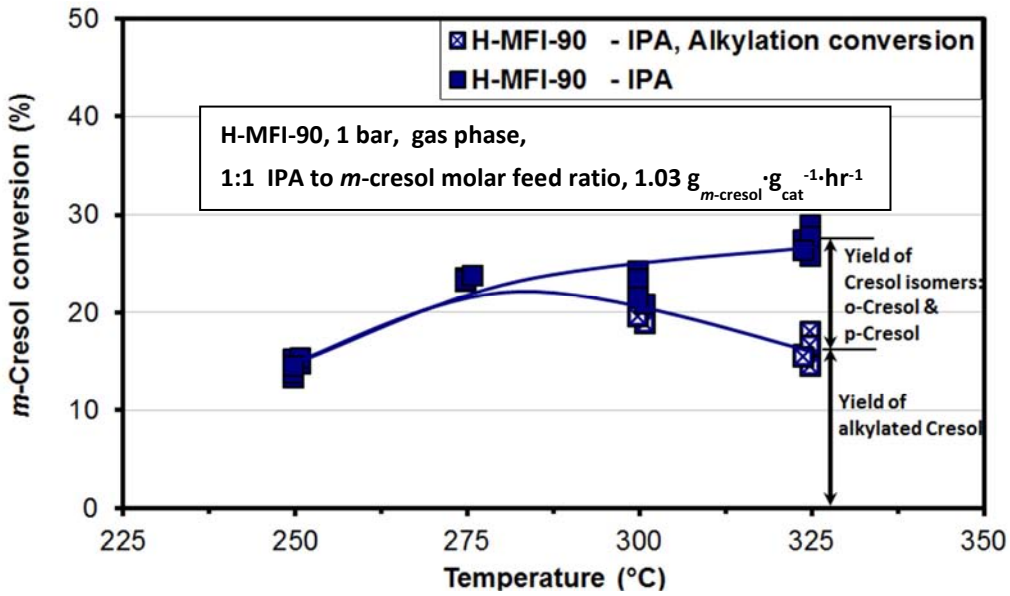

Figure 6-4: *m*-Cresol conversion and alkylation conversion vs. temperature.

6.4.3 Effect of space velocity

For the sake of clarity, selectivity-conversion data is considered separately corresponding to the "high space velocity" and the "low space velocity regimes" of the general *m*-cresol conversion vs. space velocity plot of Figure 5-7. In addition these data will be considered in terms of a "kinetically favoured" product fraction (thymol, 3-methyl-2-isopropyl-phenol, 3-methyl-4-isopropyl-phenol and di-propylated *m*-cresol) and a "secondary products" fraction (C-10, lights, 3-methyl-5-isopropyl-phenol and heavies) for data at 275℃, below the point where *m*-cresol isomerisation becomes significant.

At high space velocities (Figure 6-5) selectivity to the "kinetically favoured" products (which form immediately) is high and decreases only slightly with decreasing space velocity (while conversion increases). This trend was mirrored by an equally marginal increase in selectivity to the "secondary products" fractions.

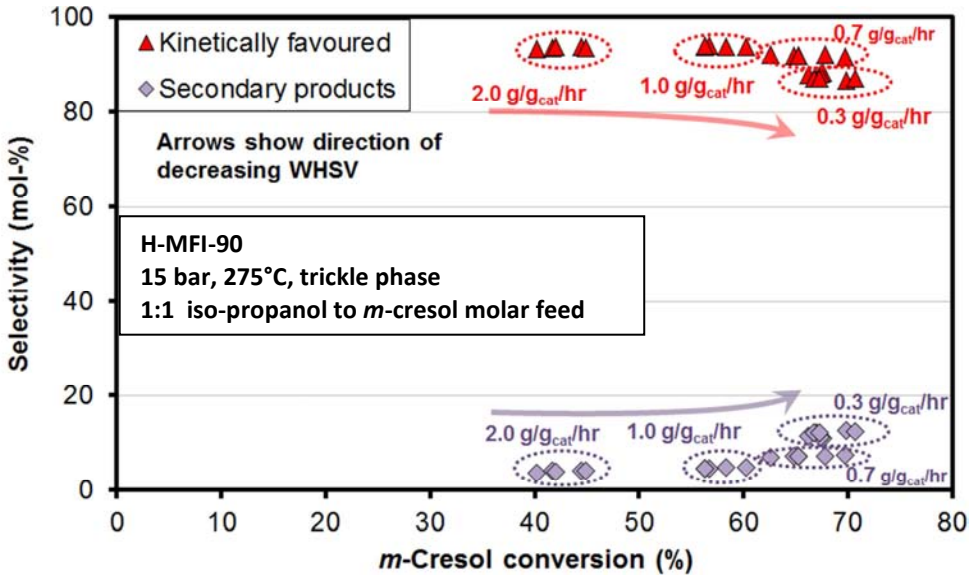

Figure 6-5: Selectivity to "kinetically favoured" and "secondary poducts" vs. *m*-cresol conversion in the "high space velocity" regime.

Refer to Appendix A (blue page) for a fold out detailing the various product fractions.

Thymol selectivity (Figure 6-6) increases only marginally with increasing *m*-cresol conversion (and corresponding decrease in space velocity). This trend has also been attributed to a shift of reaction mechanism from O-alkylation to C-alkylation (Nagooroo, 2012).

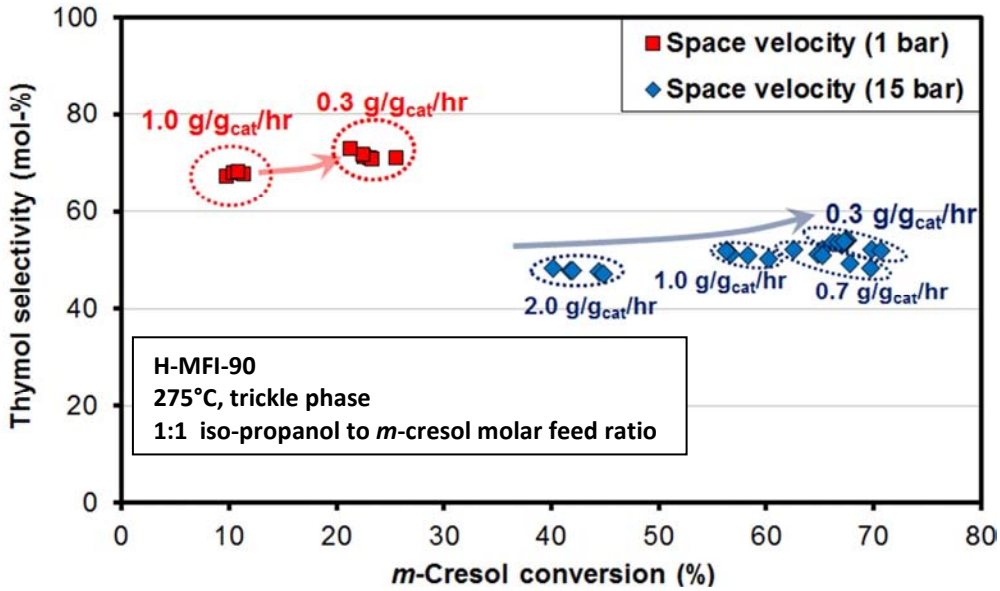

Figure 6-6: Thymol selectivity vs. *m*-cresol conversion in "high space velocity" regime.

In contrast to the trends observed in the "high space velocity" regime, selectivity to the "kinetically favoured" fraction decreases substantially with decreasing space velocity (Figure 6-7) and, correspondingly, an equivalent increase in selectivity to "secondary products" is seen. Similarly, thymol selectivity (achieved at 15 bar) decreases, as shown in Figure 6-8.

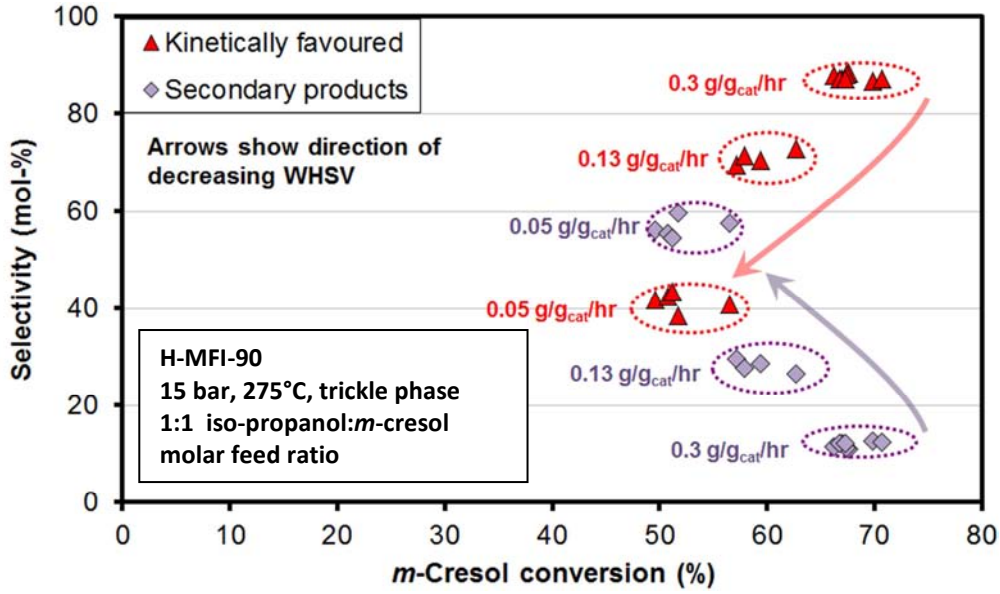

Figure 6-7: Selectivity to "kinetically favoured" and "secondary poducts" vs. *m*-cresol conversion in "low space velocity" regime.

Refer to Appendix A (blue page) for a fold out detailing the product fractions.

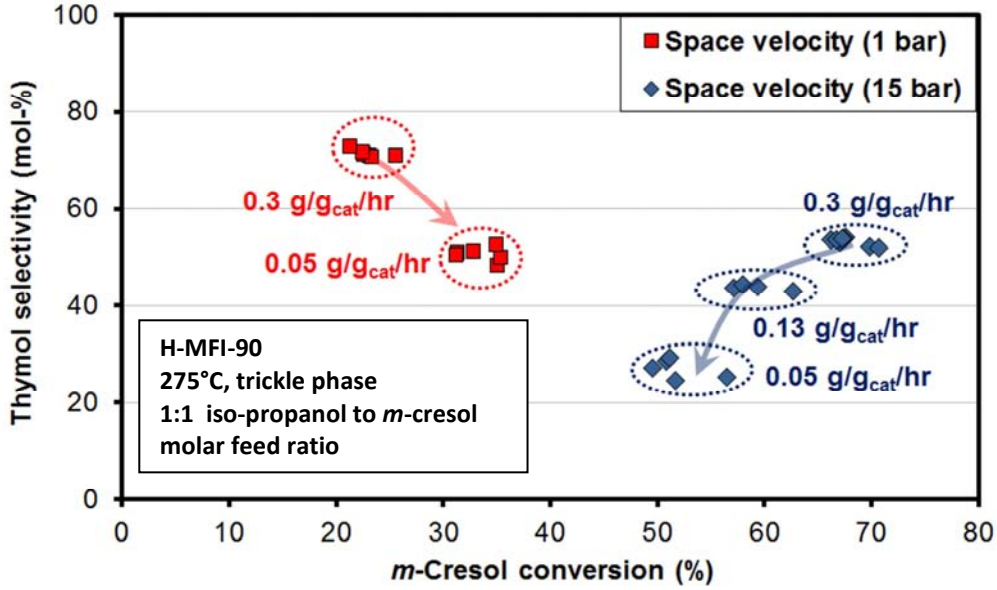

Figure 6-8: Thymol selectivity vs. *m*-cresol conversion in "low space velocity" regime.

The yield curves of Figure 5-8 show that, with decreasing space velocity, the "kinetically favoured" isomers were converted in favour of the "secondary products" in the "low space velocity" regime. In this experiment, which employed a comparatively aged catalyst of lower activity than that used in the preliminary experiments of Mathews and Tsui (2007) at 1 bar and 275℃,(Figure 5-7) the same trend with respect to *m*-cresol conversion was not observed. Even so, the relationship between thymol selectivity and space velocity in the "low space velocity" regime was similar (Figure 5-10 and Figure 6-8), and this declining thymol selectivity is characteristic of an approach to thermodynamic equilibrium as discussed in Section 2.6.1. At higher temperatures (above 275℃), the approach to thermodynamic equilibrium is more rapid as a consequence of the increased reaction kinetics and the characteristic decrease in thymol selectivity is observed at higher space velocities at these temperatures.

The same deactivated catalyst was subsequently operated at higher pressure (15 bar) and under these conditions the so-called "volcano curve" in respect of *m*-cresol conversion was observed (Figure 5-6 and Figure 5-7). As in the preliminary result (Mathews and Tsui, 2007), declining *m*-cresol conversion, was accompanied by declining thymol selectivity at space velocities below 0.5 $g_{m\text{-cresol}} \cdot g_{cat}^{-1} \cdot hr^{-1}$.

The elevated pressure allowed also for a higher equilibrium *m*-cresol conversion and the higher pressure also increased reaction rate, consequently, the *m*-cresol conversion obtained at higher pressures was at a higher level compared to that obtained at lower pressure. In all cases where the "volcano curve" was seen within the range of space velocities investigated, the *m*-cresol conversion was in close proximity to the equated thermodynamic equilibrium *m*-cresol conversion value (Figure 5-7).

6.4.4 Origin of the "volcano curve" for *m*-cresol conversion

Figure 6-9 presents the same *m*-cresol conversion vs. space velocity data of Figure 5-6 and Figure 5-7 but plotted in a vertical orientation and representing a lengthwise section through the catalyst bed of the fixed bed reactor. The primary Y-axis (left) represents the length of the catalyst bed (from top) while the X-axis depicts conversion. Space velocities corresponding to the individual groups of data points are indicated on the secondary Y-axis (right). It should be noted that the bed-length axis in this figure is linear and consequently, the space velocity axis is logarithmic and correspondingly, the shape of the conversion curve changes, - it appears compressed at the high space velocities (top end) and expanded at the low space velocities (bottom end) - in comparison to the curves in Figure 5-6 and Figure 5-7. Consequently, Figure 6-9 describes the chemical progression of the thymol synthesis system as the reaction mixture proceeds down the catalyst bed, coming into contact with more and more catalyst which is equivalent to a constantly declining space velocity (or increasing reaction / contact time), as indicated on the secondary Y-axis. The composition of the reaction mixture with position (primary Y-axis, left) in the reactor is thus given by the product composition for the experiments of chapter 5 at equivalent space velocity (secondary Y-axis, right).

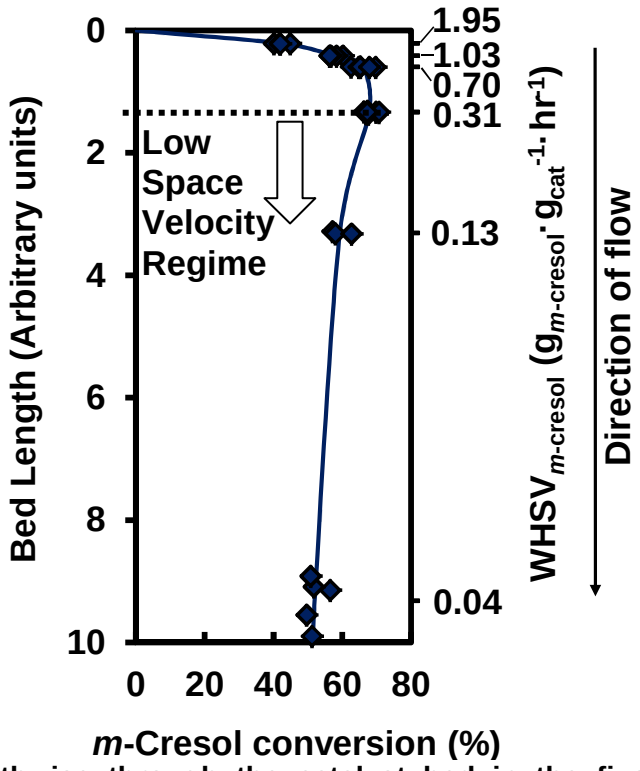

Figure 6-9: Lengthwise through the catalyst bed in the fixed bed reactor employed for thymol synthesis.

The declining *m*-cresol conversion with decreasing space velocity seen in the "low space velocity" regime (space velocity range 0.31 – 0.04 g/g·hr in Figure 6-9) suggests that the alkylated *m*-cresol product generated in the "high space velocity" (space velocity range 1.95 – 0.7 g/g·hr in Figure 6-9) is dealkylated, thereby reintroducing *m*-cresol back into the reaction mixture in the "low space velocity" regime further down the catalyst bed, as described below.

When the feed mixture enters the catalyst bed (from the top of the bed) and passes through the uppermost layers of catalyst, the co-fed iso-propanol is very rapidly and almost completely converted mostly to propene and water (as described in Section 5.4) and some isopropyl-3-tolyl-ether. The resulting propene, as the effective alkylating agent, alkylates *m*-cresol but at a rate much slower than the iso-propanol dehydration reaction. Initially this propylation forms mostly thymol and smaller amounts of its 2- and 4-isopropylated isomers as shown selectivity to the thymol and the "kinetically favoured" fraction in Figure 6-6 and Figure 6-5, respectively - the latter isomers being the other, albeit, less reactive positions on the *m*-cresol ring which become occupied also when the ether rearranges to thymol and these isomers in accordance with the mechanism described by Nagooroo (2012). *m*-Cresol conversion and, correspondingly, the yields of these isomers increase with increasing mass or volume of catalyst passed through by the reaction mixture (as shown in Figure 5-8), i.e. further down the catalyst bed. The comparatively small increase in conversion observed with decreasing space velocity in the "high space velocity" regime (top of the catalyst bed), from about 45 to 65 percentage points when the space velocity was reduced almost four-fold from its initial value, can be attributed to an approach to the thermodynamic equilibrium conversion as per the Arrhenius plot in Figure 6-2.

The above trend in conversion with respect to space velocity is as expected. However, after having passed through about 15% of the catalyst bed (corresponding to the "high space velocity" regime), *m*-cresol conversion and thymol formation cease (effectively) as reflected by the decreasing thymol yield in Figure 5-8.

This decline in thymol content, and also that of its 2- and 4-isopropylated position isomers, can partly be attributed to their consumption via isomerisation to the 5-isopropylated isomer and their conversion to other C10 compounds (mostly n-propylated *m*-cresol isomers) as can be seen in Figure 5-8 and Figure 5-9.

Further down the catalyst bed, reactions other than mono- and di-isopropylation of *m*-cresol or the isomerisation of the mono-isopropylated *m*-cresol compounds dominate, in particular the formation of alkyl-methylphenols with alkyl side chains longer than C_3 as reflected in the increasing yield of "Heavies" with decreasing space velocity (Figure 5-8 and the determination of their nature in Section 4.5.1). The C_4-C_8 side chains found in these "Heavies" may arise from a 'pool' of olefins, higher than propene, that form through propene oligomerisation and subsequent higher oligomer cracking, the presence of which has been reported in other studies concerning the reaction of small olefins over acid zeolites and other solid acid catalysts (O'Connor, 2008; Sealy *et al.,* 1994; van Niekerk, 1996; Wichterlová and Čejka, 1993; Garwood, 1983) and which has also been demonstrated to occur under the reaction conditions applied in this study (Section 5.4).

Both the aforementioned reactions, namely the formation of a 'pool' of higher olefins and their alkylation of *m*-cresol eventually consume more propene per ring alkylated than that provided by the 1:1 molar stoichiometric feed mixture (which is stoichiometric with respect to mono isopropylation, i.e. the formation of thymol and its position isomers). They are all secondary or even tertiary reactions, occurring further down the catalyst bed after thymol formation and only after the olefin pool has been established and, consequently, these reactions proceed mostly further down the catalyst bed, only, once thymol formation from propene and *m*-cresol has equilibrated in the top ("low space velocity" regime) of the bed. As a result, co-reactant propene is 'removed' from the ***m*-cresol + propene ⇔ thymol** equilibrium mixture that has established, via dealkylation of the initially formed compounds followed by transfer of the resulting propene to the olefinic pool - and consequently, the *m*-cresol / propene / thymol equilibrium shifts back to the left, as evidenced by the declining cresol conversion and thymol yields further down the bed (see Figure 5-9 and Figure 5-8) which show the selectivity and yield of the compounds whose isopropyl groups are located in reactive position essentially the 2-, 4- and 6-isopropylated *m*-cresol isomers and corresponding di-propylated *m*-cresol compounds, decreasing with decreasing space velocity in the "low space velocity" regime of the bed.

Correspondingly, after the rapid, initial mono-isopropylation phase which takes place in the top section of the catalyst bed is over, the ratio of the average carbon number of (combined) new side chains to *m*-cresol rings increases (whereby 'combined' means that, for example, two isopropyl groups count as C_6), from 3.4 after a few layers of catalyst to beyond 4 further down the catalyst bed as shown in Table 6-1 (see Figure 5-6 for reaction conditions employed and Section 4.6.6 for the calculations).

Table 6-1: Average side chain length as a function space velocity

Space velocity ($g_{m\text{-cresol}} \cdot g_{cat}^{-1} \cdot hr^{-1}$)	**Average number of total carbon atoms in side chains (in addition to the original methyl group) of cresylic rings**
1.95	3.4
1.01	3.5
0.7	3.7
0.31	3.7
0.13	4.0
0.04	4.1

Similar findings have been reported for the acid catalysed isomerisation of cresols (Böhringer, 2009) and the transalkylation of xylenols with phenol (Moeketsi, 2007) In the cresol isomerisation system, the approach to thermodynamic equilibrium resulted in consumption of the primary product to form transalkylation products via side reactions (Böhringer, 2009). Similarly, with decreasing space velocity (and the approach to equilibrium), the phenol/xylenol transalkylation system exhibited increasing yields of higher methylated phenols and a concomitant re-introduction of phenol into the reaction product. As a result, the phenol conversion passed through a maximum with decreasing space velocity (Moeketsi, 2007).

7 Conclusions and Recommendations

Systems with water present exhibited a slower rate of deactivation as compared to systems with no water present over H-MFI-90. Moreover, it is postulated that a solvent mediated washing effect which frees the catalyst of soft coke can be achieved by means of a pressure-induced liquid or trickle phase over the catalyst.

The depression in the temperature profile seen in the upper zone of the catalyst bed can be attributed to the endothermic dehydration of the alkylating agent (whether iso-propanol or di-isopropylether is used). Increased dilution of the catalyst bed with SiC was effective in reducing the extent of the depression. In separate experiments it is observed that iso-propanol completely dehydrates at the top of catalyst bed and that propene is the effective alkylation agent in all experiments.

As per previous studies involving thymol synthesis with propene and *m*-cresol (O' Connor *et al.,* 2003; Nagooroo, 2012), temperature affected thymol selectivity directly, with thymol selectivity decreasing, with increasing temperature. The maximum thymol yield also being limited by thermodynamic equilibrium.

It has been established that with the decreasing space velocity, the thymol / *m*-cresol / propene reaction system approaches thermodynamic equilibrium. Effectively, the formation of thymol ceases and competing reactions start to occur. Under these conditions a fraction of compounds consisting of *m*-cresol rings with C_4-C_8 side chains (with carbon numbers higher than that of propene) form by alkylation of *m*-cresol via a pool of olefins. As a consequence, the system becomes propene depleted and a driving force for the dealkylation of kinetically favoured isomers (such as thymol) arises, such that, a decrease in thymol yield is observed with further decreasing space velocity and the counter- intuitive volcano curve in respect of cresol conversion arises.

Based on the findings of this study, the following recommendations are made in respect of future studies aimed at optimising the thymol synthesis process, viz. that:

- a maximum temperature of 275℃ is applied;
- the use of higher pressures and mass flows, than those employed in this study, be considered;

- the effect of alkylating agent partial pressure in the reactant mixture be investigated, i.e. that the feed molar ratio be varied;

- after 72 hours on-stream and before commencing with further experiments, the system be operated at 325℃ for 6 hours to obtain q uasi steady state catalyst performance (at higher temperature, the aforesaid quasi steady state will be obtained more rapidly and it is expected that maintaining this condition for 6 hours only, will not deactivate the catalyst excessively);

- the volumetric dilution of the catalyst bed over the initial region be increased from 1:5 (Catalyst: SiC) to some higher value so as to avoid the depression of the temperature resulting from iso-propanol dehydration.

8 References

Ambrose, D., “Correlation and Estimation of Vapour-Liquid Critical Properties. I. Critical Temperatures of Organic Compounds,” National Physical Laboratory, Tedington, *NPL Rep. Chem.* vol. **92**, 1978 (corrected 1980).

Ambrose, D., “Correlation and Estimation of Vapour-Liquid Critical Properties. II. Critical Temperatures of Organic Compounds,” National Physical Laboratory, Tedington, *NPL Rep. Chem.* vol. **98**, 1979

Areshidze, K. I., Benashvili, E. M. and Chkheidze, K. I., “Alkylation of phenol by N-propyl and isopropyl alcohols in the presence of synthetic zeolites.”, Soobshcheniya Akademii Nauk Gruzinskoi SSR, vol. **75**, 2nd ed., 1974, pp. 345-348.

Ashford, R.D. (1994). Thymol. Ashford’s Dictionary of Industrial Chemicals. London: Wavelength.

Baerlocher, Ch., Meier, W.M. and Olson, D.H. (2001). Atlas of zeolite framework types, 5th revised edition. Amsterdam: Elsevier

Barnes, N. and Vallabh, H., “Shape-selective phenol alkylation”, Final year project report, Department of Chemical Engineering, University of Cape Town, 2005.

Bartholomew, C.H., “Mechanisms of catalyst deactivation”, *Applied Catalysis A: General,* 2001, vol. **212**, pp. 17-19.

Benson, S.W. and Buss, J.H., “Additivity Rules for the Estimation of Molecular Properties. Thermodynamic Properties”, J. Chem. Phys.,1958, vol. **29**, 3rd ed., pp. 279-305.

Benson, S.W., “Thermochemical Kinetics”, Wiley, New York, 1968, Chapter 2

Benson, S.W., Cruickshank, F.R., Golden, D.M., Haugen, G.R., O’Neal, H.E., Rodgers, A.S., Shaw, R. and Walsh, R., “Additivity Rules for the Estimation of Thermochemical Properties,” Chem. Rev., vol. **69**, 3rd ed., 1969, pp. 279-324.

.

Botelho, M.G., “The minimum inhibitory concentraiton of oral antibacterial against cariogenic organisms”, Microbios, **vol.** 103, 2000, pp. 31-41.

Böhringer, W.F.W., Personal communication, 2007.

Callanan van Steen, L., “Methanol ammination over hydrothermally treated zeolites RHO and Mordenite”, PhD Thesis, Catalysis Research Unit, University of Cape Town, 1999.

Calcott, W. S., Tinker, J. M. and Weinmayr, V., ”Hydrofluoric acid as a condensing agent. II. Nuclear alkylations in the presence of hydrofluoric acid.”, Journal of the American Chemical Society ,vol. **61**, 1939, pp. 1010-1015, abstract CAN 33:38201.

Chaplin, J.A. (2002). The process for preparing (-)-Menthol and similar compounds. WO 2002/036795.

Clark, G.S., **“**Menthol - Its natural sources, history, world trade, producers, substitutes, derivatives and analogs”, Perfumer & Flavorist, vol. 23, 5th ed., 1998, pp. 33.

Clark, G.S., “Aroma Chemical Profile: Menthol - History, world consumption, synthetics, by-products, substitutes and derivatives.”, Perfumer & Flavorist, vol. 32, 12th ed., 2007, pp. 38.

Constantinou, L. and Gani, R.," New Group Contribution Method for estimating properties of Organic Compounds", AIChE J., vol. **40/10**, 1697,(1994).

Csicsery, S.M., “Catalysis by shape selective zeolites – science and technology”, Pure and Appl. Chem. vol. 58, 6th ed., 1986, pp. 841 – 856.

Daubert, T. E. and Thomas E., “Physical and thermodynamic properties of pure chemicals”, Taylor & Francis, Philadelphia, 1999.

Derouane, E.G., “New aspects of molecular shape selectivity: Catalysis by zeolite ZSM-5”, *Catalysis by Zeolites*, 1990, pp. 5-17.

Dirdy, N., Dubreuil, L. and Pinkas, M., “Antibacterial activity of thymol, carvacrol and cinnamaldehyde alone or in combination”, Pharmazie, **vol**. 48, 1993, pp. 301.

Eckroth, D., Othmer, D.F., Kirk, R.E. and Grayson, M, *Kirk-Othmer Encyclopedia of Chemical Technology*, Wiley, 3rd ed., New York, 1984, pp 831-856.

Fiege, H., Phenol derivatives. *Ullmann’s Encyclopedia of Industrial Chemistry*. Wiley-VCH, Weinheim, vol**. 25**, 6th ed., 2003, pp. 605.

Fletcher, J.C.Q., Quoted by: Isaacs, Z., “New process could save millions for South African chemical industry”, Engineering News, 2004.

Fletcher, J.C.Q., Vaughan, James S.and O'Connor, Cyril T., “Heterogeneous oligomerization of propene over heteropoly acids.” Preprints - American Chemical Society, Division of Petroleum Chemistry, vol. 36, 4th ed., 1991, pp. 605-612.

Fletcher, J.V., Böhringer, W. and Fletcher, J.C.Q. (2001a). Zeolite Catalysts for Thymol synthesis. Phase II Part A (unpublished report). Centre for Catalysis Research. University of Cape Town.

Fletcher, J.V., Böhringer, W. and Fletcher, J.C.Q. (2001b). Parameter variation/optimisation – Gas Phase and Mixed Phase conversion. Phase II Part B (unpublished report). Centre for Catalysis Research. University of Cape Town.

Fletcher, J.V., Böhringer, W. and Fletcher, J.C.Q. (2002). Catalysts for conversion of thymol isomers: Catalyst screening and parameter variation. Phase III Part B (unpublished report). Catalysis Research Unit. University of Cape Town.

Fletcher, J.V., Böhringer, W. and Fletcher, J.C.Q., “ Selective Synthesis of Thymol from m-Cresol over Zeolite Catalysts”, SAIChE conference, 2003.

Fogler, H.S., “Elements of Chemical Reaction Engineering”, 3rd Ed., Prentice Hall, New Jersey, 2002, pp. 709-710, 766.

Gakh, I. G., Babin, E. P. and Gakh, L. G. “Synthesis of 2,4,6-triisopropylphenol.”, Trudy IREA, vol. **29**, 1966, pp. 319-322, abstract
CAN 67:53814.

Garwood, W.E., “Conversion of C_2-C_{10} to Higher Olefins over Synthetic Zeolite ZSM-5”, Intrazeolite Chemistry, ACS Symposium Series, vol. 218, chapter 23, 1983, pp. 383-396.

Genvresse, P., “Synthesis with Aluminium Chloride”, Comptes Rendus Hebdomadaires des Seances de l’Academie des Sciences, vol. **116**, 1893, pp. 1065-1067, abstract CAN 0:81322.

Grabowska, H. and Wrzyszcz, J., “C-alkylation of m-cresol with n- and iso-propanol over iron catalyst.”, *Res. Chem. Intermed.*, vol. **27,** 2001a **,** pp. 281 – 285.

Grabowska, H., Mista, W., Trawczynski, J., Wrzyszcz, J. and Zawadzki, M., “A method for obtaining thymol by gas phase catalytic alkylation of m-cresol over zinc aluminate spinel.”, *Appl. Catal. A: General* , vol. **220,** 2001b, pp. 207 - 213.

Hahn, W. (1963). Process for the production of ortho-substituted phenols. *DE 1,142,873/US 3,290,389* (assigned to Farbenfabriken Bayer AG, Leverkusen, Germany).

Harmer, M.A.and Qun, S., “Solid acid catalysis using ion-exchange resins”, Applied Catalysis A: General, vol. 221, Issues 1-2, 2001, pp. 45-62.

Heise, R., “Synthesis of hydrocarbons”, Berichte der Deutschen Chemischen Gesellschaft, vol**. 24**, 1891, pp. 768-772.

Helander I.M., Alakomı H.L., Latva-Kala K., Mattıla-Sandholm T., Pol I., Smıd E.J., Gorrıs L.G.M.,Von Wrıght A. (1998): Characterization of the actionof selected essential oil components on gram-negative bacteria. Journal of Agricultural and Food Chemistry, vol. **46**, 1998, pp. 3590–3595.

Ipatiew, W., Orlow, N. and Petrow, A., "The reaction between phenol and n-propylalcohol at high temperatures and pressures.", Berichte der Deutschen Chemischen Gesellschaft, vol. **60**, 1927, pp. 1006-1008.

Isaacs, Z., "New process could save millions for South African chemical industry", Engineering News, 26 March 2004

Joback, K.G., "A Unified Approach to Physical Property Estimation Using Multivariate Statistical Techniques", S.M. Thesis, Department of Chemical Engineering, Massachusetts Institute of Technology, Cambridge, MA, 1984.

Joback, K.G. and Reid, R.C., "Estimation of Pure-Component Properties from Group-Contributions", Chemical Engineering Communications, voI. **57**, issue 1 & 6, 1987, pp. 233 – 243.

Kehiaian, H.V. and Lide, D.R., "CRC Handbook of Thermophysical and Thermochemical Data", CRC Press, Florida, 1994, pp. 42.

Klemm, L.R. and Taylor, D.R., "Alumina-Catalyzed Reactions of Hydroxyaromatic Ketones. 9. Reaction of Phenol with 1-Propanol" Journal of Organic Chemistry, vol. **45**, 22nd ed.,1980a, pp. 4320-4326.

Klemm, L.R. and Taylor, D.R., "Alumina-Catalyzed Reactions of Hydroxyaromatic Ketones. 9. Reaction of Phenol with 2-Propanol", Journal of Organic Chemistry, vol. **45**, 22nd ed. ,1980b, pp. 4326-4329.

Korenskii, V. I., Plyusnin, V. G., Butina, I. V., Lysenko, A. P. and Shevchenko, N. A., "Alkylation of phenol by propylene in the presence of hydrogen fluoride.", Trudy Instituta Khimii, Akademiya Nauk SSSR, 1968, **vol.** 16, pp. 34-42, abstract CAN 70:87191

Krause, E.L., Ternes, W., "Bioavailability of the antioxidative thyme compounds thymol and p-cymene-2,3-diol in eggs", Eur Food Res Technol, vol. 209, 1999, pp. 140–144.

Kukard, R., (2008). The effect of zeolite type on the hydrocracking of long n-paraffins. MSc. Thesis. Centre for Catalysis Research. University of Cape Town.

Kuskov, V. K.; Filippova, G. F., "Preparation of alkylphenols from phenol boric acid esters and alcohols.", Zhurnal Obshchei Khimii, **vol**. 29, 1959, pp. 4063-4069, abstract CAN 54:110223.

Leffingwell, J.C. interview granted to McCoy, J., published in "Hot Market For A Cool Chemical", Chemical and Engineering News, vol. **88**, 35, 2010, pp. 15-16.

Lydersen, A.L., "Estimation of Critical Properties of Organic Compounds" University of Wisconsin, Coll. Eng., Eng. Exp. Stn. Rept. 3, Madison, WI, 1955.

Marais, S.F. (2003). Personal communication with Böhringer, W. (and affiliation). CSIR Bio/Chemtek, Modderfontain, South Africa.

Marczewski M., Perot G. and Guisnet M., "Alkylation of aromatics. Kinetics of phenol alkylation with methanol", Reaction Kinetics and Catalysis Letters, vol. **57**, 1st ed., 1996, pp. 21-27.

Marrero-Marejón, J., and Pardillo-Fontdevila, "Estimation of pure compound properties using group-interaction contributions", AIChe J., vol. 45, 3rd issue, 1999, pp. 615-621.

Matthews, D., Tsui, D., "Synthesis of Thymol via Propylation of m-Cresol and C3-alcohols", Final year research report completed in fulfilment of the requirements for CHE4045Z, Department of Chemical Engineering, University of Cape Town, 2007.

McCoy, M. "Hot Market For A Cool Chemical", Chemical and Engineering News, vol. 88, 35, 2010, pp. 15-16.

McMurry, J., "Fundamentals of organic chemistry", 3rd ed., Wadsworth Inc., Belmont, 1994, pp. 106.

Mikovsky, R.J. and Marshall, J.F., " Random aluminium-ion siting in the Faujasite lattice", *Journal of Catalysis*, vol. **44**, 1976, pp. 170-173.

Milos, M., Mastelic´, J., Jerkovic, I., Katalinic, V., “Chemical composition and antioxidant activity of the essential oil of oregano (Origanum vulgare L.) grown wild in Croatia”, Rivista Italiana Eppos, **vol.** Jan., 2000, pp. 617–624.

Moon, G., ” Alkylation of phenol with methanol over H-ZSM-5, H-Beta, H-Mordenite, H USY and H-MCM-22.”, PhD Thesis. Catalysis Research Unit. University of Cape Town, 2003.

Nagooroo, S., “Thymol Synthesis via Alkylation of m-cresol with isopropanol, The effect of the SiO2/Al2O3 ratio of H-MFI catalysts on catalyst activity and thymol selectivity”, MSc Thesis, Department of Chemical Engineering, University of Cape Town, 2012.

Nitta, M., Aomura, K. and Yamaguchi, K. (1974a). Alkylation of phenols. II. Selective formation of thymol from m-cresol and propylene with a □-alumina catalyst. Bull. Chem. Soc. Japan 47 2360 - 2364.

Nitta, M., Yamaguchi, K. and Aomura, K. (1974b). Alkylation of m-cresol with propylene by supported metal sulfates. Bull. Chem. Soc. Japan 47 2897 - 2898.

O’ Connor, C.T., Ertl, G., Knözinger, H., Schüth, F., Weitkamp, J., (eds.) “Oligomerisation”, “Handbook of Heterogeneous Catalysis”, Wiley-VCH, Weinheim, 2nd ed., vol. 6, 2008, pp. 2854-2864.

O’ Connor, C.T., Schwarz, S. and Kojima, M., “The effects of various physical and chemical parameters on the synthesis of ZSM-5 for propene oligomerisation”, *Elsevier Science Publishers B.V.,* 1991, pp. 491-500.

O’ Connor, C.T., Moon, G.C., Böhringer, W. and Fletcher, J.C.Q., “Alkylation of phenol and m-cresol over zeolites”, Collect. Czech. Chem. Commun., vol. 68, 2003, pp. 1949-1968.

Ohta, N., “Alkylation of phenol and m-cresol with isopropyl alcohol in the vapor phase.”, Kogyo Kagaku Zasshi, vol. **51**, 1948, pp. 141-143, abstract CAN 44:48552.

Ogata, Y., Sakanishi, K. and Hosoi, H., "Catalytic vapor-phase alkylations of phenol with alcohols.", Kogyo Kagaku Zasshi, vol. **72,** 5th ed., 1969, pp. 1102-1106, Translated from Japanese to English.

Pillai, B.B.C.and Pillai,C.N., "Alkylation of aniline by 2-propanol over zeolites", Indian Journal of Chemistry, Section B: Organic chemistry including medicinal chemistry, vol. **32B**, issue 5, 1993, p.p. 592-594.

Pillai, R.B.C., "Alkylation of aniline with n-propyl alcohols over zeoiltes*", Reaction Kinetics and Catalysis Letters,* Vol. **58**, 1996, pp. 145-154.

Poling, B.E., Prausnitz, J.M. and O'Connell, J.P., "The Properties of Gasses and Liquids", McGraw-Hill, 5th ed., 2001, Singapore, pp. 2.2-2.23, 2.26-2.33.

Joseph Antony Raj, K., Padma Malar, E. J.and Vijayaraghavan, V. R., "Shapeselective reactions with AEL and AFI type molecular sieves alkylation of benzene, toluene and ethylbenzene with ethanol, 2-propanol, methanol and t-butanol", Journal of Molecular Catalysis A: Chemical, 2005, vol. 243, pp. 99 -105.

Santacesaria E., Di Serio M., Ciambelli P., Gelosa D. and Carr`a S., "Catalytic alkylation of phenol with methanol: Factors influencing activities and selectivities II. Effect of intracrystalline diffusion and shape selectivity on H-ZSM-5 zeolite", Applied Catalysis, Vol. **64**, 1990, pp. 101-117.

Sandler, S.I., "Chemical and Engineering Thermodynamics", 3rd Ed, 1999, Wiley, New York, pp. 638-639.

Sasol (1997). Sasol announces major cresols expansion. Sasol media release. 15 May 1997. Sasol Chemical Industries Ltd., Rosebank, South Africa.

Schulz H., Böhringer, W., Kohl, C., Rahman, N. and Will, A., "Entwicklung und Anwendung der Kapillar-GC-Gesamptprobentechnic für Gas/Dampf-Viel-stoffgemische", DGMK-Forschungsbericht 320, 1984, DGMK Hamburg.

Sealy, S.J., Fraser, D.M., Moller, K.P. and O'Connor, C.T., "Equilibrium considerations in the modeling of propene oligomerisation", Chemical Engineering Science, vol. 49, 19th ed., 1994, pp. 3307-3312.

Shankankale, M. and Thomson, C., "Synthesis of Thymol, CHE4045Z-Project-R", BSc (Eng) Chem thesis, Department of Chemical Engineering, University of Cape Town, 2012.

Shapiro, S., "The inhibitory action of fatty acids on oral bacteria", *Oral Microbiol. Immun.,* vol. **11**, 1996, pp. 350.

Sowa, F. J., Hennion, G. F., Nieuwland, J. A., "Organic reactions with boron fluoride. IX. The alkylation of phenols with alcohols.", Journal of the American Chemical Society, **vol**. 57, 1935, pp. 709-711, abstract CAN 29:25642.

Stroh, R., Seydel, R. and Hahn, W., "Alkylation of phenols with olefins.", Angewandte Chemie, **vol**. 69, 1957, pp. 699-706, abstract CAN 52:34968.

Stull, D.R., Westrum, Jr. E.F. and Sinke, G.C., "The chemical thermodynamics of organic compounds", 1969, Wiley, New York.

Sykes, P., "A guidebook to mechanisms in organic chemistry", Longman Scientific and Technical, 6th edition, Essex, 1986, pp. 53-76.

Symrise, Interview granted to McCoy, J., published in "Hot Market For A Cool Chemical", Chemical and Engineering News, vol. 88, 35, 2010, pp. 15.

Teissedre, P., Waterhouse, A. L., "Inhibition of Oxidation of Human Low-Density Lipoproteins by Phenolic Substances in Different Essential Oils Varieties", J. Agric. Food Chem., vol. 48, 2000, pp. 3801.

Toma, N., "An investigation into the alkylation of phenol with different alcohols over selected zeolites" BSc (Eng) Chem thesis, Department of Chemical Engineering, University of Cape Town, 2005

Traynor, S.G. Interview granted to McCoy, J., published in "Hot Market For A Cool Chemical", Chemical and Engineering News, vol. 88, 35th ed., 2010, pp. 16.

Tsukervanik, I.P., Nazarova, Z.N., “Alkylation of Phenols with Alcohols in the Presence of Aluminum Chloride. II. Alkylation with Secondary and Primary Aliphatic Alcohols”, Zh. Obshch. Khim., vol. 7,1937, pp. 623. ABSTRACT.

Turova-Pollak, M. B., Rudenko, N. V. and Lin, L., “Catalytic alkylation of phenol with isopropyl alcohol.”, Zhurnal Obshchei Khimii, **vol.** 30, 1960, pp. 94-98, abstract CAN 54:110222.

Umamaheswari, V., Palanichamy, M. and Murugesan, V., “Isopropylation of m-cresol over mesopourous Al-MCM-41 molecular sieves”, *J. Catal.,* vol. **210,** 2002**,** pp. 367 - 374.

van Niekerk, Miles J., O'Connor, Cyril T. and Fletcher, Jack C. Q., “Methanol Conversion and Propene Oligomerization Productivity of Dealuminated Large-Port Mordenites”, Industrial & Engineering Chemistry Research, vol. 35, 3rd ed., 1996, pp. 697-702.

Velu, S. and Sivasanker, S., “Alkylation of m-cresol with methanol and 2-propanol over calcined magnesium-aluminium hydrotalcites.”, *Res. Chem. Intermed.,* vol. **24,** 1998, pp. 657 - 666.

Weitkamp, J. and Puppe, L., “Catalysis and Zeolites : Fundamentals and Applications”, Springer, Berlin, 1999, pp. 100, 343, 344.

Weitkamp, J. and Ernst, S., “Catalytic test reactions for probing width of large and super large pore molecular sieves”, *Catalysis Today*, vol. **19,** 1994, pp. 107-150.

Weast, R.C., “CRC Handbook of Chemistry and Physics”, 58th ed., CRC Press, Florida, 1977, pp. F-90.

Wilson, G.M., and Jasperson, L.V., “Critical Constants Tc, Pc, Estimation Based on Zero, First and Second order methods”, AIChe Spring Meeting, New Orleans, LA, 1996

Wimmer, P., Buysch, H.-J. and Puppe, L. (1991). Process for the preparation of thymol. *US 5,030,770* (assigned to Bayer AG, Leverkusen, Germany).

Yadaf, G.D. and Pathre, G.S., “Novel Mesoporous Solid Superacidic Catalysts: Activity and Selectivity in the Synthesis of Thymol by Isopropylation of m-Cresol with 2-Propanol over UDCaT-4,-5 and -6”, Journal of Physical Chemistry, vol. **109**, 2005, pp. 11080-11088.

Yamanaka, T., Nakata, F. and Komatsu, A., “o-Alkylphenols from phenols and olefins”, 1970a, *DE 1815846* (assigned to Takasago Perfumery Co. Ltd., Tokyo, Japan

Yamanaka, T., Nakata, Y. and Kobayashi, A., o-Alkylcresol, 1970b, *JP 45015491* (assigned to Takasago Perfumery Co. Ltd., Tokyo, Japan). Abstract: CAN 73:55808

Yamanaka, T., “Catalytic properties of metal sulfates supported on □-aluminium oxide in the liquid-phase isopropylation of m-cresol with propylene”, *Bull. Chem. Soc. Japan*, vol. **49,** 1976, pp. 2669 - 2673.

Yanishlieva, N.V., Marinova, E.M., Gordon, M.H., Raneva, V.G., “Antioxidant activity and mechanism of action of thymol and carvacrol in two lipid systems”, Food Chem., **vol.** 64, Issue 1, 1999, pp. 59-66.

Websites visited in May 2007

ChemCity (2007). The South African chemical industry.
http://www.chemcity.co.za/chemical.htm

IZA synthesis commission (2007)
www.iza-synthesis.org/databases

Whitaker (2007)
http://www.whitakeroil.com

Sigma Aldrich (2007)
http://www.sigmaaldrich.com

Mallinckrodt Baker (2007)
http://www.jtbaker.com

Vinquiry (2007)
http://vinquiry.com

Sciencelab (2007)
http://www.sciencelab.com

Cheric (2007)
http://www.cheric.org

Webb, M. Sasol considers Free State, Waterberg sites for new coal-to-liquids plant, accessed 11 June 2010.
http://www.engineeringnews.co.za/article/sasol-considers-free-state-waterberg-sites-for-new-coaltoliquids-plant-2007-09-10-1

Databases consulted

MS NIST (version 2.0)

Appendix A: Description of product fractions

EXPERIMENTAL PRODUCT FRACTIONS	
Fraction	**Description**
Lights	Di-and Trimethyl-phenols Ethyl-methyl-phenols Isopropyl-phenols n-Propyl-phenols Methyl-isopropyl-phenols with the methyl group not in the 3 position
C-10	Other compounds eluding in the same time frame (11.0-12.4 minutes) as the mono-isopropylated isomers e.g. n-Propylated *m*-Cresol
Σ Isomers	Isopropylated *m*-Cresol isomers: 3-Methyl-2-isopropyl-phenol Thymol 3-Methyl-5-isopropyl-phenol 3-Methyl-4-isopropyl-phenol
Di-propylated	Di-propylated *m*-Cresol (with n-Propyl and iso-Propyl)
Heavies	*m*-Cresol alkylated with side chains consisting of 4-8 carbon atoms (C_{4-8})
Kinetically favoured	Thymol 3-Methyl-2-isopropyl-phenol 3-Methyl-4-isopropyl-phenol Di-isopropylated *m*-Cresol
Secondary products	Heavies C-10 Lights 3-Methyl-5-isopropyl-phenol
THE FOLLOWING APPLIES TO FRACTIONS SIMULATED IN THERMODYNAMIC EQUILIBRIUM CALCULATIONS	
C4 remaining	n-Butenes (cis-2-, trans-2- and 1-Butene)
C3 remaining	Propene
iso-C4 substituents	n-Butenes which have alkylated *m*-Cresol to form secondary butyl substituents
2 x iso-C3 side chains	Propene which has alkylated the m-cresol ring twice to form Di-isopropylated m-cresol compounds
iso-C3 side chains	Propene which has alkylated the *m*-Cresol ring to form Thymol and Thymol position isomers
THE FOLLOWING APPLIES TO ACRONYMS DESIGNATING PRODUCT COMPOSITION IN THERMODYNAMIC CALCULATIONS	
M	*m*-Cresol
P	Propene
W	Water
T	Thymol and thymol isomers
D	Di-isopropylated *m*-Cresol derivatives
I	sec. butylated *m*-Cresol isomers
B	n-Butenes
ALKYLATING AGENT ABREVIATIONS	
IPA	Iso-propanol
DIPE	Di-isopropylether

Appendix A: Description of product fractions

EXPERIMENTAL PRODUCT FRACTIONS	
Fraction	**Description**
Lights	Di-and Trimethyl-phenols Ethyl-methyl-phenols Isopropyl-phenols n-Propyl-phenols Methyl-isopropyl-phenols with the methyl group not in the 3 position
C-10	Other compounds eluding in the same time frame (11.0-12.4 minutes) as the mono-isopropylated isomers e.g. n-Propylated *m*-Cresol
Σ Isomers	Isopropylated *m*-Cresol isomers: 3-Methyl-2-isopropyl-phenol Thymol 3-Methyl-5-isopropyl-phenol 3-Methyl-4-isopropyl-phenol
Di-propylated	Di-propylated *m*-Cresol (with n-Propyl and iso-Propyl)
Heavies	*m*-Cresol alkylated with side chains consisting of 4-8 carbon atoms (C_{4-8})
Kinetically favoured	Thymol 3-Methyl-2-isopropyl-phenol 3-Methyl-4-isopropyl-phenol Di-isopropylated *m*-Cresol
Secondary products	Heavies C-10 Lights 3-Methyl-5-isopropyl-phenol
THE FOLLOWING APPLIES TO FRACTIONS SIMULATED IN THERMODYNAMIC EQUILIBRIUM CALCULATIONS	
C4 remaining	n-Butenes (cis-2-, trans-2- and 1-Butene)
C3 remaining	Propene
iso-C4 substituents	n-Butenes which have alkylated *m*-Cresol to form secondary butyl substituents
2 x iso-C3 side chains	Propene which has alkylated the m-cresol ring twice to form Di-isopropylated m-cresol compounds
iso-C3 side chains	Propene which has alkylated the *m*-Cresol ring to form Thymol and Thymol position isomers
THE FOLLOWING APPLIES TO ACRONYMS DESIGNATING PRODUCT COMPOSITION IN THERMODYNAMIC CALCULATIONS	
M	*m*-Cresol
P	Propene
W	Water
T	Thymol and thymol isomers
D	Di-isopropylated *m*-Cresol derivatives
I	sec. butylated *m*-Cresol isomers
B	n-Butenes
ALKYLATING AGENT ABREVIATIONS	
IPA	Iso-propanol
DIPE	Di-isopropylether

Appendix B: Temperature profiles

The tips of the thermocouples associated with the controllers which regulated the heat input to the individual heating bands were located in such a way that they touched the outer surface of the reactor heating block. The temperatures measured inside the reactor tube corresponding to the zones regulated by these controllers, differed significantly (by up to 20℃) from the tem peratures measured at the tips of the heating band thermocouples.

Optimised temperature profiles were generated at the temperatures at which experiments were intended to be conducted. The initial approximate controller set points were generated under N_2 flow and later fine-tuned during the actual experiments (see Table B-1).

Table B-1: Temperature controller set points to achieve a 250℃ isothermal zone

Heating zone	Temperature setpoints of heating zones (℃)			
	N_2 *)	Iso-propanol/ N_2 **)	Iso-propanol/ *m*-Cresol **)	Iso-propanol/ *m*-Cresol, increased bed dilution ***)
Zone 1	243	243	221	243
Zone 2	234	231	235	243
Zone 3	229	223	222	226
Zone 4	231	224	225	231
Zone 5	240	242	****)	240

*) SiC was employed as reactor packing, N_2 flow of 60ml·min^{-1} at 1 bar.

**) Dilution of catalyst with SiC: 1:1 (by volume), 0.57 $g_{iso\text{-}propanol} \cdot g_{cat}^{-1} \cdot hr^{-1}$ at 1 bar, 1:1 molar mixture iso-propanol/N_2 and iso-propanol/*m*-cresol respectively

***) Dilution of first section of catalyst bed with SiC (14% of total catalyst packed in this section): 5:1 (by volume), Dilution in second section: 1:1, 0.57 $g_{iso\text{-}propanol} \cdot g_{cat}^{-1} \cdot hr^{-1}$, 1 bar, 1.03 $g_{m\text{-}cresol} \cdot g_{cat}^{-1} \cdot hr^{-1}$, 1:1 molar mixture iso-propanol/*m*-cresol.

****) 4 Zone heating block employed for this experiment instead of the 5-zone heating block and therefore the setpoints used to achieve the isothermal zone is significantly different to the 5-Zone systems

The temperature profiles in question were such that the top of the reactor packing was maintained at least 10 °C below the boiling poi nt of the intended reagent feed mixture at 1 bar (pressure corresponding to the “standard conditions”), so that this liquid feed was drawn into the void spaces between the SiC particles above the reactor bed (see Figure 4-4) at a constant flow rate and slowly heated up and gradually evaporated as it made its way down the SiC bed.

In order to maintain the inlet temperature of the liquid feed below the normal boiling point of its lowest boiling constituent (iso-propanol or di-isopropylether), a cooling fan was used to cool the top end of the reactor system where the liquid feed was introduced.

Downstream of the feed inlet point, the bed temperature increased with a moderate gradient, so that the entire volume of liquid feed evaporated before the boiling point of the highest boiling constituent of the feed mixture (*m*-cresol) was reached so as to enable slow and smooth evaporation and thus to eliminate pulsing of the feed. Finally, the bed temperature increased to that of the reaction, before the catalyst bed was reached.

Appendix C: Further dehydration experiments with n-propanol

Figure C-1 compares the propene selectivity obtained for different alkylating agents over a range of temperatures. Under all conditions studied total conversion of the respective alkylating agents was observed. The propene selectivity obtained at 250 ℃ with n-propanol was much higher than that given by the use of iso-propanol and di-isopropyl-ether. This result suggests that the dehydration of n-propanol proceeds much slower as opposed to that of iso-propanol and di-isopropylether at 250℃. This observation can be attributed to the difference in stability between the primary carbenium ion (formed by direct acid catalysed dehydration of n-propanol) which is much less stable than the secondary carbenium ion (formed by direct acid catalysed dehydration of iso-propanol) (McMurry, 1994).

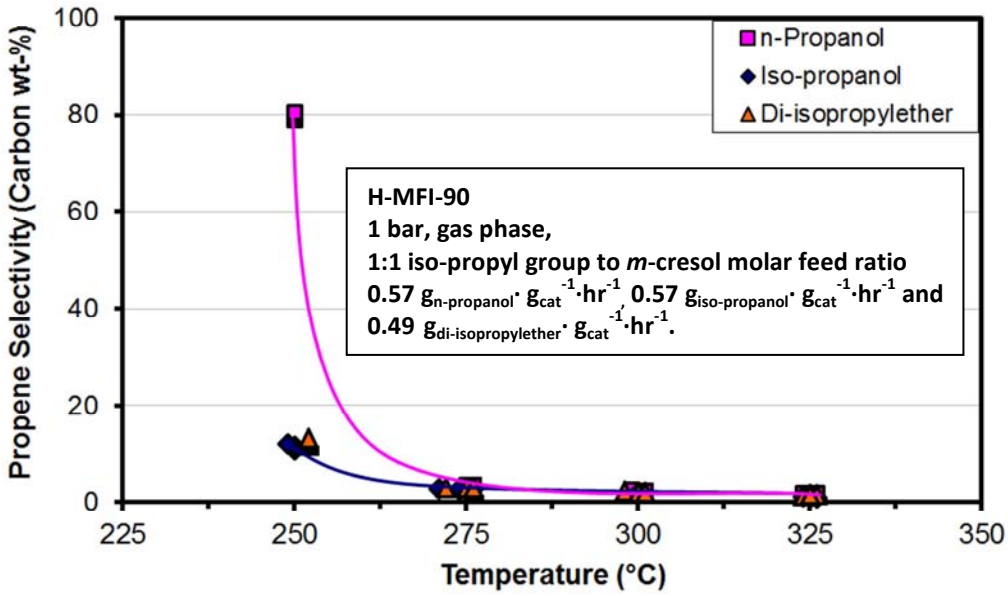

Figure C-1: Propene selectivity vs. temperature for dehydration experiments.

Appendix D: Cause of depression in temperature profiles at catalyst bed inlet

Figure D-1 compares the temperature profiles obtained by reacting different feed mixtures over a catalytic bed. The red dotted lines mark the beginning and end of the catalyst bed for the experiment with iso-propanol/N_2. The characteristic depression in temperature profiles shown in Figure D-1 was observed in all experiments irrespective of reagent feed or conditions, though the extent of the depression depended on these parameters as will be illustrated in this appendix.

Table D-1 lists the equilibrium conversion, heat of reaction, heat change in the system and adiabatic temperature drop of the system in which iso-propanol is dehydrated to propene and water at 250℃. The large temperature drop under adiabatic conditions and the high positive change in enthalpy of the system indicates the extent of the endothermic nature of this dehydration reaction. Hence the depression in the temperature profile observed in the experiments with iso-propanol. Similar to the dehydration of iso-propanol, the experiments with n-propanol/N_2 and di-isopropylether/N_2 also showed a depression which can be attributed to the dehydration of these components. Although the molar flow rates of the C_3-alcohols and di-isopropylether were similar, the extent of the depression in the example with n-propanol/N_2 was less severe compared to that corresponding to the experiments with iso-propanol/N_2 and di-isopropylether/N_2.

From the results of the dehydration experiments it is evident that at these conditions, the rate at which n-propanol was dehydrated is slower as compared to that of iso-propanol and di-isopropylether at equivalent conditions (see *Appendix C*). Therefore, if the rate of the endothermic dehydration reaction of n-propanol is slower compared to di-isopropylether and iso-propanol, less heat will be consumed and that corresponds to a lesser depression of the temperature profile - as was observed. Hence, the differences in the extent of the depression of the temperature profiles corresponding to the n-propanol/N_2 and di-isopropylether/N_2 & iso-propanol/N_2 at the conditions in question corroborate the findings pertaining to the rate of the dehydration of n-propanol compared to that of di-isopropylether and iso-propanol (discussed in *Appendix C*).

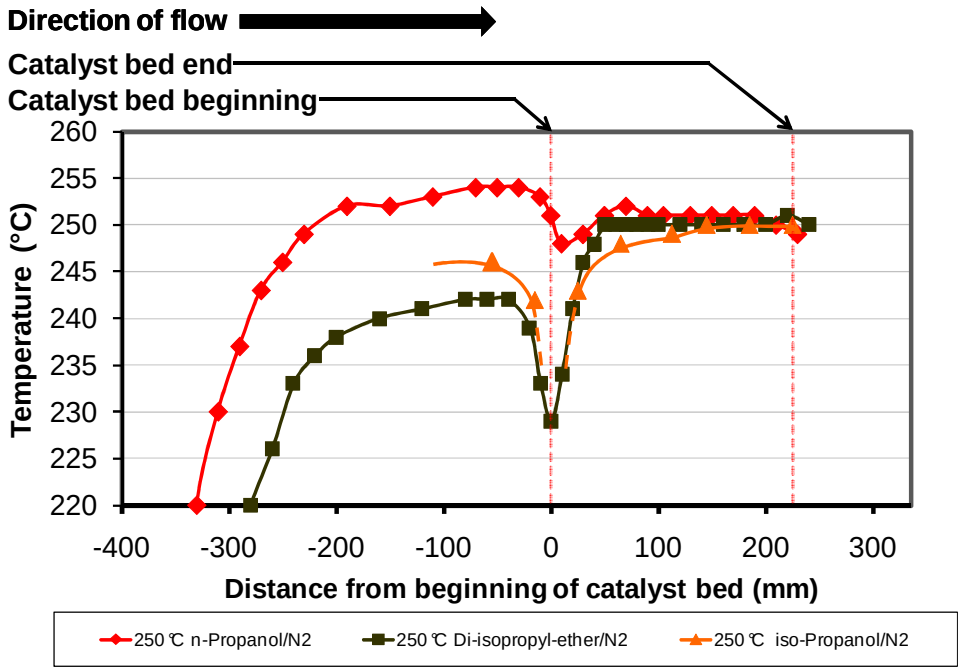

Figure D-1: Temperature profiles obtained at standard reaction conditions

The following table displays the results of a simulation of the adiabatic temperature drop and heat of reaction corresponding to the equilibrium conversion of iso-propanol to water and propene. These results correspond to 1 bar, 1:1 molar feed mixture of iso-propanol/N_2 fed to the system at a feed rate of 1.0 mol/min iso-propanol and 250℃.

Table D-1: Adiabatic temperature drop and heat of IPA dehydration reaction.

Equilibrium conversion of iso-propanol	99.9 %
Enthalpy change	40 kJ·mol$_{\text{iso-propanol}}^{-1}$·min^{-1}
Heat of dehydration reaction at 250℃	52 kJ·mol$_{\text{iso-propanol}}^{-1}$
Initial temperature	250 ℃
Final temperature (adiabatic)	-137 ℃
Adiabatic temperature drop	387 ℃

In Figure D-2, temperature profiles obtained during experiments with N_2 (60 ml·min^{-1}) iso-propanol/N_2 (0.128 mol·hr^{-1}) and iso-propanol/*m*-cresol (0.056 mol·hr^{-1}). These feed mixtures were reacted at 1 bar over a catalyst bed with a 1:1 (vol.) dilution with SiC. iso-propnaol/*m*-cresol (0.17 mol·hr^{-1}) was also reacted over a bed with increased dilution- 1:5 (vol.) in the first section and 1:1 (vol.) in the second section. The 2 red dotted lines in Figure D-2 (at 0 mm and 225 mm) indicate the start and end

of the catalyst bed corresponding to the experiment with iso-propanol/N_2 at ambient pressure and 0.57 $g_{iso\text{-}propanol}.g_{cat}^{-1}.hr^{-1}$.

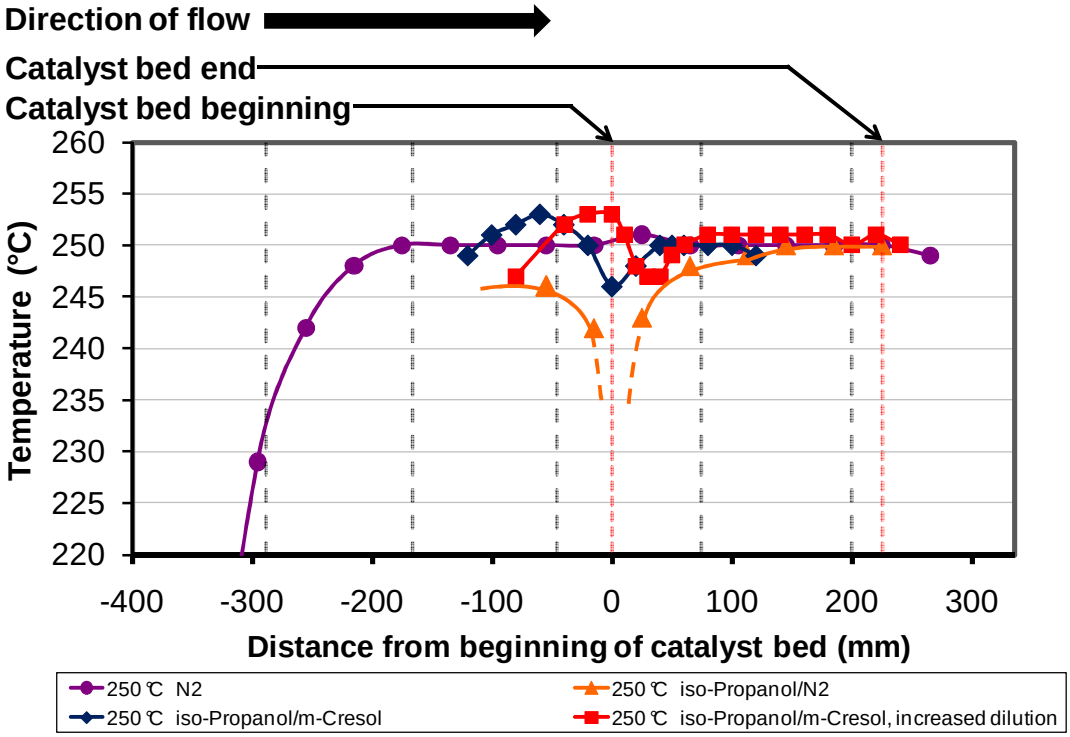

Figure D-2: Temperature profiles obtained during experiments

The temperature profiles corresponding to the experiments with iso-propanol/N_2, iso-propanol/*m*-cresol and di-isopropylether/N_2 (wherein a SiC-to-catalyst dilution ratio of 1:1(vol.) was employed) exhibited a depression before the beginning of the catalyst bed. In these instances, the extent of the temperature depression increased with molar flow rate of the propyl groups.

As the dehydration reaction is rapid and reaches completion in the upper most layers of the catalyst bed (or initial contact zone at the beginning of the catalyst bed), the more severe temperature depression at higher flow rate shows that at the higher flow rate, more molecules are converted per time unit in the same volume (initial bed contact zone) as compared to the lower flow system finally resulting in this increased temperature depression.

The experiment with n-propanol/N_2 illustrates that with the lower rate of dehydration (discussed earlier) the depression is observed from the beginning of the catalyst bed and not before the catalyst bed as mentioned in the cases above. Similarly, with the

experiment in which iso-propanol/*m*-cresol was reacted over the catalyst bed of which the initial section was diluted to a 5:1 (vol.) SiC:Catalyst ratio and larger molar flow rate of iso-propanol, a smaller temperature depression which occurred later in the bed was observed compared to that where iso-propanol/*m*-cresol was reacted over a catalyst bed with SiC:Catalyst dilution ratio 1:1 (vol.) (0.17 $mol \cdot hr^{-1}$ compared to 0.056 $mol \cdot hr^{-1}$). This lesser temperature depression can be attributed to the lower catalyst concentration-which resulted in a less molecules reacting per given volume.

The position of the temperature depression with respect to the catalyst bed, points to the conductive effect of the system (wherein heat was conducted through the thermowell and/or SiC), by which the sections upstream from that in which a relatively high rate of dehydration occurred, was cooled down even though no dehydration reaction occurred there. The fact that lesser temperature depressions were observed which only occurred downstream from the beginning of the catalyst bed in cases where less molecules were dehydrated per unit time in a particular section of the catalyst bed also point to the said conductive effect.

This finding together with the results of the simulation suggests that the actual temperature depression in the gas phase may have been more severe than that measured in these experiments.

Appendix E: Dehydration equilibria and adiabatic temperature drop

In the modelling of the adiabatic temperature drop during the dehydration of iso-propanol to propene and water, the equilibrium composition of the reaction system was equated by minimising the Gibbs free energy of formation. This calculation showed that the dehydration reaction reaches 100% conversion at 250℃ and 1 bar. The results of this simulation is displayed in Table E-1.

Table E-1: Results yielded by the model used to derive the chemical equilibrium composition of the iso-propanol dehydration system.

Stream	Feed	Effluent
Mole Flow mol/min		
IPA	1	1.35E-03
Propene	0	9.99E-01
Water	0	9.99E-01
Total Flow mol/min	1	2.00E+00
Total Flow kg/min	6.01E-02	6.01E-02
Total Flow l/min	43.49642	86.93411
Temperature (℃)	250	250
Pressure (atm)	0.9869233	0.9869233
Vapor Frac	1	1
Liquid Frac	0	0
Solid Frac	0	0
Enthalpy cal/mol	-58993.12	-23368.07
Entropy cal/mol-K	-64.40973	-13.22058
Density mol/cc	2.30E-05	2.30E-05

To model the decrease in temperature of the system under adiabatic condition the "Rplug" reaction module within the ASPEN software package. The dehydration system was simulated at 250℃ and ambient pressure. Iso-propanol and nitrogen was fed to the reactor at a 1:1 molar ratio. The reactor length and inner diameter was specified as 0.5 m and 19 mm, respectively. The ideal gas law equation of state was used in the simulation. The rest of the parameters were the default values assigned by the package.

Table E-2: Constants yielding the equilibrium conversion of iso-propanol at 250℃ and 1 bar, iso-propanol was co-fed with N_2 at a 1:1 molar ratio.

k	**0.417902**
n	**0.5**
E	**1 kcal/mol**
To	**200 ℃**

Table E-3 shows the results of the model used to calculate the adiabatic temperature decrease in the dehydration of iso-propanol to water and propene.

Table E-3: Results from the adiabatic model with the feed and product stream specifications.

Stream	Feed	Effluent
Mole Flow mol/min		
IPA	1	1.35E-03
Propene	0	0.99865
Water	0	0.99865
Nitrogen	1	1
Total Flow mol/min	2	1.00E+00
Total Flow kg/min	88.1094	88.1094
Total Flow l/min	86.99283	33.85957
Temperature (℃)	250	-137.341
Pressure atm	0.986923	0.986923
Vapor Frac	1	1
Liquid Frac	0	0
Solid Frac	0	0
Enthalpy cal/mol	-28708.7	-19147.7
Entropy cal/mol-K	-64.4097	-13.2206
Density mol/cc	2.30E-05	2.30E-05

Appendix F: Thermodynamic data from functional analysis

The "Dmol" module (a Quantum mechanical molecular model) in the **Materials Studio 4.0** software package (Accelrys, 2005) was employed for the purpose of generating thermodynamic data which could be used to calculate the theoretical thermodymic equilibrium distribution of the product pool (or its major constituents respectively), seen in this study.

Dmol was used to conduct a normal mode analysis on these molecules using Density Functional Theory (DFT). DFT calculates the total energy of the molecule from the electron density distribution as the energy of the electron is expressed as a unique functional of the electron density.

The aforementioned functional is expressed as the sum of the **Energy of Interaction between the Electrons and the Nucleus** (given by electron nuclear Coulomb interaction), **Electron Kinetic Energy** (calculated directly with Hartree Fock theory), **Hartree Electrostatic Energy** (also calculated directly using Hartree Fock theory) and the **Exchange-Correlation Functional energy.**

The **Exchange-Correlation Functional Energy** may either be approximated by the **Liquid Density Approximation (LDA)** or by the **Generalised Gradient Approximation (GGA).**

The **LDA** treats the local electron density as constant and therefore is less accurate than the **GGA** which does not use this somewhat flawed approximation and therefore provides a more accurate approximation of the **Exchange-Correlation Functional Energy.** Therefore, GGA type functionals were used to approximate the **Exchange-Correlation Functional Energy** in this study**.**

Structures were generated for each of the compounds considered in the thermodynamic equilibria. The results of the normal mode analyses were examined and in cases where negative frequencies were observed, the structures were altered and the normal mode analyses repeated. This procedure was repeated until no negative frequencies were observed in the results.

In this regard, Toma (2011) modelled the thermodynamic xylene isomer equilibrium with a great deal of accuracy compared to the measured equilibrium composition over a range of temperatures. This was accomplished by considering all possible conformational isomers of each of the position isomers.

In the case of this study, the generation of all of the conformation isomers for each of the molecules considered, would have proven to be too time intensive and therefore only one of the conformational isomers of each of the compounds was considered in the calculation of the equilibrium composition.

The following GGA functionals were employed: PW91, RPBE, HCTH and BLYP to generate this thermodynamic data. The results yielded by the use of these functionals are displayed in Table F-1 - Table F-12.

Table F-1: Pure component values for the respective compounds computed with the PW91 GGA functional

	$\Delta H_f^{\circ}{}_{est}$ (kcal·mol^{-1})	$\Delta G_f^{\circ}{}_{est}$ (kcal·mol^{-1})	Cp (cal·mol^{-1}·K^{-1})										
Temperature (K) →	**298.15**	**298.15**	**25**	**50**	**75**	**100**	**125**	**150**	**175**	**200**	**225**	**250**	**275**
Compounds													
Water	-47949.39411	-47963.26311	7.949	7.949	7.949	7.949	7.949	7.949	7.949	7.951	7.955	7.964	7.978
Propene	-73925.12642	-73944.09742	7.955	8.237	8.779	9.333	9.891	10.48	11.12	11.83	12.63	13.5	14.44
Iso-propanol	-121890.177	-121911.534	7.957	8.361	9.441	10.86	12.33	13.7	14.98	16.23	17.47	18.75	20.07
1-Butene	-98572.73204	-98593.91004	7.994	8.814	10.02	11.14	12.15	13.12	14.11	15.17	16.33	17.58	18.91
cis-Butene	-98575.3501	-98596.4491	7.955	8.412	9.575	10.86	12.04	13.15	14.24	15.35	16.51	17.75	19.05
trans-Butene	-98576.6845	-98597.7525	7.95	8.258	9.467	10.96	12.31	13.49	14.58	15.66	16.8	17.99	19.26
Di-isopropylether	-195828.2977	-195855.3647	120	120.2	120.5	120.9	121.3	121.8	122.4	123	123.7	124.4	125.2
m-Cresol	-217525.4156	-217550.9206	49.04	55.72	60.08	63.62	66.78	69.72	72.53	75.26	77.93	80.56	83.16
o-Cresol	-217525.2069	-217549.6379	48.18	53.85	57.65	60.86	63.8	66.58	69.27	71.9	74.49	77.06	79.6
p-Cresol	-217524.7028	-217549.7078	48.27	54.47	58.7	62.16	65.25	68.15	70.93	73.64	76.29	78.9	81.49
Thymol	-291471.1203	-291501.9573	9.114	12.05	15.68	19.53	23.23	26.75	30.15	33.49	36.85	40.24	43.66
2-Isopropyl-3-methyl-phenol	-291466.6378	-291497.2198	9.048	11.73	15.27	19.14	22.9	26.47	29.91	33.3	36.7	40.12	43.56
4-Isopropyl-3-methyl-phenol	-291469.9508	-291501.2938	9.943	12.45	15.99	19.77	23.41	26.88	30.24	33.57	36.92	40.31	43.73
5-Isopropyl-3-methyl-phenol	-291472.0807	-291503.1477	9.103	12.06	15.98	19.93	23.62	27.09	30.43	33.74	37.06	40.44	43.84
6-(1-Methyl-propyl)-3-methyl-phenol	-316119.0289	-316153.0049	11.56	14.94	18.66	22.57	26.38	30.04	33.62	37.2	40.83	44.53	48.3
2-(1-Methyl-propyl)-3-methyl-phenol	-316113.5798	-316146.0398	9.589	12.9	16.87	21.15	25.27	29.18	32.94	36.66	40.4	44.2	48.03
4-(1-Methyl-propyl)-3-methyl-phenol	-316117.1466	-316150.0726	9.873	13.41	17.64	21.87	25.85	29.6	33.24	36.86	40.53	44.26	48.05
5-(1-Methyl-propyl)-3-methyl-phenol	-316120.0661	-316153.7861	10.32	14.54	18.97	23.14	26.97	30.57	34.07	37.57	41.15	44.82	48.56
4,6-Di-isopropyl-3-methyl-phenol	-365415.3295	-365452.3395	11.23	15.48	20.6	26.15	31.43	36.32	40.91	45.37	49.79	54.25	58.76
5,6-Di-isopropyl-3-methyl-phenol	-365411.5426	-365448.2746	10.06	14.85	20.88	26.81	32.17	37.02	41.57	45.98	50.37	54.81	59.3
4,5-Di-isopropyl-3-methyl-phenol	-365409.8754	-365446.6914	10.65	14.99	20.42	26.15	31.54	36.52	41.19	45.71	50.19	54.69	59.23

Table F-2: Pure component values for the respective compounds computed with the PW91 GGA functional

	Cp (T) ($cal \cdot mol^{-1} \cdot K^{-1}$)														
Temperature (K)→	298.15	300	325	350	375	400	425	450	475	500	525	550	575	600	625
Compounds															
Water	7.998	7.999	8.027	8.062	8.103	8.149	8.2	8.255	8.312	8.372	8.434	8.497	8.562	8.627	8.693
Propene	15.342	15.416	16.42	17.44	18.45	19.44	20.41	21.35	22.26	23.14	23.98	24.78	25.56	26.3	27.02
Iso-propanol	21.322	21.423	22.8	24.17	25.54	26.89	28.2	29.47	30.7	31.89	33.03	34.12	35.17	36.17	37.14
1-Butene	20.195	20.3	21.72	23.16	24.58	25.99	27.35	28.68	29.96	31.19	32.37	33.5	34.59	35.63	36.63
cis-Butene	20.293	20.394	21.77	23.16	24.54	25.91	27.24	28.54	29.8	31.01	32.18	33.3	34.38	35.42	36.42
trans-Butene	20.484	20.584	21.94	23.32	24.69	26.05	27.38	28.67	29.92	31.13	32.3	33.42	34.5	35.54	36.54
Di-isopropylether	126.02	126.09	127	128	129.1	130.2	131.4	132.7	134	135.3	136.8	138.2	139.8	141.3	143
m-Cresol	85.545	85.735	88.29	90.83	93.34	95.83	98.3	100.7	103.1	105.5	107.8	110.2	112.4	114.7	116.9
o-Cresol	81.939	82.126	84.64	87.13	89.61	92.07	94.5	96.91	99.29	101.6	104	106.3	108.5	110.7	112.9
p-Cresol	83.867	84.056	86.6	89.13	91.63	94.11	96.56	98.99	101.4	103.8	106.1	108.4	110.6	112.9	115.1
Thymol	46.839	47.093	50.51	53.89	57.19	60.39	63.49	66.46	69.31	72.04	74.63	77.11	79.47	81.72	83.86
2-Isopropyl-3-methyl-phenol	46.756	47.011	50.44	53.83	57.14	60.35	63.45	66.43	69.28	72	74.6	77.08	79.44	81.68	83.83
4-Isopropyl-3-methyl-phenol	46.91	47.164	50.59	53.96	57.26	60.47	63.56	66.54	69.39	72.11	74.7	77.18	79.53	81.78	83.92
5-Isopropyl-3-methyl-phenol	47.014	47.268	50.68	54.04	57.34	60.54	63.63	66.6	69.44	72.16	74.75	77.22	79.58	81.82	83.96
6-(1-Methyl-propyl)-3-methyl-phenol	51.818	52.1	55.9	59.67	63.37	66.96	70.44	73.79	77.01	80.08	83.01	85.81	88.48	91.03	93.46
2-(1-Methyl-propyl)-3-methyl-phenol	51.61	51.896	55.75	59.55	63.28	66.9	70.4	73.77	76.99	80.08	83.02	85.83	88.5	91.06	93.49
4-(1-Methyl-propyl)-3-methyl-phenol	51.595	51.878	55.7	59.49	63.2	66.81	70.3	73.66	76.88	79.96	82.9	85.71	88.38	90.93	93.36
5-(1-Methyl-propyl)-3-methyl-phenol	52.072	52.353	56.15	59.92	63.61	67.21	70.69	74.03	77.24	80.31	83.24	86.04	88.7	91.24	93.66
4,6-Di-isopropyl-3-methyl-phenol	62.961	63.297	67.84	72.34	76.76	81.07	85.25	89.28	93.15	96.86	100.4	103.8	107	110.1	113.1
5,6-Di-isopropyl-3-methyl-phenol	63.498	63.833	68.36	72.85	77.27	81.57	85.73	89.75	93.61	97.3	100.8	104.2	107.4	110.5	113.5
4,5-Di-isopropyl-3-methyl-phenol	63.461	63.799	68.36	72.87	77.29	81.6	85.78	89.8	93.66	97.35	100.9	104.3	107.5	110.6	113.5

Table F-3: Pure component values for the respective compounds computed with the PW91 GGA functional

	Cp (T) ($cal \cdot mol^{-1} \cdot K^{-1}$)														
Temperature (K)→	650	675	700	725	750	775	800	825	850	875	900	925	950	975	1000
Compounds															
Water	8.76	8.827	8.895	8.963	9.033	9.102	9.172	9.243	9.314	9.385	9.456	9.528	9.599	9.671	9.742
Propene	27.706	28.367	29	29.62	30.21	30.78	31.33	31.86	32.38	32.87	33.35	33.81	34.26	34.7	35.11
Iso-propanol	38.061	38.95	39.81	40.63	41.42	42.19	42.92	43.63	44.32	44.98	45.62	46.24	46.84	47.41	47.97
1-Butene	37.585	38.506	39.39	40.24	41.07	41.86	42.62	43.35	44.06	44.75	45.41	46.04	46.66	47.25	47.83
cis-Butene	37.383	38.309	39.2	40.06	40.89	41.68	42.45	43.2	43.91	44.61	45.27	45.92	46.54	47.14	47.73
trans-Butene	37.497	38.421	39.31	40.17	40.99	41.79	42.56	43.3	44.02	44.71	45.37	46.02	46.64	47.24	47.82
Di-isopropylether	144.63	146.33	148.1	149.9	151.7	153.6	155.5	157.4	159.4	161.4	163.4	165.5	167.5	169.7	171.8
m-Cresol	119.03	121.16	123.3	125.3	127.3	129.3	131.3	133.2	135.1	137	138.8	140.6	142.4	144.2	145.9
o-Cresol	115.07	117.19	119.3	121.3	123.3	125.3	127.3	129.2	131.1	133	134.8	136.6	138.4	140.1	141.9
p-Cresol	117.23	119.35	121.4	123.5	125.5	127.5	129.5	131.4	133.3	135.2	137	138.8	140.6	142.3	144.1
Thymol	85.909	87.864	89.73	91.52	93.23	94.87	96.45	97.95	99.4	100.8	102.1	103.4	104.7	105.9	107
2-Isopropyl-3-methyl-phenol	85.874	87.828	89.7	91.48	93.19	94.83	96.4	97.91	99.36	100.7	102.1	103.4	104.6	105.8	106.9
4-Isopropyl-3-methyl-phenol	85.964	87.916	89.78	91.57	93.27	94.91	96.48	97.99	99.44	100.8	102.2	103.4	104.7	105.9	107
5-Isopropyl-3-methyl-phenol	86.005	87.956	89.82	91.61	93.31	94.95	96.52	98.03	99.48	100.9	102.2	103.5	104.7	105.9	107.1
6-(1-Methyl-propyl)-3-methyl-phenol	95.785	98.004	100.1	102.2	104.1	106	107.8	109.5	111.1	112.7	114.2	115.7	117.1	118.5	119.8
2-(1-Methyl-propyl)-3-methyl-phenol	95.815	98.036	100.2	102.2	104.1	106	107.8	109.5	111.2	112.7	114.3	115.7	117.1	118.5	119.8
4-(1-Methyl-propyl)-3-methyl-phenol	95.686	97.905	100	102.1	104	105.9	107.7	109.4	111	112.6	114.1	115.6	117	118.4	119.7
5-(1-Methyl-propyl)-3-methyl-phenol	95.971	98.18	100.3	102.3	104.2	106.1	107.9	109.6	111.2	112.8	114.3	115.8	117.2	118.5	119.8
4,6-Di-isopropyl-3-methyl-phenol	115.92	118.63	121.2	123.7	126.1	128.4	130.5	132.7	134.7	136.6	138.5	140.3	142	143.7	145.3
5,6-Di-isopropyl-3-methyl-phenol	116.28	118.97	121.5	124	126.4	128.6	130.8	132.9	134.9	136.9	138.7	140.5	142.3	143.9	145.5
4,5-Di-isopropyl-3-methyl-phenol	116.31	118.99	121.6	124	126.4	128.7	130.8	132.9	134.9	136.9	138.7	140.5	142.2	143.9	145.5

Table F-4: Pure component values for the respective compounds computed with the HCTH GGA functional

	$\Delta H_f^{\circ}{}_{est}$ (kcal·mol^{-1})	$\Delta G_f^{\circ}{}_{est}$ (kcal·mol^{-1})	Cp (cal·mol^{-1}·K^{-1})										
Temperature (K) →	298.15	298.15	25	50	75	100	125	150	175	200	225	250	275
Compounds													
Water	-47959.65556	-47973.50956	7.949	7.949	7.949	7.949	7.949	7.949	7.949	7.951	7.955	7.963	7.976
Water	-73952.24681	-73970.77081	7.949	7.953	8.044	8.347	8.849	9.483	10.21	11	11.86	12.78	13.75
Propene	-121921.8599	-121942.4259	7.949	7.97	8.28	9.144	10.39	11.78	13.19	14.59	15.98	17.39	18.81
Iso-propanol	-98607.62099	-98628.12199	7.951	8.16	8.814	9.739	10.76	11.82	12.9	14.05	15.27	16.58	17.95
1-Butene	-98611.63665	-98633.05365	8.013	9.004	10.28	11.45	12.53	13.55	14.57	15.64	16.77	17.97	19.24
cis-Butene	-98613.0913	-98634.3873	7.967	8.656	9.979	11.33	12.58	13.73	14.83	15.96	17.12	18.35	19.64
trans-Butene	-195880.791	-195906.968	8.377	10.21	12.14	14.57	17.22	19.82	22.3	24.7	27.09	29.5	31.95
Di-isopropylether	-217540.7414	-217564.3094	48.34	53.87	57.3	60.09	62.65	65.1	67.5	69.87	72.22	74.56	76.89
m-Cresol	-217543.1676	-217567.3736	48.18	53.84	57.55	60.63	63.43	66.11	68.72	71.29	73.84	76.36	78.87
o-Cresol	-217544.134	-217568.858	48.24	54.2	58.14	61.38	64.35	67.17	69.92	72.62	75.28	77.91	80.52
p-Cresol	-291509.3261	-291538.3111	8.186	10.08	13	16.49	20.14	23.75	27.27	30.73	34.17	37.61	41.07
Thymol	-291504.0288	-291533.6158	9.723	11.42	13.63	16.57	19.87	23.33	26.83	30.34	33.87	37.41	40.96
2-Isopropyl-3-methyl-phenol	-291507.7026	-291536.4216	8.109	9.729	12.54	15.98	19.64	23.28	26.85	30.35	33.82	37.29	40.76
4-Isopropyl-3-methyl-phenol	-291511.7033	-291541.0123	8.184	10.29	13.39	16.91	20.54	24.15	27.7	31.23	34.74	38.27	41.8
5-Isopropyl-3-methyl-phenol	-316162.6237	-316193.8927	8.999	12.38	16.13	19.76	23.28	26.74	30.19	33.69	37.25	40.88	44.59
6-(1-Methyl-propyl)-3-methyl-phenol	-316156.5255	-316187.3455	9.139	11.62	14.64	18.22	22.06	25.95	29.82	33.67	37.52	41.39	45.28
2-(1-Methyl-propyl)-3-methyl-phenol	-316163.1418	-316194.1278	8.724	11.61	14.94	18.69	22.61	26.53	30.39	34.21	38.03	41.87	45.73
4-(1-Methyl-propyl)-3-methyl-phenol	-316167.7287	-316199.6317	8.829	12.19	16.3	20.53	24.61	28.48	32.2	35.87	39.54	43.25	47
5-(1-Methyl-propyl)-3-methyl-phenol	-365474.8914	-365508.9314	9.028	12.7	17.12	21.9	26.82	31.71	36.53	41.27	45.96	50.64	55.32
4,6-Di-isopropyl-3-methyl-phenol	-365469.0536	-365503.4586	8.85	12.78	17.74	23	28.13	33.03	37.72	42.29	46.82	51.35	55.92
5,6-Di-isopropyl-3-methyl-phenol	-365468.1596	-365502.6776	9.439	13.04	17.45	22.51	27.69	32.71	37.55	42.25	46.9	51.53	56.17

Table F-5: Pure component values for the respective compounds computed with the HCTH GGA functional

	Cp (T) ($cal \cdot mol^{-1} \cdot K^{-1}$)														
Temperature (K)→	298.15	300	325	350	375	400	425	450	475	500	525	550	575	600	625
Compounds															
Water	7.994	7.996	8.022	8.056	8.095	8.14	8.189	8.243	8.299	8.357	8.418	8.48	8.543	8.606	8.671
Propene	14.68	14.75	15.77	16.79	17.81	18.81	19.79	20.73	21.65	22.53	23.38	24.19	24.98	25.73	26.46
Iso-propanol	20.136	20.243	21.68	23.11	24.52	25.91	27.25	28.56	29.81	31.02	32.18	33.3	34.36	35.39	36.37
1-Butene	19.268	19.375	20.83	22.28	23.73	25.15	26.54	27.89	29.18	30.43	31.63	32.78	33.88	34.94	35.96
cis-Butene	20.458	20.557	21.91	23.28	24.64	25.99	27.31	28.6	29.85	31.05	32.22	33.34	34.41	35.45	36.45
trans-Butene	20.872	20.972	22.33	23.7	25.06	26.41	27.72	29	30.24	31.43	32.58	33.69	34.75	35.78	36.76
Di-isopropylether	34.273	34.46	37	39.55	42.09	44.6	47.05	49.45	51.77	54.01	56.18	58.27	60.27	62.2	64.06
m-Cresol	79.045	79.217	81.54	83.86	86.16	88.46	90.75	93.02	95.27	97.5	99.7	101.9	104	106.2	108.3
o-Cresol	81.188	81.372	83.86	86.33	88.78	91.21	93.63	96.01	98.37	100.7	103	105.3	107.5	109.7	111.9
p-Cresol	82.923	83.114	85.69	88.24	90.76	93.27	95.74	98.19	100.6	103	105.3	107.6	109.9	112.1	114.3
Thymol	44.263	44.518	47.95	51.34	54.65	57.88	61	64.01	66.9	69.67	72.31	74.84	77.24	79.54	81.74
2-Isopropyl-3-methyl-phenol	44.24	44.501	48.01	51.45	54.81	58.08	61.23	64.25	67.15	69.93	72.57	75.09	77.5	79.79	81.98
4-Isopropyl-3-methyl-phenol	43.977	44.233	47.68	51.08	54.41	57.65	60.79	63.81	66.7	69.48	72.13	74.67	77.08	79.39	81.59
5-Isopropyl-3-methyl-phenol	45.059	45.318	48.81	52.24	55.58	58.83	61.96	64.97	67.86	70.61	73.23	75.74	78.12	80.4	82.56
6-(1-Methyl-propyl)-3-methyl-phenol	48.053	48.331	52.09	55.82	59.51	63.11	66.61	69.99	73.25	76.37	79.37	82.23	84.97	87.59	90.09
2-(1-Methyl-propyl)-3-methyl-phenol	48.877	49.165	53.03	56.85	60.59	64.22	67.74	71.13	74.38	77.5	80.47	83.31	86.03	88.61	91.08
4-(1-Methyl-propyl)-3-methyl-phenol	49.312	49.598	53.45	57.25	60.98	64.61	68.12	71.5	74.75	77.86	80.83	83.67	86.38	88.97	91.44
5-(1-Methyl-propyl)-3-methyl-phenol	50.504	50.784	54.56	58.31	61.98	65.57	69.04	72.39	75.61	78.69	81.63	84.45	87.13	89.7	92.14
4,6-Di-isopropyl-3-methyl-phenol	59.64	59.985	64.61	69.18	73.65	78	82.22	86.29	90.2	93.96	97.55	101	104.3	107.4	110.4
5,6-Di-isopropyl-3-methyl-phenol	60.16	60.499	65.07	69.6	74.05	78.39	82.6	86.67	90.58	94.32	97.91	101.3	104.6	107.7	110.7
4,5-Di-isopropyl-3-methyl-phenol	60.46	60.802	65.41	69.96	74.42	78.76	82.97	87.03	90.93	94.67	98.25	101.7	104.9	108.1	111

Table F-6: Pure component values for the respective compounds computed with the HCTH GGA functional

	Cp (T) ($cal \cdot mol^{-1} \cdot K^{-1}$)														
Temperature (K)→	650	675	700	725	750	775	800	825	850	875	900	925	950	975	1000
Compounds															
Water	8.736	8.802	8.868	8.935	9.002	9.07	9.139	9.207	9.276	9.346	9.416	9.485	9.555	9.625	9.695
Propene	27.152	27.822	28.47	29.09	29.69	30.27	30.83	31.37	31.89	32.4	32.89	33.36	33.81	34.25	34.68
Iso-propanol	37.315	38.221	39.09	39.93	40.74	41.52	42.27	42.99	43.69	44.36	45.01	45.64	46.25	46.84	47.4
1-Butene	36.932	37.869	38.77	39.64	40.47	41.28	42.05	42.8	43.52	44.22	44.89	45.54	46.16	46.77	47.35
cis-Butene	37.414	38.34	39.23	40.09	40.92	41.72	42.5	43.24	43.96	44.65	45.32	45.97	46.6	47.2	47.78
trans-Butene	37.709	38.621	39.5	40.35	41.16	41.95	42.71	43.44	44.15	44.83	45.49	46.13	46.75	47.34	47.92
Di-isopropylether	65.844	67.562	69.21	70.81	72.34	73.81	75.24	76.61	77.93	79.21	80.44	81.63	82.77	83.88	84.95
m-Cresol	110.34	112.38	114.4	116.4	118.3	120.3	122.2	124	125.9	127.7	129.5	131.2	133	134.7	136.4
o-Cresol	114.02	116.13	118.2	120.2	122.2	124.2	126.2	128.1	130	131.8	133.6	135.4	137.2	138.9	140.7
p-Cresol	116.51	118.64	120.7	122.8	124.8	126.8	128.8	130.7	132.6	134.5	136.3	138.1	139.9	141.7	143.4
Thymol	83.832	85.834	87.75	89.58	91.34	93.02	94.63	96.18	97.67	99.1	100.5	101.8	103.1	104.3	105.5
2-Isopropyl-3-methyl-phenol	84.064	86.057	87.96	89.79	91.53	93.21	94.81	96.35	97.83	99.25	100.6	101.9	103.2	104.4	105.6
4-Isopropyl-3-methyl-phenol	83.696	85.706	87.63	89.47	91.23	92.92	94.54	96.1	97.59	99.03	100.4	101.7	103	104.2	105.4
5-Isopropyl-3-methyl-phenol	84.633	86.608	88.5	90.3	92.03	93.69	95.28	96.8	98.27	99.68	101	102.3	103.6	104.8	106
6-(1-Methyl-propyl)-3-methyl-phenol	92.486	94.776	96.97	99.07	101.1	103	104.9	106.6	108.3	110	111.6	113.1	114.6	116	117.3
2-(1-Methyl-propyl)-3-methyl-phenol	93.441	95.695	97.85	99.92	101.9	103.8	105.6	107.4	109	110.6	112.2	113.7	115.1	116.5	117.9
4-(1-Methyl-propyl)-3-methyl-phenol	93.798	96.053	98.21	100.3	102.3	104.2	106	107.7	109.4	111	112.6	114.1	115.5	116.9	118.2
5-(1-Methyl-propyl)-3-methyl-phenol	94.484	96.721	98.86	100.9	102.9	104.8	106.6	108.3	110	111.6	113.1	114.6	116	117.4	118.7
4,6-Di-isopropyl-3-methyl-phenol	113.29	116.05	118.7	121.2	123.6	126	128.2	130.3	132.4	134.4	136.3	138.1	139.9	141.6	143.3
5,6-Di-isopropyl-3-methyl-phenol	113.59	116.33	118.9	121.5	123.9	126.2	128.4	130.5	132.6	134.5	136.4	138.3	140	141.7	143.3
4,5-Di-isopropyl-3-methyl-phenol	113.9	116.63	119.2	121.8	124.2	126.5	128.7	130.8	132.9	134.8	136.7	138.5	140.3	142	143.6

Table F-7: Pure component values for the respective compounds computed with the RPBE GGA functional

	$\Delta H_f^{\circ}{}_{est}$ (kcal·mol^{-1})	$\Delta G_f^{\circ}{}_{est}$ (kcal·mol^{-1})	Cp (cal·mol^{-1}·K^{-1})										
Temperature (K) →	298.15	298.15	25	50	75	100	125	150	175	200	225	250	275
Compounds													
Water	-47962.68646	-47976.55946	7.949	7.949	7.949	7.949	7.949	7.949	7.949	7.951	7.955	7.964	7.978
Propene	-73969.01871	-73988.09471	7.968	8.402	8.983	9.506	10.03	10.6	11.23	11.94	12.73	13.61	14.55
Iso-propanol	-121942.1089	-121963.3179	7.951	8.207	9.154	10.52	11.98	13.38	14.69	15.96	17.23	18.53	19.86
1-Butene	-98629.35321	-98650.28221	7.955	8.365	9.412	10.59	11.7	12.76	13.83	14.95	16.16	17.45	18.81
cis-Butene	-98631.21023	-98652.15023	7.949	8.174	9.14	10.44	11.7	12.88	14.02	15.18	16.38	17.64	18.96
trans-Butene	-98632.76407	-98653.29207	7.949	8.028	8.604	9.682	10.93	12.17	13.37	14.56	15.79	17.08	18.41
Di-isopropylether	-195918.2789	-195945.3469	9.211	10.88	12.92	15.62	18.44	21.11	23.62	26.05	28.46	30.92	33.43
m-Cresol	-217620.4235	-217645.4955	48.5	54.71	58.91	62.37	65.47	68.38	71.16	73.86	76.51	79.13	81.71
o-Cresol	-217619.9159	-217644.4779	48.21	53.92	57.77	61.04	64.02	66.86	69.59	72.26	74.88	77.46	80.03
p-Cresol	-217619.4344	-217643.8664	48.23	53.97	57.75	60.9	63.79	66.56	69.24	71.88	74.48	77.05	79.6
Thymol	-291603.5744	-291634.4804	9.845	11.96	15.13	18.82	22.53	26.12	29.6	33.03	36.45	39.91	43.38
2-Isopropyl-3-methyl-phenol	-291598.0669	-291628.3329	8.992	11.33	14.56	18.38	22.23	25.91	29.46	32.93	36.39	39.86	43.34
4-Isopropyl-3-methyl-phenol	-291601.9545	-291632.1095	8.911	11.22	14.32	18.04	21.84	25.54	29.11	32.62	36.11	39.61	43.11
5-Isopropyl-3-methyl-phenol	-291604.4438	-291634.5668	8.579	10.95	14.38	18.21	22.01	25.66	29.18	32.65	36.1	39.57	43.06
6-(1-Methyl-propyl)-3-methyl-phenol	-316264.0416	-316297.3046	10.35	14.07	18.14	22.1	25.89	29.56	33.17	36.78	40.45	44.18	47.97
2-(1-Methyl-propyl)-3-methyl-phenol	-316257.3148	-316289.2438	9.236	12.1	15.9	20.22	24.48	28.51	32.39	36.19	40	43.83	47.71
4-(1-Methyl-propyl)-3-methyl-phenol	-316261.7378	-316294.4718	9.783	13.41	17.36	21.47	25.44	29.24	32.92	36.58	40.27	44.02	47.82
5-(1-Methyl-propyl)-3-methyl-phenol	-316264.568	-316296.693	9.484	12.2	16.1	20.34	24.48	28.43	32.24	36	39.78	43.61	47.47
4,6-Di-isopropyl-3-methyl-phenol	-365584.8365	-365620.8915	10.33	14.66	19.43	24.78	30.08	35.08	39.81	44.39	48.93	53.47	58.05
5,6-Di-isopropyl-3-methyl-phenol	-365579.9482	-365615.8882	10.03	14.04	19.22	24.91	30.39	35.46	40.24	44.85	49.41	53.98	58.57
4,5-Di-isopropyl-3-methyl-phenol	-365577.8793	-365613.5233	9.419	13.7	18.95	24.67	30.18	35.29	40.1	44.72	49.28	53.85	58.43

Table F-8: Pure component values for the respective compounds computed with the RPBE GGA functional

	Cp (T) ($cal \cdot mol^{-1} \cdot K^{-1}$)														
Temperature (K)→	298.15	300	325	350	375	400	425	450	475	500	525	550	575	600	625
Compounds															
Water	7.996	7.998	8.025	8.059	8.1	8.145	8.196	8.25	8.308	8.367	8.429	8.492	8.556	8.622	8.688
Propene	15.455	15.529	16.54	17.55	18.56	19.55	20.52	21.46	22.37	23.24	24.08	24.88	25.65	26.39	27.11
Iso-propanol	21.121	21.223	22.6	23.98	25.36	26.7	28.02	29.29	30.53	31.71	32.85	33.94	34.99	36	36.96
1-Butene	20.115	20.221	21.66	23.11	24.54	25.95	27.32	28.65	29.93	31.16	32.34	33.48	34.56	35.6	36.6
cis-Butene	20.225	20.327	21.72	23.11	24.5	25.87	27.21	28.51	29.76	30.97	32.14	33.26	34.33	35.36	36.36
trans-Butene	19.688	19.792	21.2	22.62	24.03	25.42	26.78	28.11	29.39	30.62	31.81	32.96	34.06	35.11	36.13
Di-isopropylether	35.802	35.993	38.59	41.18	43.75	46.28	48.75	51.15	53.46	55.69	57.84	59.9	61.87	63.77	65.59
m-Cresol	84.091	84.28	86.83	89.35	91.86	94.34	96.8	99.23	101.6	104	106.3	108.6	110.9	113.1	115.3
o-Cresol	82.383	82.571	85.1	87.6	90.09	92.56	95	97.42	99.8	102.2	104.5	106.8	109	111.3	113.4
p-Cresol	81.945	82.132	84.65	87.15	89.63	92.09	94.53	96.94	99.32	101.7	104	106.3	108.5	110.7	112.9
Thymol	46.595	46.852	50.3	53.7	57.02	60.25	63.36	66.34	69.2	71.93	74.53	77.01	79.38	81.63	83.78
2-Isopropyl-3-methyl-phenol	46.56	46.817	50.27	53.67	56.99	60.22	63.32	66.31	69.16	71.89	74.49	76.97	79.33	81.58	83.73
4-Isopropyl-3-methyl-phenol	46.351	46.609	50.08	53.48	56.81	60.04	63.15	66.14	69	71.73	74.33	76.82	79.18	81.44	83.59
5-Isopropyl-3-methyl-phenol	46.288	46.546	50	53.41	56.74	59.96	63.07	66.06	68.93	71.66	74.27	76.76	79.12	81.38	83.53
6-(1-Methyl-propyl)-3-methyl-phenol	51.515	51.798	55.62	59.4	63.1	66.71	70.2	73.56	76.78	79.86	82.8	85.6	88.28	90.83	93.27
2-(1-Methyl-propyl)-3-methyl-phenol	51.304	51.591	55.46	59.28	63.01	66.64	70.15	73.52	76.76	79.84	82.79	85.61	88.29	90.84	93.28
4-(1-Methyl-propyl)-3-methyl-phenol	51.365	51.649	55.47	59.26	62.97	66.58	70.07	73.43	76.65	79.73	82.67	85.47	88.15	90.7	93.13
5-(1-Methyl-propyl)-3-methyl-phenol	51.067	51.355	55.23	59.05	62.79	66.42	69.93	73.31	76.54	79.63	82.58	85.39	88.07	90.62	93.06
4,6-Di-isopropyl-3-methyl-phenol	62.303	62.643	67.22	71.76	76.2	80.54	84.74	88.78	92.67	96.4	99.96	103.4	106.6	109.7	112.7
5,6-Di-isopropyl-3-methyl-phenol	62.83	63.17	67.76	72.29	76.73	81.06	85.25	89.28	93.16	96.87	100.4	103.8	107	110.1	113.1
4,5-Di-isopropyl-3-methyl-phenol	62.688	63.028	67.61	72.14	76.58	80.9	85.09	89.13	93	96.71	100.3	103.7	106.9	110	112.9

Table F-9: Pure component values for the respective compounds computed with the RPBE GGA functional

	Cp (T) ($cal \cdot mol^{-1} \cdot K^{-1}$)														
Temperature (K)→	650	675	700	725	750	775	800	825	850	875	900	925	950	975	1000
Compounds															
Water	8.755	8.823	8.891	8.96	9.03	9.1	9.17	9.241	9.313	9.384	9.456	9.528	9.6	9.672	9.744
Propene	27.789	28.448	29.08	29.69	30.28	30.85	31.4	31.93	32.44	32.93	33.41	33.87	34.32	34.75	35.16
Iso-propanol	37.891	38.782	39.64	40.46	41.26	42.02	42.76	43.47	44.16	44.82	45.46	46.08	46.68	47.26	47.82
1-Butene	37.555	38.475	39.36	40.21	41.03	41.82	42.58	43.31	44.02	44.7	45.36	45.99	46.61	47.2	47.77
cis-Butene	37.309	38.226	39.11	39.96	40.78	41.57	42.33	43.07	43.78	44.46	45.12	45.76	46.38	46.98	47.56
trans-Butene	37.105	38.044	38.95	39.82	40.66	41.46	42.24	42.99	43.72	44.42	45.09	45.75	46.38	46.98	47.57
Di-isopropylether	67.338	69.018	70.63	72.19	73.68	75.12	76.51	77.84	79.13	80.37	81.57	82.73	83.84	84.92	85.96
m-Cresol	117.49	119.62	121.7	123.8	125.8	127.8	129.7	131.7	133.6	135.4	137.3	139.1	140.9	142.6	144.4
o-Cresol	115.6	117.72	119.8	121.9	123.9	125.9	127.8	129.7	131.6	133.5	135.3	137.1	138.9	140.7	142.4
p-Cresol	115.08	117.2	119.3	121.3	123.3	125.3	127.3	129.2	131.1	132.9	134.8	136.6	138.4	140.1	141.8
Thymol	85.829	87.787	89.66	91.45	93.16	94.8	96.38	97.89	99.34	100.7	102.1	103.4	104.6	105.8	106.9
2-Isopropyl-3-methyl-phenol	85.772	87.725	89.59	91.38	93.09	94.73	96.3	97.8	99.25	100.6	102	103.3	104.5	105.7	106.8
4-Isopropyl-3-methyl-phenol	85.641	87.601	89.47	91.27	92.98	94.63	96.2	97.72	99.17	100.6	101.9	103.2	104.4	105.6	106.8
5-Isopropyl-3-methyl-phenol	85.589	87.551	89.43	91.22	92.94	94.58	96.16	97.68	99.13	100.5	101.9	103.2	104.4	105.6	106.8
6-(1-Methyl-propyl)-3-methyl-phenol	95.596	97.82	99.95	102	103.9	105.8	107.6	109.3	111	112.6	114.1	115.5	117	118.3	119.6
2-(1-Methyl-propyl)-3-methyl-phenol	95.611	97.836	99.96	102	103.9	105.8	107.6	109.3	111	112.6	114.1	115.6	117	118.3	119.6
4-(1-Methyl-propyl)-3-methyl-phenol	95.453	97.672	99.79	101.8	103.8	105.6	107.4	109.1	110.8	112.4	113.9	115.4	116.8	118.1	119.4
5-(1-Methyl-propyl)-3-methyl-phenol	95.384	97.604	99.73	101.8	103.7	105.6	107.4	109.1	110.7	112.3	113.8	115.3	116.7	118.1	119.4
4,6-Di-isopropyl-3-methyl-phenol	115.52	118.24	120.8	123.3	125.7	128	130.2	132.3	134.3	136.3	138.2	140	141.7	143.4	145
5,6-Di-isopropyl-3-methyl-phenol	115.9	118.6	121.2	123.7	126	128.3	130.5	132.6	134.6	136.6	138.4	140.2	142	143.6	145.2
4,5-Di-isopropyl-3-methyl-phenol	115.76	118.46	121	123.5	125.9	128.2	130.4	132.5	134.5	136.4	138.3	140.1	141.8	143.5	145.1

Table F-10: Pure component values for the respective compounds computed with the PLYB GGA functional

	$\Delta H_f^{\circ}{}_{est}$ (kcal·mol^{-1})	$\Delta G_f^{\circ}{}_{est}$ (kcal·mol^{-1})	Cp (cal·mol^{-1}·K^{-1})										
Temperature (K) →	298.15	298.15	25	50	75	100	125	150	175	200	225	250	275
Compounds													
Water	-47956.23455	-47970.11055	7.949	7.949	7.949	7.949	7.949	7.949	7.949	7.951	7.955	7.964	7.978
Propene	-73921.65235	-73940.58435	7.952	8.178	8.685	9.236	9.802	10.4	11.05	11.78	12.58	13.46	14.39
Iso-propanol	-121887.3743	-121908.5873	7.949	8.121	9.023	10.46	12.01	13.46	14.81	16.11	17.4	18.71	20.05
1-Butene	-98565.596	-98586.886	8.055	9.049	10.23	11.29	12.26	13.2	14.17	15.22	16.37	17.61	18.93
cis-Butene	-98568.0023	-98589.5753	8.092	9.289	10.59	11.71	12.72	13.69	14.67	15.71	16.82	18.03	19.3
trans-Butene	-98569.5324	-98591.1074	8.014	8.993	10.56	12.01	13.21	14.24	15.22	16.22	17.29	18.44	19.67
Di-isopropylether	-195817.0155	-195844.8325	9.157	11.57	14.38	17.35	20.15	22.69	25.06	27.36	29.67	32.05	34.5
m-Cresol	-217525.1509	-217549.1009	48.38	53.96	57.56	60.53	63.25	65.84	68.35	70.81	73.25	75.68	78.1
o-Cresol	-217524.1796	-217548.8196	48.21	53.95	57.86	61.17	64.19	67.05	69.79	72.47	75.1	77.7	80.28
p-Cresol	-217524.1129	-217549.1269	48.27	54.38	58.57	62.02	65.13	68.05	70.86	73.58	76.26	78.89	81.5
Thymol	-291457.649	-291489.099	9.895	12.68	16.28	20.06	23.71	27.18	30.54	33.88	37.23	40.62	44.05
2-Isopropyl-3-methyl-phenol	-291452.4057	-291482.8157	8.755	11.44	15.02	18.93	22.73	26.35	29.83	33.25	36.67	40.11	43.58
4-Isopropyl-3-methyl-phenol	-291456.2742	-291487.4312	9.422	12.36	16.04	19.86	23.54	27.03	30.41	33.76	37.13	40.53	43.96
5-Isopropyl-3-methyl-phenol	-291458.7829	-291489.9689	9.275	12.28	16.06	19.93	23.61	27.09	30.46	33.79	37.14	40.53	43.96
6-(1-Methyl-propyl)-3-methyl-phenol	-316101.3941	-316135.1261	10.78	14.83	18.81	22.78	26.58	30.23	33.82	37.41	41.06	44.78	48.57
2-(1-Methyl-propyl)-3-methyl-phenol	-316094.9944	-316128.3054	10.6	13.9	17.86	22.06	26.08	29.88	33.56	37.23	40.93	44.69	48.51
4-(1-Methyl-propyl)-3-methyl-phenol	-316099.302	-316132.086	9.947	13.16	17.11	21.33	25.41	29.29	33.04	36.75	40.49	44.29	48.13
5-(1-Methyl-propyl)-3-methyl-phenol	-316102.6923	-316136.2483	10.16	14.01	18.49	22.79	26.73	30.43	34.02	37.6	41.24	44.95	48.73
4,6-Di-isopropyl-3-methyl-phenol	-365389.1205	-365426.2315	10.95	15.63	20.96	26.58	31.88	36.76	41.36	45.82	50.25	54.72	59.23
5,6-Di-isopropyl-3-methyl-phenol	-365384.5541	-365422.1421	10.67	16.03	22.22	28.08	33.29	38.01	42.44	46.76	51.09	55.48	59.94
4,5-Di-isopropyl-3-methyl-phenol	-365382.4937	-365419.4197	10.4	15.04	20.8	26.69	32.11	37.06	41.7	46.19	50.65	55.14	59.68

Table F-11: Pure component values for the respective compounds computed with the PLYB GGA functional

	Cp (T) ($cal \cdot mol^{-1} \cdot K^{-1}$)														
Temperature (K)→	**298.15**	**300**	**325**	**350**	**375**	**400**	**425**	**450**	**475**	**500**	**525**	**550**	**575**	**600**	**625**
Compounds															
Water	7.997	7.999	8.027	8.061	8.102	8.149	8.2	8.255	8.313	8.373	8.435	8.499	8.564	8.63	8.697
Propene	15.299	15.373	16.38	17.39	18.4	19.39	20.36	21.3	22.21	23.09	23.93	24.74	25.52	26.27	26.99
Iso-propanol	21.314	21.416	22.8	24.18	25.55	26.9	28.21	29.49	30.72	31.91	33.05	34.14	35.19	36.2	37.17
1-Butene	20.214	20.317	21.74	23.16	24.58	25.98	27.35	28.67	29.95	31.18	32.36	33.5	34.59	35.63	36.64
cis-Butene	20.535	20.635	22	23.38	24.76	26.12	27.45	28.75	30	31.21	32.38	33.5	34.58	35.62	36.62
trans-Butene	20.869	20.966	22.3	23.65	25.01	26.35	27.66	28.94	30.19	31.39	32.55	33.66	34.74	35.77	36.76
Di-isopropylether	36.831	37.018	39.57	42.13	44.68	47.18	49.63	52	54.29	56.51	58.63	60.68	62.64	64.53	66.34
m-Cresol	80.331	80.51	82.92	85.31	87.7	90.06	92.41	94.74	97.05	99.33	101.6	103.8	106	108.1	110.3
o-Cresol	82.644	82.833	85.37	87.9	90.4	92.88	95.34	97.77	100.2	102.5	104.9	107.2	109.4	111.7	113.9
p-Cresol	83.899	84.09	86.66	89.2	91.73	94.23	96.7	99.14	101.6	103.9	106.3	108.6	110.9	113.1	115.3
Thymol	47.232	47.486	50.91	54.28	57.58	60.78	63.87	66.84	69.68	72.4	74.99	77.46	79.82	82.07	84.21
2-Isopropyl-3-methyl-phenol	46.793	47.049	50.5	53.89	57.21	60.43	63.54	66.52	69.38	72.11	74.71	77.2	79.56	81.82	83.97
4-Isopropyl-3-methyl-phenol	47.154	47.409	50.84	54.22	57.53	60.74	63.83	66.81	69.66	72.38	74.98	77.45	79.81	82.06	84.21
5-Isopropyl-3-methyl-phenol	47.14	47.394	50.82	54.19	57.5	60.7	63.8	66.77	69.62	72.34	74.94	77.41	79.78	82.03	84.17
6-(1-Methyl-propyl)-3-methyl-phenol	52.103	52.386	56.2	59.98	63.68	67.28	70.77	74.12	77.33	80.4	83.34	86.14	88.81	91.36	93.79
2-(1-Methyl-propyl)-3-methyl-phenol	52.073	52.358	56.2	59.99	63.7	67.31	70.8	74.16	77.38	80.45	83.39	86.19	88.86	91.41	93.84
4-(1-Methyl-propyl)-3-methyl-phenol	51.71	51.996	55.85	59.66	63.39	67.01	70.52	73.89	77.11	80.2	83.15	85.96	88.64	91.19	93.63
5-(1-Methyl-propyl)-3-methyl-phenol	52.265	52.548	56.36	60.14	63.84	67.45	70.93	74.28	77.49	80.56	83.5	86.29	88.96	91.5	93.93
4,6-Di-isopropyl-3-methyl-phenol	63.44	63.776	68.32	72.81	77.23	81.53	85.7	89.72	93.59	97.29	100.8	104.2	107.5	110.6	113.5
5,6-Di-isopropyl-3-methyl-phenol	64.103	64.436	68.94	73.41	77.8	82.08	86.23	90.23	94.08	97.76	101.3	104.7	107.9	110.9	113.9
4,5-Di-isopropyl-3-methyl-phenol	63.897	64.234	68.78	73.29	77.7	82.01	86.17	90.18	94.04	97.73	101.3	104.6	107.8	110.9	113.9

Table F-12: Pure component values for the respective compounds computed with the PLYB GGA functional

	Cp (T) ($cal \cdot mol^{-1} \cdot K^{-1}$)														
Temperature (K)→	650	675	700	725	750	775	800	825	850	875	900	925	950	975	1000
Compounds															
Water	8.765	8.834	8.903	8.973	9.044	9.115	9.187	9.259	9.332	9.405	9.478	9.551	9.624	9.697	9.77
Propene	27.684	28.351	28.99	29.61	30.21	30.79	31.34	31.88	32.4	32.9	33.38	33.85	34.3	34.74	35.16
Iso-propanol	38.103	38.998	39.86	40.69	41.49	42.26	43	43.72	44.41	45.08	45.72	46.34	46.95	47.53	48.09
1-Butene	37.604	38.532	39.43	40.28	41.11	41.91	42.68	43.42	44.13	44.82	45.49	46.13	46.75	47.35	47.93
cis-Butene	37.586	38.512	39.4	40.26	41.09	41.89	42.66	43.4	44.12	44.81	45.48	46.13	46.75	47.35	47.93
trans-Butene	37.72	38.641	39.53	40.39	41.21	42.01	42.77	43.51	44.23	44.92	45.58	46.23	46.85	47.45	48.02
Di-isopropylether	68.077	69.749	71.36	72.9	74.39	75.83	77.21	78.54	79.82	81.06	82.25	83.4	84.51	85.58	86.61
m-Cresol	112.36	114.42	116.5	118.4	120.4	122.3	124.3	126.1	128	129.8	131.6	133.3	135.1	136.8	138.5
o-Cresol	116.05	118.18	120.3	122.3	124.4	126.4	128.3	130.3	132.2	134	135.9	137.7	139.5	141.2	143
p-Cresol	117.51	119.64	121.7	123.8	125.8	127.8	129.8	131.8	133.7	135.5	137.4	139.2	141	142.8	144.5
Thymol	86.254	88.208	90.08	91.86	93.58	95.22	96.79	98.3	99.75	101.1	102.5	103.8	105	106.2	107.3
2-Isopropyl-3-methyl-phenol	86.023	87.984	89.86	91.65	93.37	95.02	96.6	98.11	99.56	101	102.3	103.6	104.8	106	107.2
4-Isopropyl-3-methyl-phenol	86.254	88.21	90.08	91.87	93.58	95.22	96.79	98.3	99.75	101.1	102.5	103.8	105	106.2	107.3
5-Isopropyl-3-methyl-phenol	86.22	88.178	90.05	91.84	93.55	95.2	96.77	98.28	99.73	101.1	102.5	103.8	105	106.2	107.3
6-(1-Methyl-propyl)-3-methyl-phenol	96.11	98.33	100.5	102.5	104.4	106.3	108.1	109.8	111.5	113	114.6	116	117.4	118.8	120.1
2-(1-Methyl-propyl)-3-methyl-phenol	96.157	98.374	100.5	102.5	104.5	106.3	108.1	109.8	111.5	113.1	114.6	116	117.5	118.8	120.1
4-(1-Methyl-propyl)-3-methyl-phenol	95.963	98.189	100.3	102.4	104.3	106.2	108	109.7	111.3	112.9	114.5	115.9	117.3	118.7	120
5-(1-Methyl-propyl)-3-methyl-phenol	96.251	98.466	100.6	102.6	104.6	106.4	108.2	109.9	111.6	113.1	114.7	116.1	117.5	118.9	120.2
4,6-Di-isopropyl-3-methyl-phenol	116.33	119.04	121.6	124.1	126.5	128.8	131	133.1	135.1	137	138.9	140.7	142.5	144.1	145.7
5,6-Di-isopropyl-3-methyl-phenol	116.7	119.39	122	124.4	126.8	129.1	131.2	133.3	135.4	137.3	139.2	140.9	142.7	144.3	145.9
4,5-Di-isopropyl-3-methyl-phenol	116.67	119.36	121.9	124.4	126.8	129	131.2	133.3	135.3	137.3	139.1	140.9	142.6	144.3	145.9

Appendix G: Thermodynamic data from group contribution methods

As an alternative to thermodynamic data generated with the use of density functional theory, the ideal gas Gibbs free energy of formation, enthalpy of formation and gas heat capacity of the respective compounds was also estimated with **group contribution methods** such as that of Joback (1984;1987) and Constantinou and Gani (1994).

Group contribution methods were also used to estimate pure component properties such as boiling points and critical properties for the compounds for which no experimentally measured values were found in literature.

As a means of method validation i.e., to determine which of the group contribution methods was most likely to predict the pure component properties with the greatest accuracy, such properties were calculated and compared to the measured values for a control group of phenolic compounds (for which this data was available literature). Results for these calculations are presented in Table G-1- Table G-4.

It is evident from Table G-2 that the method of Marrero and Pardillo (1999) consistently predicted the normal boiling points of thymol and its position isomers with the greatest degree of accuracy compared to the other methods. Therefore, this method was used to estimate the normal boiling points for the compounds for which this data could not be found in literature.

In turn, the method described by Wilson and Jasperson (1996) with the first and second order group contribution parameters was used to estimate the critical temperature. Table G-3 shows that although the methods by Gani and Constantinou (1994) with first and/or second order parameters predict the smaller phenolic molecules with a fair degree of accuracy, they overpredict this value for thymol by a much larger margin as compared to that of Wilson and Jasperson (1996) which predict thymol's critical temperature with the greatest degree of accuracy.

The methods by Ambrose (1978, 1979) and Marrero and Pardillo (1999) predicted the critical pressures of the control group with the greatest degree of accuracy (see Table G-4). As the method by Ambrose predicted the Thymol's critical pressure

more accurately than that of Marrero and Pardillo (1999), it was used to predict the critical pressures in this study.

The estimates for the normal boiling points, critical data, ideal gas Gibbs free energy of formation and enthalpy of formation used in this study, are shown in Table G-1.

Table G-1: Estimated pure component physico-chemical and thermodynamic property values for the respective compounds

	Sg (4℃, 1Atm)	$T_{b,est}$ (K)	$T_{c,est}$ (K)	$P_{c,est}$ (bar)	$\Delta H_f°_{est}$ (kJ·mol^{-1})	$\Delta H_f°_{est}$ (kJ·mol^{-1})	$\Delta H_f°_{est}$ (kJ·mol^{-1})	$\Delta G_f°_{est}$ (kJ·mol^{-1})	$\Delta G_f°_{est}$ (kJ·mol^{-1})	$\Delta G_f°_{est}$ (kJ·mol^{-1})
Estimation Method⟶	Specific gravity	Marrero/ Pardillo	Wilson/ Jasperson (2nd order)	Ambrose	Joback	Gani/ Constantinou (1st order)	Gani/ Constantinou (2nd order)	Joback	Gani/ Constantinou (1st order)	Gani/ Constantinou (2nd order)
Compounds										
Thymol	0.975*	505.7*	698*	33.4*	-207.3	-203.7	-204.5	-21.0	-19.9	-19.6
2-Isopropyl-3-methyl-phenol	0.946*	501.7*	704.4	34.9	-207.3	-203.7	-204.5	-21.0	-19.9	-19.6
4-Isopropyl-3-methyl-phenol	0.974**	511.2*	717.7	33.2	-207.3	-203.7	-204.5	-21.0	-19.9	-19.6
5-Isopropyl-3-methyl-phenol	0.973*	514.2*	722.0	31.7	-207.3	-203.7	-204.5	-21.0	-19.9	-19.6
6-(1-Methyl-propyl)-3-methyl-phenol	0.992*	532.9	737.2	29.7	-227.9	-224.4	-224.4	-12.5	-11.7	-11.7
2-(1-Methyl-propyl)-3-methyl-phenol	0.962***	531.7	735.6	31.0	-227.9	-224.4	-224.4	-12.5	-11.7	-11.7
4-(1-Methyl-propyl)-3-methyl-phenol	0.962***	530.7	734.3	29.7	-227.9	-224.4	-224.4	-12.5	-11.7	-11.7
5-(1-Methyl-propyl)-3-methyl-phenol	0.962***	531.9	735.9	28.5	-227.9	-224.4	-224.4	-12.5	-11.7	-11.7
4,6-Di-isopropyl-3-methyl-phenol	0.945**	557.3	750.6	25.1	-285.9	-279.1	-280.8	-7.77	-5.58	-4.99
5,6-Di-isopropyl-3-methyl-phenol	0.941**	557.3	750.6	25.1	-285.9	-279.1	-280.8	-7.77	-5.58	-4.99
4,5-Di-isopropyl-3-methyl-phenol	0.941****	557.3	750.6	25.1	-285.9	-279.1	-280.8	-7.77	-5.58	-4.99

*) Actual measured values obtained from literature

**) Estimated values calculated using ACD/Labs (Advanced Chemistry Development) Software V ersion 8.14 for Solaris (1994-2009 ACD/Labs)

***) Estimated with the method of Marrero and Pardillo (1999)

****) Assumed to be the same value as that of 5,6-Di-isopropyl-3-methyl-phenol

Figure G-1 compares the results of the different simulations of the system with MPWTDIB (*m*-cresol, propene, water, thymol isomers, and di-isopropylated *m*-cresol) corresponding to thermodynamic data obtained with Molecular modelling (PW91, HCTH, RPBE and BLYB) and group contribution methods (Gani and Constantinou (1st and 2nd order) and Joback (Daubert and Thomas,1999). All cases showed that the *m*-cresol equilibrium conversion decreased once the transition from liquid to gas phase started, with increasing temperature.

The data obtained with molecular modelling showed a transition from gas to liquid phase at lower temperatures as compared to the thermodynamic data obtained with the group contribution methods. In contrast to the results obtained with the respective group contribution method data which showed similar *m*-cresol conversion, the results obtained with the different molecular modelling functionals did not correspond.

The results corresponding to the following functionals employed for the molecular model are shown: PW91, HCTH, RPBE, BLYP. The following Group contribution methods were used to generate thermodynamic data: Gani and Constantinou with 1st and 2nd order parameters and Joback. These curves model systems at 1 bar and iso-propanol/*m*-cresol molar ratio of 1:1. The following components were taken into account for this model: MPWTDIB - *m*-cresol, propene, water, thymol isomers, di-isopropylated *m*-cresol isomers, sec. butylated *m*-cresol isomers and butenes.

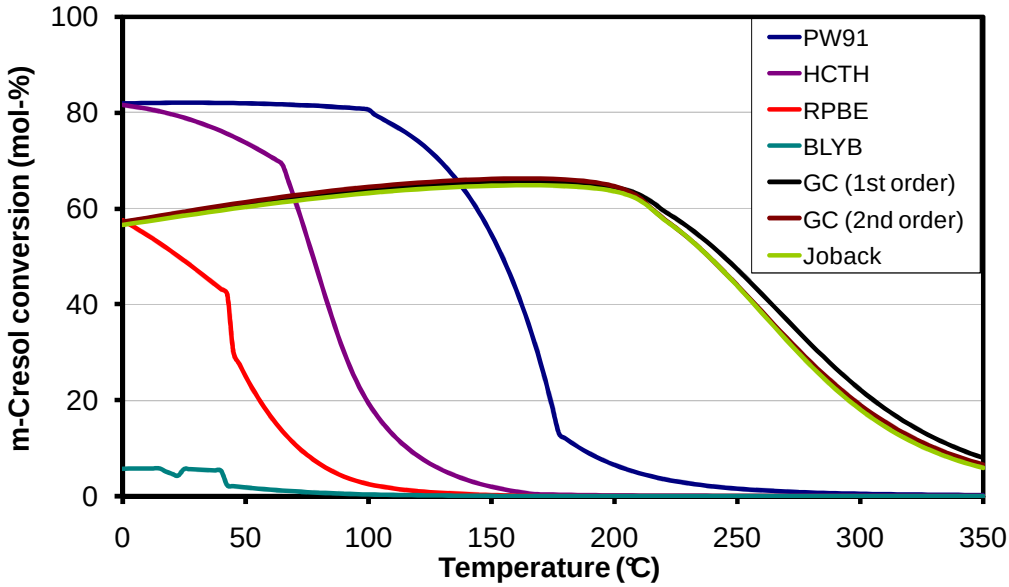

Figure G-1: *m*-Cresol conversion at thermodynamic equilibrium as a function of temperature.

Table G-2: Comparison of the normal boiling points estimated

Compounds	$T_{b,est}$ (K)				$T_{b,exp}$ (K)
	Joback	Gani/Constantinou (1st order)	Gani/Constantinou (2nd order)	Marrero/ Pardillo	**Experimental values**
2-Ethyl-phenol	489.7	489.2	489.2	480.7	**477.67**
3-Ethyl-phenol	489.7	489.2	489.2	482.1	**491.58**
4-Ethyl-phenol	489.7	489.2	489.2	482.1	**491.15**
2,4-Dimethyl-phenol	494.7	492.3	492.3	489.4	**484.09**
3,4-Dimethyl-phenol	494.7	492.3	492.3	489.4	**500.11**
3,5-Dimethyl-phenol	494.7	492.3	492.3	490.7	**494.85**
m-Cresol	466.9	472.3	472.3	465.9	**475.425**
Thymol	540.0	519.1	517.2	514.5	**505.7**
2-Isopropyl-3-methyl-phenol	540.0	519.1	517.2	513.3	**501.65**
4-Isopropyl-3-methyl-phenol	540.0	519.1	517.2	512.3	**511.15**
5-Isopropyl-3-methyl-phenol	540.0	519.1	517.2	513.5	**514.2**

Table G-3: Comparison of the critical temperatures estimated using different group contribution methods

Compounds	**$T_{c,est}$ (K)**								**$T_{c,exp}$ (K)**
	Lydersen	Ambrose	Joback	Gani/ Constantinou (1st order)	Gani/ Constantinou (2nd order)	Wilson/ Jasperson (1st)	Wilson/ Jasperson (2nd)	Marrero/ Pardillo	**Experimental values**
2-Ethyl-phenol	694.2	702.6	698.1	718.6	718.6	702.9	693.6	699.8	**718.8**
3-Ethyl-phenol	714.4	717.7	718.4	718.6	718.6	723.4	713.8	718.3	**716.4**
4-Ethyl-phenol	713.8	717.1	717.8	718.6	718.6	722.7	713.1	717.6	**729.8**
2,4-Dimethyl-phenol	703.5	708.8	706.5	721.0	721.0	712.3	702.9	705.7	**715.6**
3,4-Dimethyl-phenol	726.8	731.2	729.9	721.0	721.0	735.9	726.1	729.1	**703.0**
3,5-Dimethyl-phenol	719.1	719.4	722.2	721.0	721.0	728.2	718.5	719.5	**707.6**
m-Cresol	706.0	705.5	709.5	705.1	705.1	714.1	703.6	709.4	**705.9**
Thymol	712.2	717.6	715.9	739.0	737.4	718.1	710.1	723.7	**698.0**

Table G-4: Comparison of the Critical pressures obtained using different group contribution methods compared to experimental values

Compounds	**$P_{c,est}$ (bar)**							**$P_{c,exp}$ (bar)**
	Lydersen	Ambrose	Joback	Gani/ Constantinou (1st order)	Gani/ Constantinou (2nd order)	Wilson/ Jasperson (1st)	Marrero/ Pardillo	**Experimental values**
2-Ethyl-phenol	42.4	44.3	44.1	43.0	43.0	37.9	42.2	**43.0**
3-Ethyl-phenol	42.4	41.8	44.1	43.0	43.0	38.8	41.3	**41.5**
4-Ethyl-phenol	42.4	41.8	44.1	43.0	43.0	38.7	41.3	**40.5**
2,4-Dimethyl-phenol	42.4	43.3	43.2	43.5	43.5	38.2	42.8	**42.8**
3,4-Dimethyl-phenol	42.4	43.3	43.2	43.5	43.5	39.4	42.8	**42.8**
3,5-Dimethyl-phenol	42.4	40.8	43.2	43.5	43.5	38.6	41.8	**41.3**
m-Cresol	50.0	49.1	50.3	50.8	50.8	44.8	49.4	**45.6**
Thymol	33.0	33.2	34.4	33.2	33.0	28.6	32.3	**33.4**

Appendix H: Group contribution method sample calculations

The following equations were employed in the calculation of pure component data using the method proposed by **Lydersen (1955).**

Equation H-1: Calculation of critical temperature, T_c (Lydersen, 1955)

$$T_C = \frac{T_b}{\theta}$$

Equation H-2: Denominator in critical temperature eqn. (Lydersen, 1955)

$$\theta = 0.567 + \sum \Delta_T - \left(\sum \Delta_T\right)^2$$

Equation H-3: Calculation of critical pressure

$$P_C = \frac{M}{(\Phi + 0.34)^2}$$

Sample calculation of T_c with method proposed by Lydersen for 5-Isopropyl-3-methyl-phenol:

$\Sigma\Delta_T$ = 3 (=CH$_{ring}$) + 3 (=C<$_{ring}$) + 3(-CH$_3$) + 1(-OH$_{phenol}$) + 1(-CH<)
= 3 (0.011) + 3 (0.011) + 3(0.020) + 1(0.035) + 1(0.012)
= 0.173

θ = 0.567 + $\Sigma\Delta_T$ - ($\Sigma\Delta_T$)^2
= 0.567 + 0.173 - (0.173)^2
= 0.710

T_c = $\frac{T_b}{\theta}$
= $\frac{514.2}{0.71}$
= 724 K

Sample calculation of *Pc* for 5-Isopropyl-3-methyl-phenol

Φ = 4 (=CH-$_{ring}$) + 2(=C<$_{ring}$) + 3(-CH$_3$) + 1(-OH$_{phenol}$) + 1(-CH<)
= 3 (0.154) + 3(0.154) + 3(0.227) + 1(–0.02) + 1(0.21)
= 1.795

Pc = $\frac{M}{(\Phi+0.34)^2}$
= $\frac{150.22}{(1.795+0.34)^2}$
= 33 atm

Appendix I: Catalyst drying and activation sequence

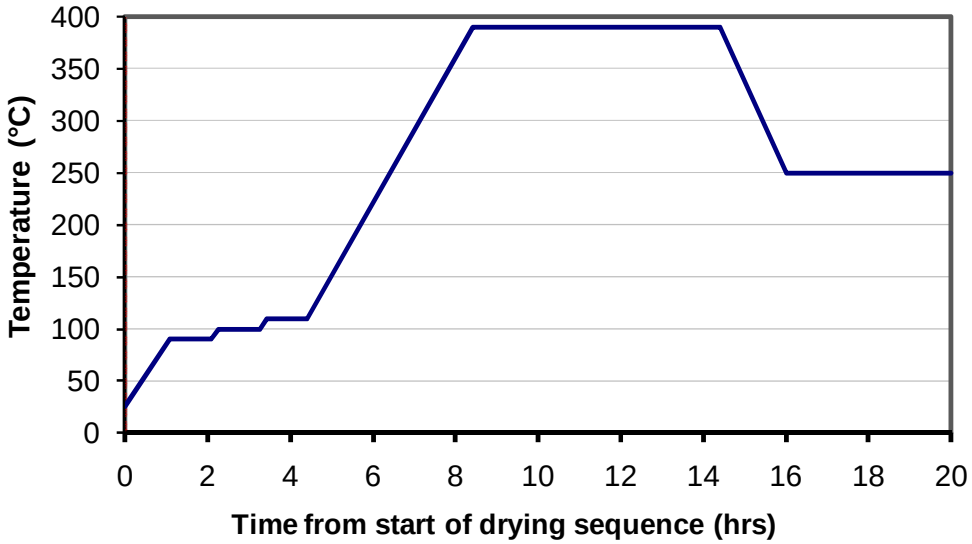

Figure I-1: Catalyst drying and activation sequence (1 bar, 50 ml·min^{-1} N_2)

Appendix J: Phase calculations for thymol synthesis system

The Aspen Plus User Interface (Aspen Technology, Inc. 2006) software package was employed for the simulation of phases in the system under reaction conditions used. Figure J-1 was employed to verify whether the temperature at the inlet of the reactor was below the boiling point of the IPA / *m*-cresol mixture.

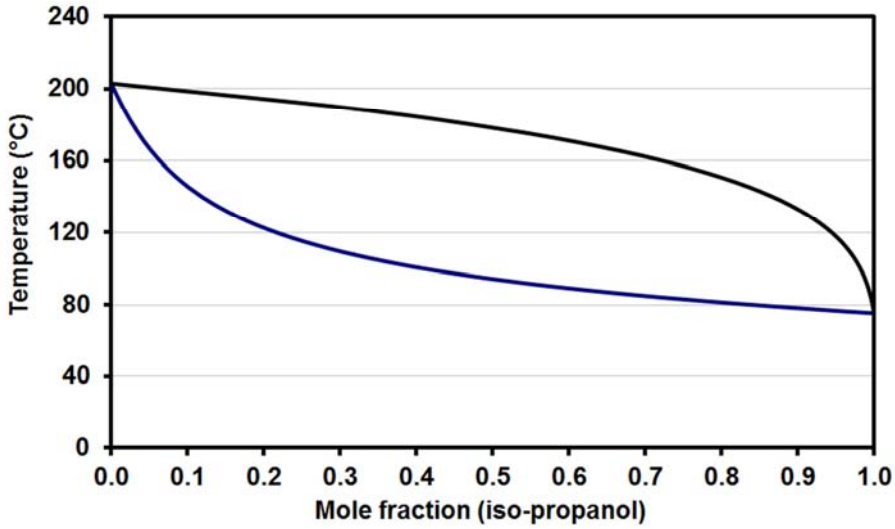

Figure J-1: Txy diagrams for IPA/*m*-cresol mixture

The dew point pressure curves for various equations of state are displayed in Figure J-2. In this simulation iso-propanol and *m*-cresol was fed to the reactor at a 1:1 molar ratio. The dehydration of iso-propanol to propene and water was complete before *m*-cresol was alkylated. The results for different equations-of-state are displayed in this graph.

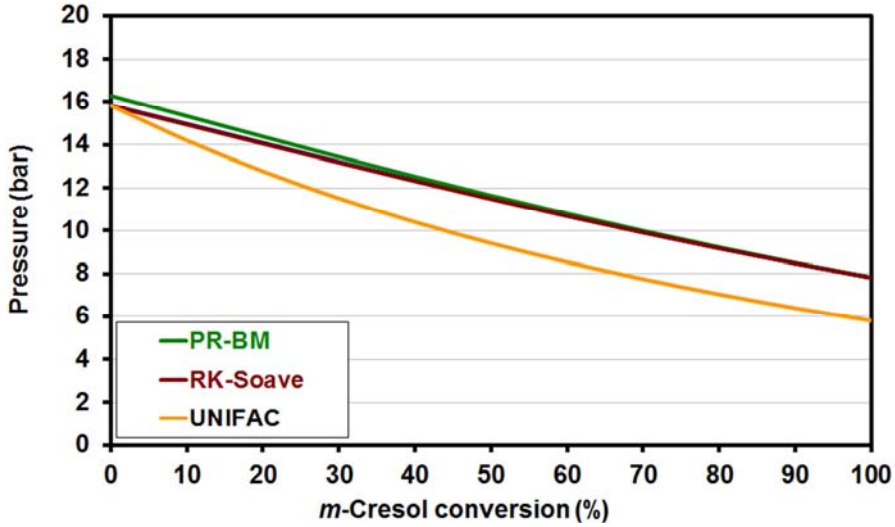

Figure J-2: Dew point pressure of a propene-water-*m*-cresol-thymol system as a function of *m*-cresol conversion.

Appendix K: GC methods and apparatus

Table K-1: Gas chromatography equipment and methods

Experiment	Thymol synthesis	Thymol synthesis	Iso-propanol dehydration
Analysis type	Quantitative	Qualitative	Quantitative/ Qualitative
Equipment	GC	GCMS	GC / GCMS
GC manufacturer (product name)	Varian (3600)	Agilent	Varian(3600)/ Agilent
GC column supplier	Supelco	Varian	Varian
Stationary phase	α-Dex-120*	CP-Sil 5 CB	CP-Sil 5 CB
GC column part number	24310	CP7691	CP7692
GC capillary column type	Fused silica, wall coated	Fused silica, wall coated	Fused silica, wall coated
GC column length (m)	30	25	25
GC column Internal diameter (mm)	0.25	0.15	0.15
GC column film thickness (µm)	0.25	2	2
Sample diluent	Acetone	Acetone	N_2
Ratio of sample to diluent (vol.)	1:3	1:3	1:50
Mode of sample injection	CP-8400 Autosampler (liquid syringe)	Manual liquid syringe injection	Online analysis with sample valve / Ampoule breaker
Initial injector head pressure (bar)	0.23	2	N/A
Carrier gas	H_2	He	H_2
Mode of carrier gas control	Constant flow	Constant pressure	Constant flow
Carrier gas flow rate (mL/min)	0.5	N/A	0.4
Injector temperature (℃)	280	230	250
Volume injected (µL)	5	0.1	0.5 / $15x10^3$
Split ratio	1 : 340	1 : 45	1:50
Split flow		170 mL/min	
Initial column temperature (℃)	50	40	-20
Holding time at initial temperature	None	5 min	None
Temperature ramp rate (℃/min)	30	10	8
First intermediate temperature (℃)	170	130	140
Holding time at first intermediate temperature (min)	2 min	25 min	None
Temperature ramp rate (℃/min)	0.5	20	4
Second intermediate temperature (℃)	174 ℃	N/A	188° C
Holding time at second intermediate temperature (min)	None	N/A	None
Temperature ramp rate (℃/min)	40 ℃/min	N/A	8 ℃/m in
Final temperature (℃)	200 ℃	220 ℃	290℃
Holding time at final temperature (min)	3 min	7 min	15.25 min
Detector	FID	Faraday cup	FID
Detector temperature (℃)	320 ℃	250 ℃	300 ℃

* stationary phase consisting of 20% permethylated α-cyclodextrin (a crown ether) in 35% diphenyl/ 65% dimethyl siloxane (Supelco, 2006)

** 100% dimethylpolysiloxane phase

Appendix L: Peak identification by means of GC/MS

Mass spectrums of model compounds finally aided in the identification of isopropyl-3-tolylether [3-methyl-1-(1-methylethoxy)-benzene], 6-n-propyl-3-methyl phenol and *m*-cresol rings alkylated with olefins higher than C_3 are outlined below.

The interpretation of thymol's (6-isopropyl-3-methyl phenol's) and 6-n-propyl-3-methylphenol' s fragmentation patterns (model compounds) follows in this appendix.

At higher conversions a small peak appeared short after thymol in the chromatogram. The mass spectra of this peak did not resemble the spectra of iso-propylated compounds.

Figure L-2 and Figure L-1 show the fragmentation pattern of this compound, which was finally identified as 6-propyl-3-methylphenol. Figure 4.5.2 shows the fragmentation pattern of the iso-analog, thymol. In both cases, the structures of the molecular ions ("molecule peak") are shown in **Frame i** of the respective spectrum whereas the structure of the ion corresponding to the base peak is shown in **Frame ii** of the respective spectra.

From the isopropyl group of the thymyl radical cation (with a molecular weight of 150 atomic mass units / m/z) a methyl radical is easily abstracted and a 6-ethyl-3-methylphenyl cation is formed. This structure has a molecular weight of 135 m/z and is represented by the base peak (Figure L-2).

In contrast to thymol, an ethyl radical is preferably abstracted from the 6-propyl-3-methylphenol thus forming a 3,6-dimethylphenyl cation with a molecular weight of 121 m/z, as represented by the base peak (Figure L-1).

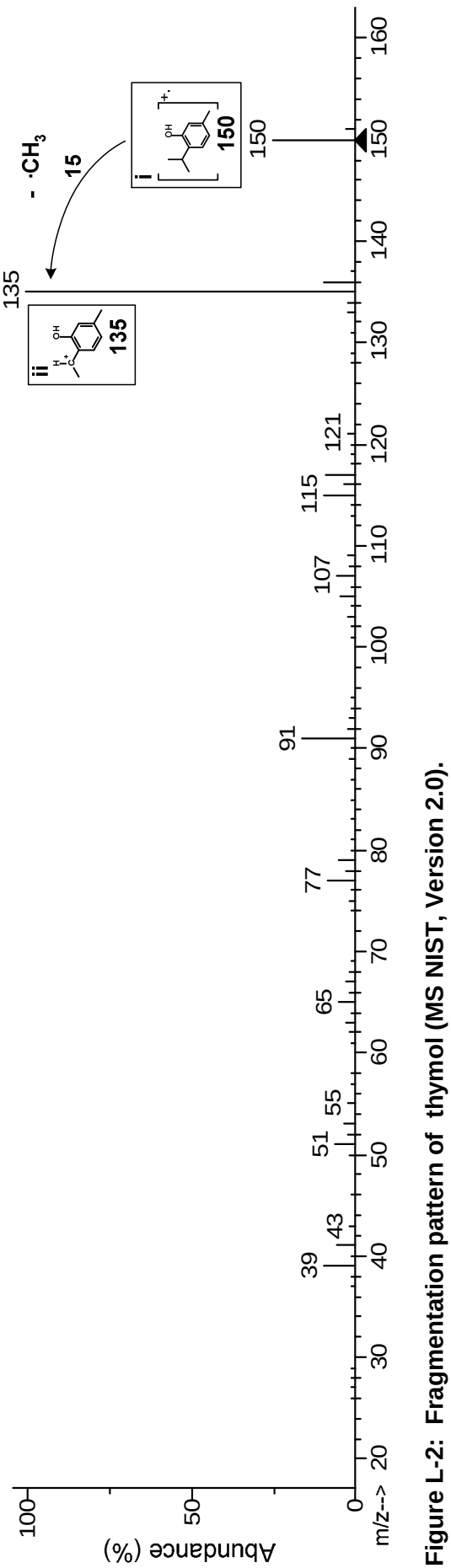

Figure L-2: Fragmentation pattern of thymol (MS NIST, Version 2.0).

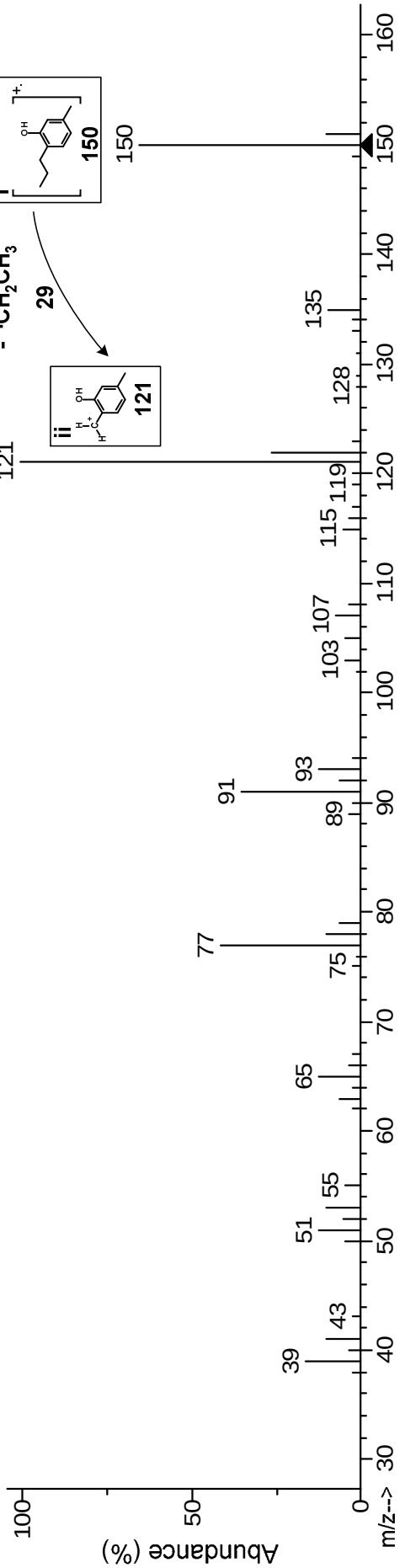

Figure L-1: Fragmentation pattern of 6-propyl-3-methylphenol (MS NIST, Version 2.0).

Appendix M: Identification of 1-methylpropyl-3-methylphenol isomers

The gas chromatograms of the product mixture obtained at severe reaction conditions showed additional peaks. “Additional” in the sense that these peaks were left after all of the mono- and di-isopropylated *m*-cresol derivatives have been identified.

The MS of the respective peaks showed masses of the parent peak of 164, 178, and 192 atomic mass units / m/z and increase, indicating 4, 5 or 6 etc. carbon atoms in the additional side chains of *m*-cresol.

In all instances where the mass spectrum of the particular unidentified compound, was not found in the MS NIST (version 2.0) database it was assumed that the compound was *m*-cresol alkylated with olefins having carbon numbers > 3.

Figure M-1 shows, as an example, the mass spectrum of the compound identified as a 1-methylpropyl-3-methyl-phenol isomer. The molecular ion peak appears at 164 m/z and the base peak corresponds to 135 m/z i.e. the abstraction of an ethyl group. The significant peak at 150 m/z indicates the abstraction of a methyl group as from thymol (Figure L-2). Hence the structure corresponding to the base peak matches up to that of an ethyl-3-methyl-phenyl cation.

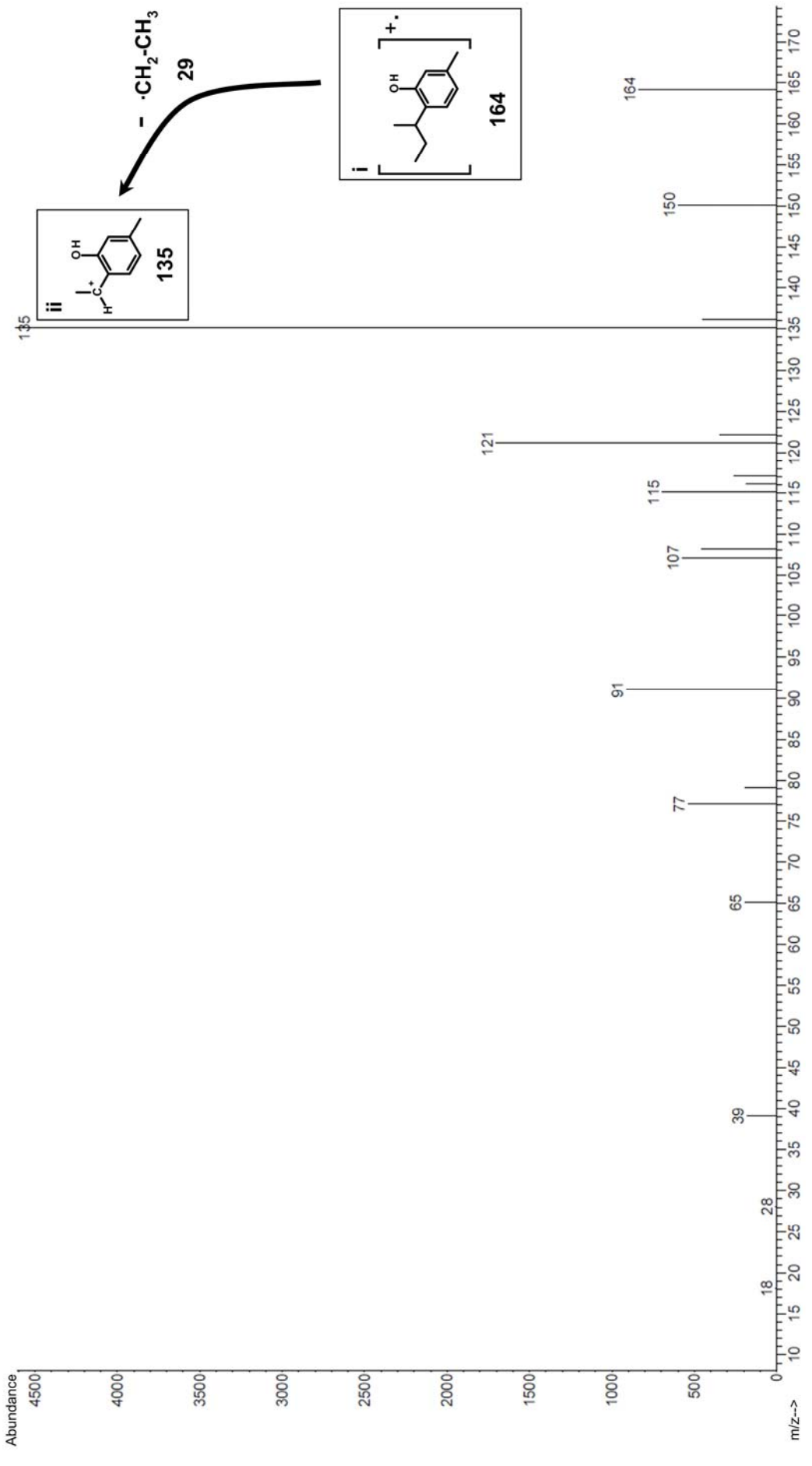

Figure M-1: Fragmentation pattern of 6-(1-methylpropyl)-3-methylphenol (H-MFI-400, 1 bar, gas phase, 300°C, iso-propanol to *m*-cresol ratio =1:1 and 0.04 $g_{m\text{-cresol}} \cdot g_{cat}^{-1} \cdot hr^{-1}$).

Appendix N: Thymol synthesis chromatograms

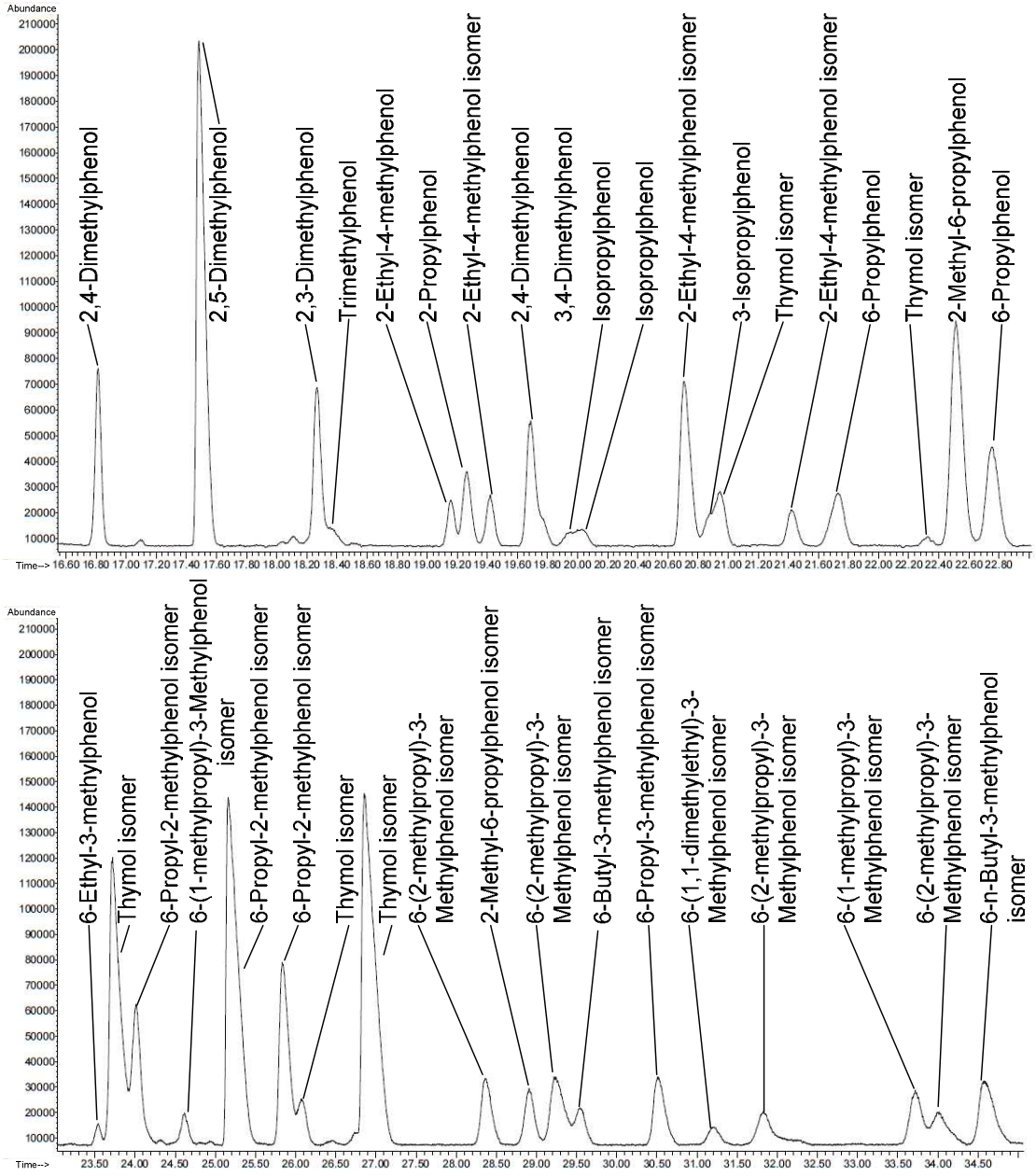

Figure N-1: Sample GCMS Chromatogram for reaction conditions: 300℃, 1 bar, gas phase, iso-propanol to *m*-cresol molar ratio 1:1, 0.04 $g_{m\text{-cresol}} \cdot g_{cat}^{-1} \cdot hr^{-1}$, H-MFI-400.

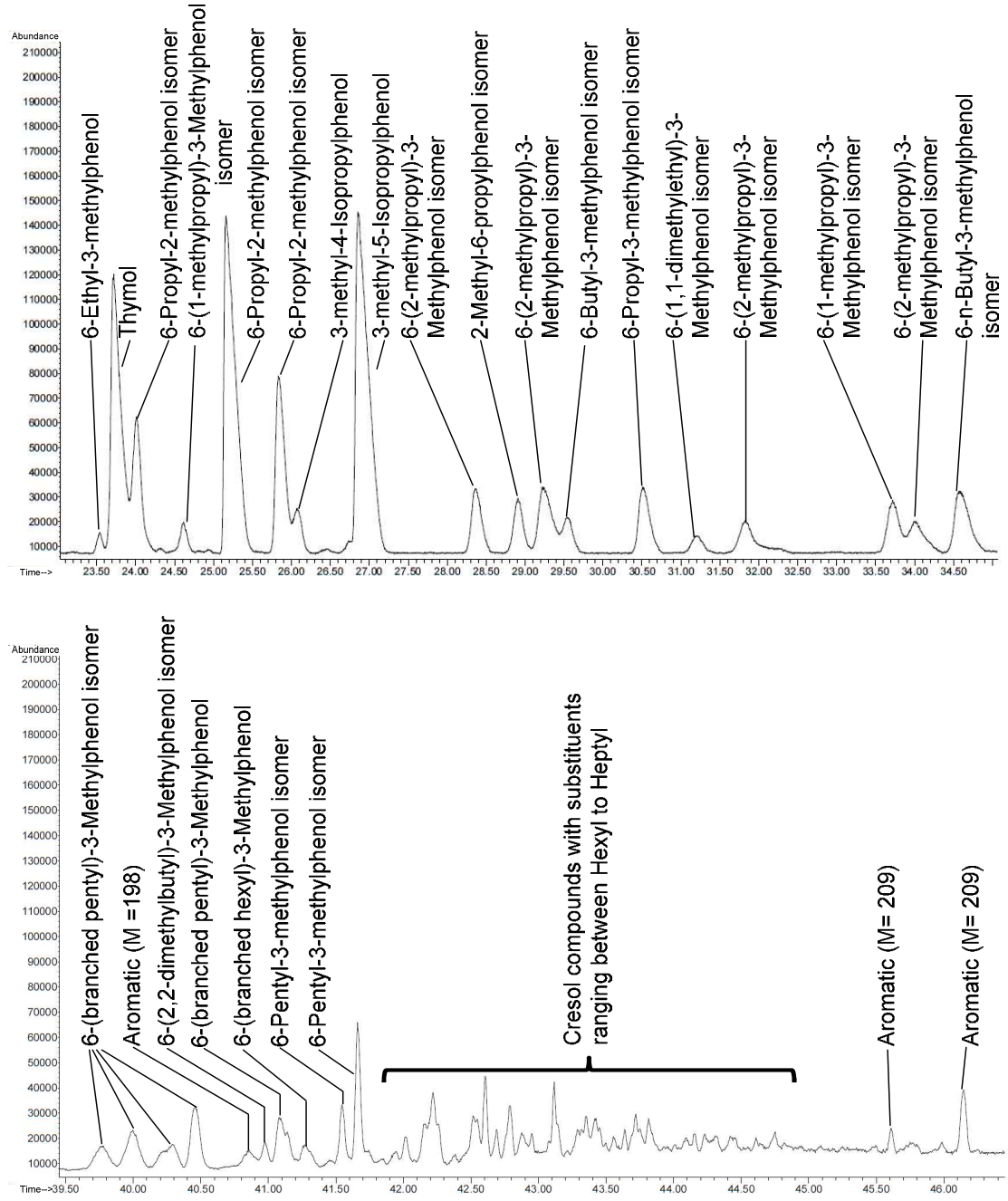

Figure N-2: Sample GCMS Chromatogram for reaction conditions: 300℃, 1 bar, gas phase, IPA to *m*-cresol molar ratio 1:1, 0.04 $g_{m\text{-cresol}} \cdot g_{cat}^{-1} \cdot hr^{-1}$, H-MFI-400.

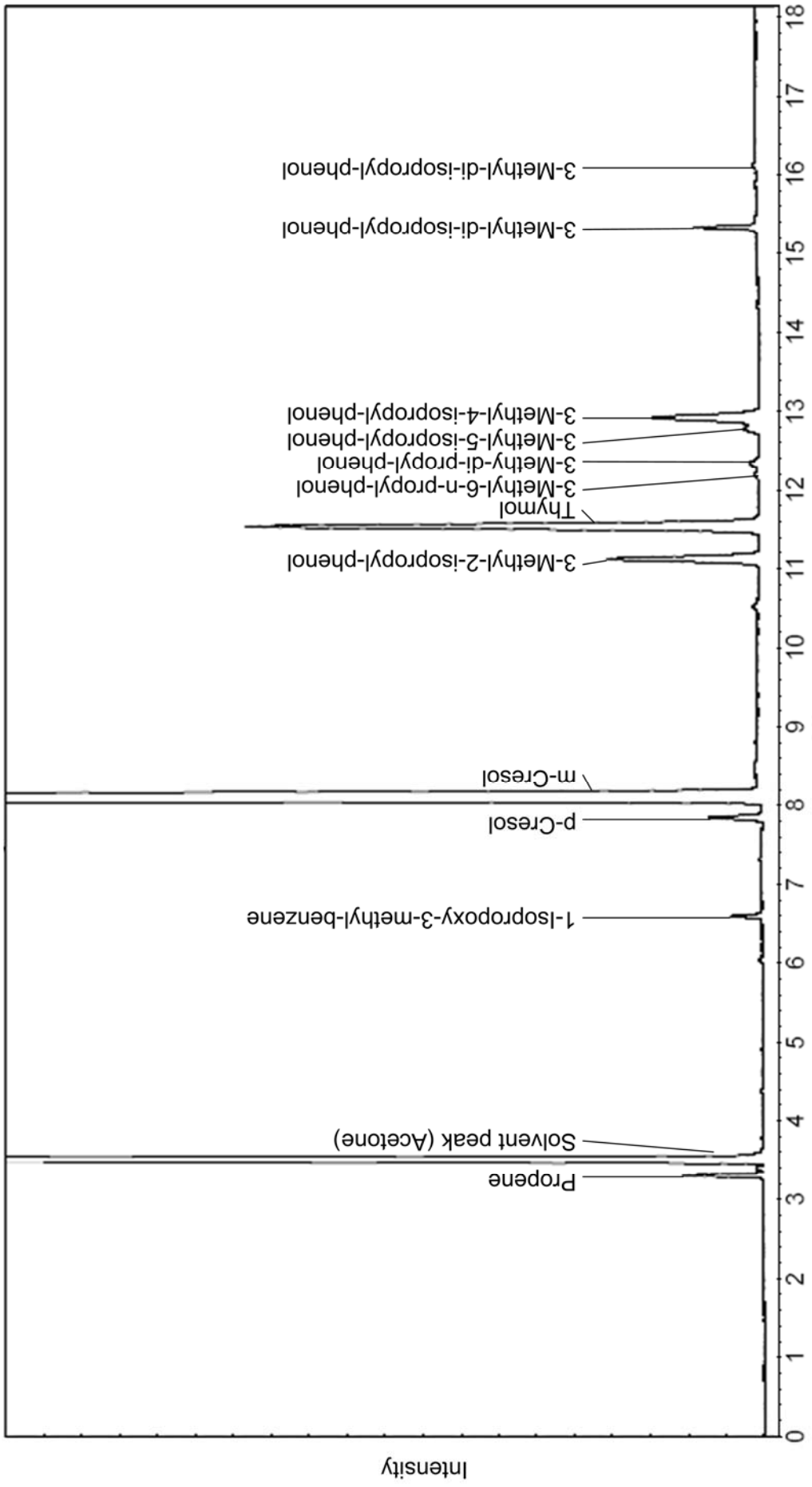

Figure N-3: FID Chromatogram of sample (H-MFI-90, iso- propanol:*m*-cresol molar ratio = 1:1, 250°C, 1 bar, gas phase, 1.03 $g_{m\text{-cresol}} \cdot g_{cat}^{-1} \cdot hr^{-1}$, catalyst bed diluted with SiC at a 1:1 (vol.) ratio).

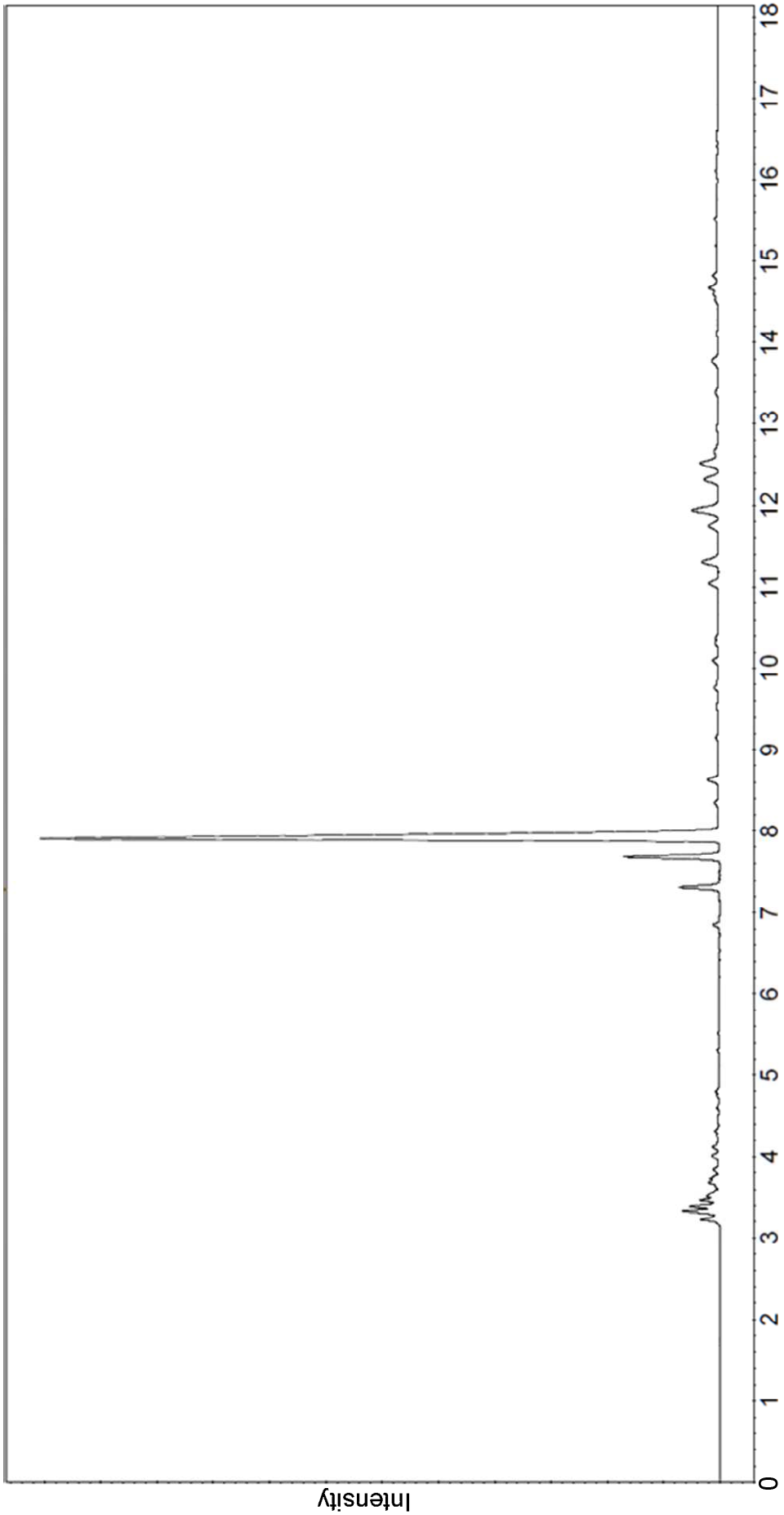

Figure N-4: FID sample chromatogram of (H-MFI-90, iso- propanol:*m*-cresol molar ratio = 1:1, 325℃, 1 bar, gas phase, 1.03 $g_{m\text{-cresol}} \cdot g_{cat}^{-1} \cdot hr^{-1}$, catalyst bed diluted with SiC at a 1:1 (vol.) ratio).

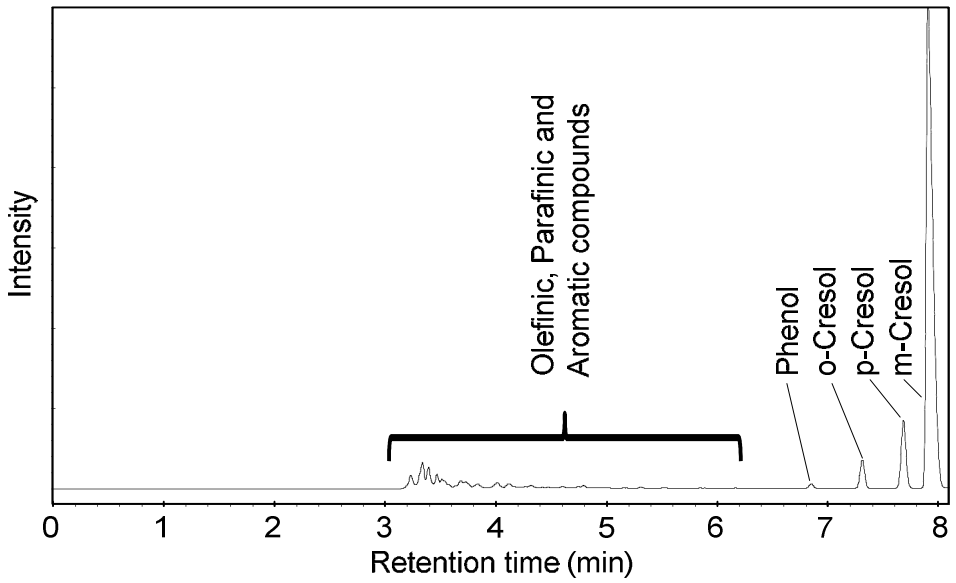

Figure N-5: First section of FID chromatogram showing grouping of peaks to compound fractions shown in Figure N-4.

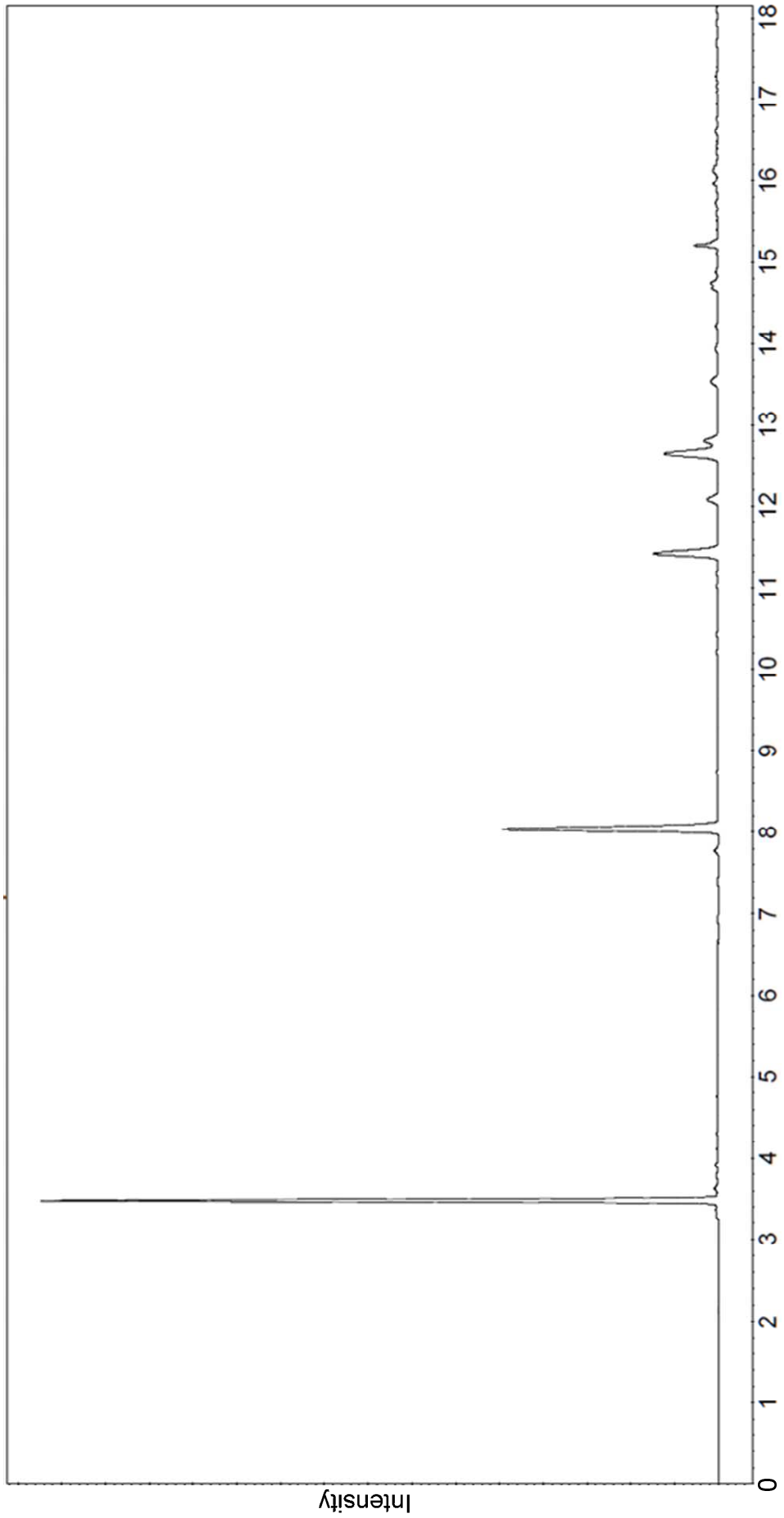

Figure N-6: FID sample chromatogram (H-MFI-90, iso- propanol:*m*-cresol molar ratio = 1:1, 275℃, 15 bar, trickle b ed phase, 0.05 $g_{m\text{-cresol}} \cdot g_{cat}^{-1} \cdot hr^{-1}$, catalyst bed diluted with SiC at a 1:1 (vol.) ratio).

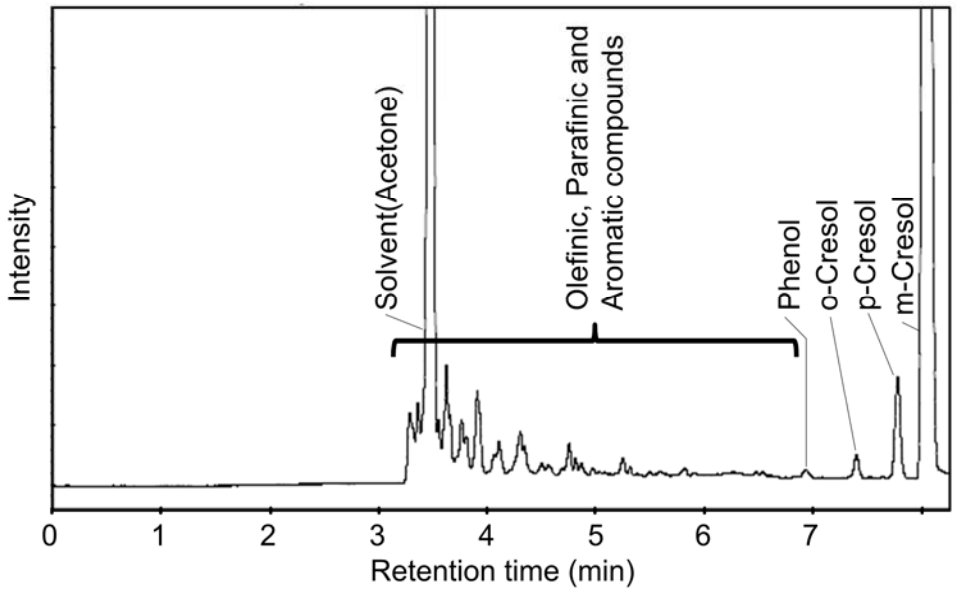

Figure N-7: Section of FID chromatogram showing grouping of peaks to compound fractions shown in Figure N-6.

Appendix O: Iso-propanol dehydration sample chromatograms

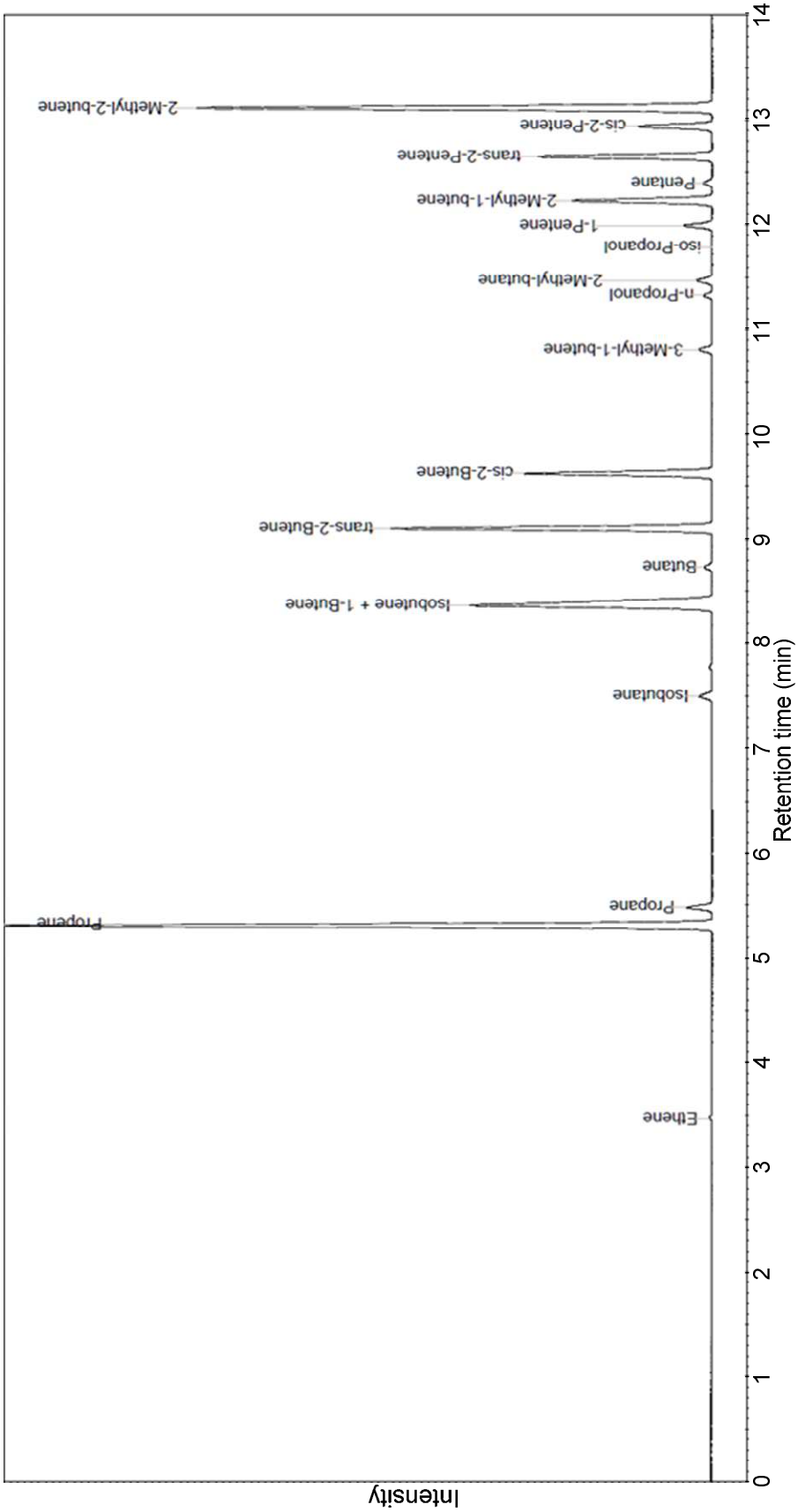

Figure N-1: Section of FID sample chromatogram (H-MFI-90 at 1 bar, 250℃ in the gas phase, IPA to N_2 molar ratio of 1:1 and 0.57 $g_{iso\text{-}propanol} \cdot g_{cat}^{-1} \cdot hr^{-1}$).

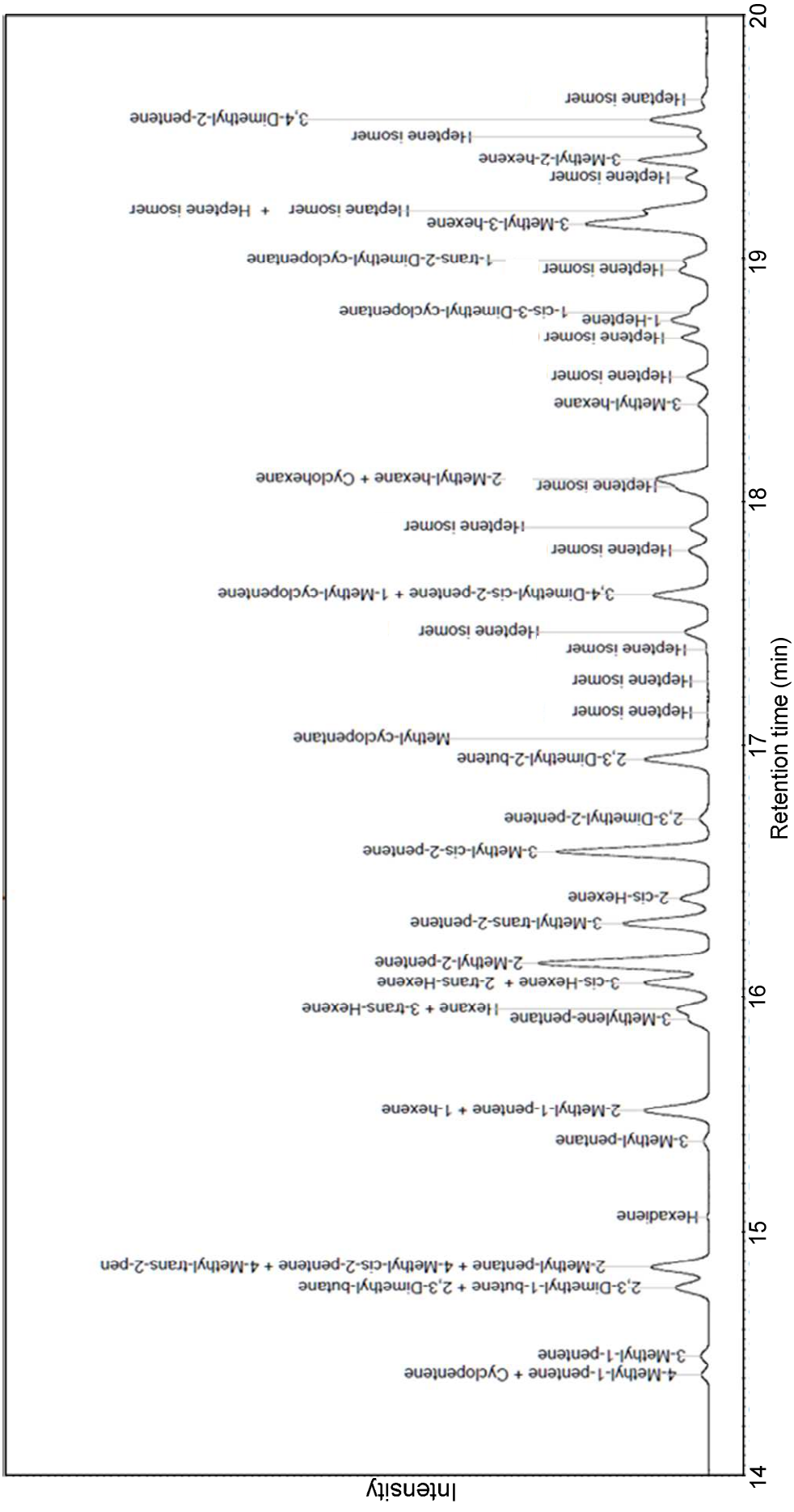

Figure O-2: Section of FID sample chromatogram (H-MFI-90 at 1 bar, 250℃ in the gas phase, IPA to N_2 molar ratio of 1:1 and 0.57 $g_{iso\text{-}propanol} \cdot g_{cat}^{-1} \cdot hr^{-1}$).

Table O-1: Sample of compounds identified during dehydration experiment.

#	Retention time (min)	Name	Identification by
1	3.47	Ethene	GC/MS
2	5.31	Propene	GC/MS
3	5.48	Propane	Model compound
4	7.5	Isobutane	Model compound
5	8.36	Isobutene + 1-Butene	Model compound
6	8.73	Butane	Model compound
7	9.1	trans-2-Butene	Model compound
8	9.63	cis-2-Butene	Model compound
9	10.81	3-Methyl-1-butene	GC/MS
10	11.33	n-Propanol	Model compound
11	11.47	2-Methyl-butane	GC/MS
12	11.79	Iso-propanol	Model compound
13	11.99	1-Pentene	GC/MS
14	12.23	2-Methyl-1-butene	GC/MS
15	12.4	Pentane	GC/MS
16	12.65	trans-2-Pentene	GC/MS
17	12.94	cis-2-Pentene	GC/MS
18	13.12	2-Methyl-2-butene	GC/MS
19	14.41	4-Methyl-1-pentene + Cyclopentene	GC/MS
20	14.49	3-Methyl-1-pentene	GC/MS
21	14.77	2,3-Dimethyl-1-butene + 2,3-Dimethyl-butane	GC/MS
22	14.86	2-Methyl-pentane + 4-Methyl-cis-2-pentene + 4-Methyl-trans-2-pentene	GC/MS
23	15.06	Hexadiene	GC/MS
24	15.37	3-Methyl-pentane	GC/MS
25	15.5	2-Methyl-1-pentene + 1-hexene	GC/MS
26	15.87	3-Methylene-pentane	GC/MS
27	15.92	Hexane + 3-trans-Hexene	GC/MS
28	16.03	3-cis-Hexene + 2-trans-Hexene	GC/MS
29	16.11	2-Methyl-2-pentene	GC/MS
30	16.27	3-Methyl-trans-2-pentene	GC/MS
31	16.37	2-cis-Hexene	GC/MS
32	16.56	3-Methyl-cis-2-pentene	GC/MS
33	16.7	2,3-Dimethyl-2-pentene	GC/MS
34	16.94	2,3-Dimethyl-2-butene	GC/MS
35	17.03	Methyl-cyclopentane	GC/MS
36	17.14	Heptene isomer	GC/MS
37	17.26	Heptene isomer	GC/MS
38	17.39	Heptene isomer	GC/MS
39	17.47	Heptene isomer	GC/MS
40	17.62	3,4-Dimethyl-cis-2-pentene + 1-Methyl-cyclopentene	GC/MS
41	17.8	Heptene isomer	GC/MS
42	17.9	Heptene isomer	GC/MS
43	18.07	Heptene isomer	GC/MS
44	18.1	2-Methyl-hexane + Cyclohexane	GC/MS
45	18.4	3-Methyl-hexane	GC/MS
46	18.52	Heptene isomer	GC/MS
47	18.68	Heptene isomer	GC/MS
48	18.75	1-Heptene	GC/MS
49	18.78	1-cis-3-Dimethyl-cyclopentane	GC/MS
50	18.95	Heptene isomer	GC/MS
51	19	1-trans-2-Dimethyl-cyclopentane	GC/MS
52	19.15	3-Methyl-3-hexene	GC/MS
53	19.2	Heptane isomer + Heptene isomer	GC/MS
54	19.34	Heptene isomer	GC/MS
55	19.41	3-Methyl-2-hexene	GC/MS
56	19.51	Heptene isomer	GC/MS
57	19.57	3,4-Dimethyl-2-pentene	GC/MS
58	19.66	Heptane isomer	GC/MS